JOURNAL OF GEOPHYSICAL RESEARCH, VOL. 106, NO. E11, PAGES 27,933–27,968, NOVEMBER 25, 2001

Lunar rotational dissipation in solid body and molten core

James G. Williams, Dale H. Boggs, Charles F. Yoder,
J. Todd Ratcliff, and Jean O. Dickey

Jet Propulsion Laboratory, California Institute of Technology, Pasadena, California, USA

Abstract. Analyses of Lunar Laser ranges show a displacement in direction of the Moon's pole of rotation which indicates that strong dissipation is acting on the rotation. Two possible sources of dissipation are monthly solid-body tides raised by the Earth (and Sun) and a fluid core with a rotation distinct from the solid body. Both effects have been introduced into a numerical integration of the lunar rotation. Theoretical consequences of tides and core on rotation and orbit are also calculated analytically. These computations indicate that the tide and core dissipation signatures are separable. They also allow unrestricted laws for tidal specific dissipation Q versus frequency to be applied. Fits of Lunar Laser ranges detect three small dissipation terms in addition to the dominant pole-displacement term. Tidal dissipation alone does not give a good match to all four amplitudes. Dissipation from tides plus fluid core accounts for them. The best match indicates a tidal Q which increases slowly with period plus a small fluid core. The core size depends on imperfectly known properties of the fluid and core-mantle interface. The radius of a core could be as much as 352 km if iron and 374 km for the Fe-FeS eutectic composition. If tidal Q versus frequency is assumed to be represented by a power law, then the exponent is –0.19±0.13. The monthly tidal Q is 37 (–4,+6), and the annual Q is 60 (–15,+30). The power presently dissipated by solid body and core is small, but it may have been dramatic for the early Moon. The outwardly evolving Moon passed through a change of spin state which caused a burst of dissipated power in the mantle and at the core-mantle boundary. The energy deposited at the boundary plausibly drove convection in the core and temporarily powered a dynamo. The remanent magnetism in lunar rocks may result from these events, and the peak field may mark the passage of the Moon through the spin transition.

1. Introduction

The Moon keeps one face toward the Earth. This simple statement of the equality of the rotational and orbital periods has a deeper implication. Since there is no reason to expect that the Moon formed in such a special rotational state, there must have been one or more mechanisms for changing the lunar rotational angular momentum and energy.

Laser ranges from the Earth to the Moon started in 1969. The analyses of laser ranges discovered active lunar rotational dissipation nearly a decade later, and during the past 2 decades the detection has improved [*Yoder et al.,* 1978; *Ferrari et al.,* 1980; *Cappallo et al.,* 1981; *Dickey et al.,* 1982; *Williams et al.,* 1987; *Dickey et al.,* 1994]. The Moon's rotation is locked in a spin state (Cassini state) such that the 18.6 year retrograde precession of the lunar equator plane along the ecliptic plane matches the precession of the lunar orbit plane. In the absence of dissipation the equator's average descending node aligns with the orbit's average ascending node. Laser range analysis finds an average shift between the two nodes which indicates ongoing dissipation. The presently measured shift is –9.8" in the node of the equator on the ecliptic equivalent to an arc length shift of 0.263" in the pole direction. The arrangement and precession of spin and orbit poles is shown in Figure 1. Over the past 2 decades the significance of the pole shift has improved from the first detection to the present 1% uncertainty.

Copyright 2001 by the American Geophysical Union.

Paper number 2000JE001396.
0148-0227/01/2000JE001396$09.00

There are two proposed mechanisms for the lunar rotational dissipation: solid-body tidal dissipation [*Yoder,* 1979; *Cappallo et al.,* 1981] and dissipation at a liquid-core/solid-body boundary [*Yoder,* 1981]. Tidal dissipation must exist for the Moon at some strength. Core dissipation requires a fluid lunar core. While there are several reasons to suspect that a core is present (see section 19), and the recent Lunar Prospector mission has strengthened the evidence, the consequences of a small core are subtle, and it has remained unclear whether it is solid or liquid.

Both tidal and core dissipation can displace the equator plane in the observed manner. In the past it has not been possible to distinguish between them. Improvements in the range accuracy and increasing data span now make it possible to use small additional signatures to discriminate.

This paper explores the two dissipation models used for numerical or analytical computation of the lunar rotation (sections 2 and 3 for tides and section 9 for core). It presents analytical developments for the effect of each model on the rotation (tides: sections 4, 5, 7, core: sections 10, 12–14) and orbit (tides: section 8, core: section 15). Results from fits to the Lunar Laser Ranging (LLR) data using the two dissipation models are presented (section 18). Results are discussed and compared with other evidence on the lunar interior (sections 19 and 20).

2. Rotational Dynamics

The attraction of the Earth and Sun on the nonspherical figure of the Moon applies torques. The Earth dominates the torques. As a consequence, the lunar equator plane precesses along the

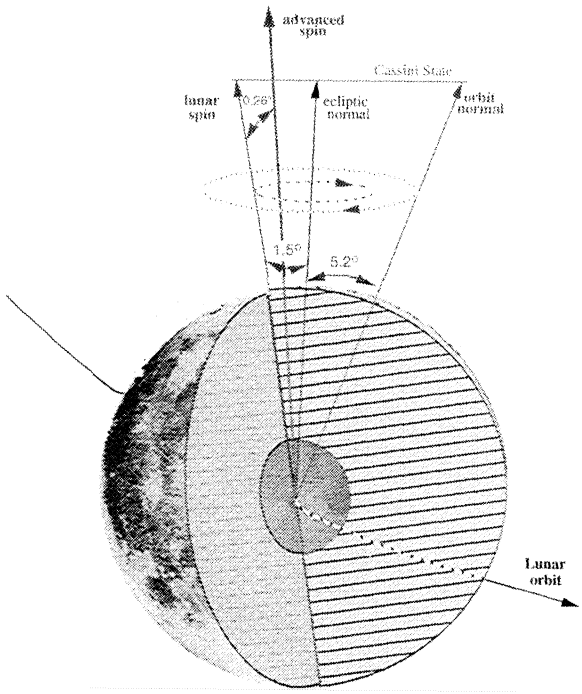

Figure 1. The spin axis and orbit normal precess in 18.6 years about the ecliptic pole in a retrograde direction. Without dissipation the three poles would be coplanar. Dissipation in the Moon causes a small displacement of the spin pole orthogonal to that plane.

ecliptic plane in 18.6 years (tilt 1.54°) with a superimposed sequence of periodic variations in pole direction, and the rotation is synchronous with variations in rotation about the polar axis. Much of the sensitivity of the LLR data to lunar science information comes through this time-varying three-dimensional rotation of the Moon called physical libration. These parameters include the moment of inertia combinations $\beta=(C-A)/B$ and $\gamma=(B-A)/C$, seven third-degree gravitational harmonics, dissipation due to solid-body tides and core, and Love number k_2. *Dickey et al.* [1994] review the Lunar Laser-Ranging technique and results.

The range accuracy has improved with time, and the most recent data are fit with a 2 cm rms residual. A highly accurate model for the orbit and rotation of the Moon is needed to fit the lunar ranges. The orbits of the Moon and planets and the rotation of the Moon are simultaneously numerically integrated. The lunar initial conditions for these integrations and the parameters of the previous paragraph come from least squares fits to the lunar range data.

The numerical integration of the lunar rotation requires the equations of motion and a model for torques. The orientation of the Moon is specified by three Euler angles. The angular velocities are computed from the Euler angles and their rates. The lunar rotation is computed from differential equations for the angular momentum. The vector differential equation is the Euler equation when expressed in a frame rotating with the body (Moon):

$$\frac{d(\mathbf{I}\omega)}{dt} + \omega \mathrm{x} \mathbf{I}\omega = \mathbf{T} . \qquad (1)$$

$\mathbf{I}$ is the moment of inertia matrix, ω is the angular velocity vector, and t is time. The angular momentum vector is the product $\mathbf{I}\omega$.

The torque $\mathbf{T}$ includes the gravitational interaction of the lunar figure with external bodies. In the integration model these are Earth, Sun, Venus, and Jupiter. For a spherical attracting body, the second-degree torques depend on $\mathbf{I}$ and take the form

$$\mathbf{T}_2 = \frac{3GM}{r^5} \mathbf{r}\mathrm{x}\mathbf{I}\mathbf{r} . \qquad (2)$$

M is the mass of the attracting body, and $\mathbf{r}$ is its position with respect to the Moon's center. G is the gravitational constant. In the Jet Propulsion Laboratory (JPL) model, additional torques come from third- and fourth-degree lunar gravitational harmonics and figure-figure interactions (triaxial Moon with oblate Earth). Since the orbits used for torque computation include the influence of gravitational harmonics, planetary perturbations, and relativity, the torques include indirect effects due to those perturbations. The lunar orientation is required to compute the torques, and the body-referenced angular velocities depend on the Euler angles and their rates.

$$\omega = \begin{pmatrix} -\dot{\psi} \sin\theta \sin\varphi - \dot{\theta} \cos\varphi \\ -\dot{\psi} \sin\theta \cos\varphi + \dot{\theta} \sin\varphi \\ \dot{\psi} \cos\theta + \dot{\varphi} \end{pmatrix} . \qquad (3)$$

In the JPL numerical integration model the Euler angles consist of a node-like angle ψ from the J2000 equinox along the J2000 Earth's equator to the descending node of the lunar equator, a tilt θ between the two equators, and an angle φ from the node along the lunar equator to the lunar zero meridian. For analytical calculations it is more useful to give Euler angles defined so that the Earth's equator plane replaces the ecliptic plane in the foregoing sequence of three angles. Equation (1) is equivalent to three second-order, nonlinear differential equations for the Euler angles.

Tidal effects cause $\mathbf{I}$ and the gravitational harmonics to be time varying. This will be described in the next section. If there is a fluid core, then in addition to (1) a vector differential equation is needed to describe the core rotation. There would be torques from interactions at a core-mantle interface which must be applied with equal magnitude and opposite sign to the mantle and core (section 9).

3. Computational Model for Tidal and Rotational Deformation

In addition to causing torques, the attraction of the Earth and Sun also raises tides on the Moon. The time-varying tidal distortion of the Moon changes both the moments of inertia and the torques, thereby modifying the rotation. Spin also distorts the Moon, and that time-varying deformation can be treated along with tides.

The Moon must be distorted by solid-body tides. The elastic tidal response of the Moon is modeled with Love numbers. The amount of anelastic tidal dissipation is not known a priori, but dissipation must be present. Consequently, for 2 decades a tidal dissipation model has been used to fit the observed lunar dissipation for Lunar Laser range data analysis. A time-varying expression for the lunar moments of inertia is used in the program which numerically integrates the rotation of the Moon and the orbits of the Moon and planets.

An early theoretical investigation by *Peale* [1973] of elastic tidal effects on rotation about the pole concluded that the effects were small, but he did not find the larger effect in pole direction. Analytical theories for both elastic tides and tidal dissipation

have been presented by *Yoder* [1979] and *Eckhardt* [1981]. *Bois and Journet* [1993] attempted a numerical approach. An equation for time-delayed lunar moments of inertia is used by *Newhall and Williams* [1997] for numerical LLR data analysis.

The moment-of-inertia expression can be split up into a fixed part, a part for tidal deformation, and a part for spin-related distortion:

$$\mathbf{I} = \mathbf{I}_{\text{rigid}} + \mathbf{I}_{\text{tide}} + \mathbf{I}_{\text{spin}} . \tag{4}$$

In the principal axis system the rigid-body principal moments of inertia are $A<B<C$. The first axis, associated with A, is approximately toward the Earth, and the third axis, associated with C, is nearly in the direction of the spin vector:

$$\mathbf{I}_{\text{rigid}} = \begin{pmatrix} A & 0 & 0 \\ 0 & B & 0 \\ 0 & 0 & C \end{pmatrix} . \tag{5}$$

The rigid-body moments are used to define $\alpha=(C-B)/A$, $\beta=(C-A)/B$ and $\gamma=(B-A)/C$. Only two are independent with $\alpha=(\beta-\gamma)/(1-\beta\gamma)$. Those relative differences and the ratios $A/C=(1-\beta\gamma)/(1+\beta)$ and $B/C=(1+\gamma)/(1+\beta)$ can be determined much more accurately than the moments of inertia.

The tides affect the moments. The second-degree tide-raising potential at a point on the lunar surface (Moon-centered unit vector $\mathbf{u}'$) is

$$V_{\text{tide}} = \frac{G\,M\,R^2}{r^3}\, P_2(\mathbf{u}\cdot\mathbf{u}') . \tag{6}$$

For the tide-raising body, M is the mass, and $\mathbf{r}$ is its Moon-centered position vector (components r_i, distance r, unit vector $\mathbf{u}=\mathbf{r}/r$, components u_i). For the Moon, R is the radius 1738 km. $P_2(\mathbf{u}\cdot\mathbf{u}') = (3/2)[(\mathbf{u}\cdot\mathbf{u}')^2-1/3]$ is the second-degree Legendre polynomial. To calculate forces, the positive gradient of (6) is taken with respect to the position $R\mathbf{u}'$ (potential sign convention is plus for the point mass potential). Along the Earth-Moon line the acceleration is outward from the Moon. For the tidal part of the moment the nine matrix components (indices i, j) are

$$I_{\text{tide},\,ij} = -\frac{k_2\,M\,R^5}{r^3}\left(u_i u_j - \frac{\delta_{ij}}{3} \right) , \tag{7}$$

where k_2 is the second-degree potential lunar Love number and the delta function δ_{ij} modifies the diagonal components.

An elastic body will also distort from rotation. In a rotating frame the additional potential at the surface is separated into two parts: one spherically symmetric and the other multiplying a second-degree spherical harmonic.

$$V_{\text{spin}} = \frac{R^2\,\omega^2}{3}\left[\, 1 - P_2(\mathbf{u}'\cdot\hat{\boldsymbol{\omega}}) \,\right] . \tag{8}$$

The angular velocity vector is $\boldsymbol{\omega}$ (components ω_i, scalar ω, unit vector $\hat{\boldsymbol{\omega}}$). Distortion from both parts of the potential contributes to the moment of inertia components.

$$I_{\text{spin},\,ij} = \frac{R^5}{3\,G}\left[\, k_2\left(\omega_i\,\omega_j - \frac{\omega^2}{3}\,\delta_{ij} \right) + s\,\omega^2\,\delta_{ij} \,\right] . \tag{9}$$

The Love number k_2 and the spherical parameter s depend on the elastic properties of the Moon. See Appendix A for a discussion of the spherical term. Rotational acceleration can also distort the Moon. These distortions are shown to be small in Appendix B.

Since $\omega_3/\omega \approx 1$ and $r_1/r \approx 1$, there are static-deformation contributions to both the spin and tidal parts of the moments. It is a matter of definition whether such constant parts are left in the tidal and spin parts of the moments or moved to the "rigid" part. In the work by *Newhall and Williams* [1997] the average values of the three diagonal terms of the spin part were nearly nulled by ignoring the s term and adding to the diagonal $n^2/3$, $n^2/3$, $-2n^2/3$, respectively, inside the parenthesis of (9). Here n is the sidereal mean motion. This is a wise choice for a rapidly spinning object like the Earth, where significant oblateness is caused by spin, but for the slowly rotating Moon the spin-induced oblateness is smaller than the permanent figure and either choice is reasonable (see section 6).

In the tidal and spin parts of **I,** the position $\mathbf{r}$ and spin rate $\boldsymbol{\omega}$ are functions of time. If the moments $\mathbf{I}_{\text{tide}}$ and $\mathbf{I}_{\text{spin}}$ are evaluated using $\mathbf{r}(t)$ and $\boldsymbol{\omega}(t)$, respectively, then the elastic response of the Moon will be accounted for in the resulting rotation. The sensitivity of the LLR analysis to the Love number k_2 comes through these terms. Tidal and spin dissipation effects arise if the distortion is not an instantaneous response. In the program which numerically integrates the rotation and orbits the tidal dissipation is introduced with a time delay Δt by using $\mathbf{r}(t-\Delta t)$ and $\boldsymbol{\omega}(t-\Delta t)$ when computing the distorted moments. In the differential equations (1) and the torque (2) it is **I** which is time delayed. The time-delayed position and spin rate appear only in the moments and not in the $\boldsymbol{\omega}$ explicit in (1) or the $\mathbf{r}$ explicit in (2). With an analytical expansion more generality can be introduced through a separate time delay, or, equivalently, a separate phase shift, for each periodic term in the moments. Such an analytical solution will be developed in the next section.

Some numerical values can be assigned to the above effects. The model used for the lunar and planetary ephemeris DE403 included tidal dissipation but not core dissipation, so the DE403 solution generated in 1995 represents a limiting possibility with the Love number $k_2 = 0.0300$, the time delay $\Delta t = 0.1673$ day, and the polar moment normalized with the lunar mass and radius $C/mR^2 = 0.3944$. With these values the ratio of the tidal moment factor to C is $(k_2 MR^5/Ca^3) = 5.7\text{x}10^{-7}$, where a = 384,399 km is the semimajor axis of the lunar orbit. Similarly, take the common factor in (9) with $\omega = n$ (for constant part) and normalize by C to get $(k_2 n^2 R^5/3GC) = 1.9\text{x}10^{-7}$. The time variation is even smaller than these values. The direction of the Earth as seen in the lunar principal axis frame varies 0.1 radian in both the north-south and east-west directions. The eccentricity e of the lunar orbit is 0.055, so that the $(a/r)^3$ tidal factor varies by $3e$. The spin rate direction varies <0.001 radian with respect to the principal axes, and the spin rate relative magnitude varies about 10^{-4}. Thus the relative time variation of the moments is of order 10^{-7} for tides and 10^{-10} for spin. The relative variation due to time delay is smaller yet since it involves the factor $n\Delta t$, which is 0.039 = 1/26 for DE403 values.

4. Tidal and Rotational Dissipation: Analytical Development

What are the dynamical consequences for the rotation angles of the tidal and rotational deformation and dissipation? Series solutions with numerical coefficients have previously been given by *Yoder* [1979] and *Eckhardt* [1981]. The results depend on how the specific dissipation Q varies with deformation frequency. The specific dissipation used here is a whole-body Q, and just as k_2 depends on elastic properties of lunar material as a function of radius, k_2/Q is a function of the distribution of internal dissipation. The numerical model with constant time delay is equivalent to Q proportional to 1/frequency. For the

values of time delay and k_2 given in the previous paragraph, $Q = 26$, which, as will be seen below, is for a 1 month period. Yoder gives series for the inverse frequency case, and he gives the difference between series for that case and a constant Q case (no frequency dependence). Eckhardt gives series for the constant Q case. The solution in this and the next section will have a separate Q for each deformation frequency. Thus the coefficients of each periodic term in the rotation series can be functions of more than one deformation frequency.

The torque expression (2) involves $\mathbf{u}\times\mathbf{I}\mathbf{u}/r^3$, where the unit vector $\mathbf{u} = \mathbf{r}/r$. The Euler equation (1) involves $\boldsymbol{\omega}\times\mathbf{I}\boldsymbol{\omega}$. Restricting the following development to the second-degree torques and tides yields

$$\frac{d(\mathbf{I}\boldsymbol{\omega})}{dt} = -\boldsymbol{\omega}\times\mathbf{I}\boldsymbol{\omega} + \frac{3\,G\,M}{r^3}\,\mathbf{u}\times\mathbf{I}\mathbf{u}\,. \qquad (10)$$

The tidal and spin parts of $\mathbf{I}$ depend on r, $\mathbf{u}$, and $\boldsymbol{\omega}$. With a dyad form for products of components the moment matrices can be written as

$$\mathbf{I}_{\text{tide}} = -\frac{k_2\,M\,R^5}{r^3}\left(\mathbf{u}\mathbf{u} - \frac{1}{3}\,\mathbf{i}\right), \qquad (11)$$

$$\mathbf{I}_{\text{spin}} = \frac{R^5}{3\,G}\left[\,k_2\left(\boldsymbol{\omega}\boldsymbol{\omega} - \frac{\omega^2}{3}\,\mathbf{i}\right) + s\,\omega^2\,\mathbf{i}\,\right]. \qquad (12)$$

where $\mathbf{i}$ is the identity matrix. It is immediately evident that the parts involving the identity matrix will disappear in the cross products. With dissipation the tidal and spin deformation parts of $\mathbf{I}$ have delayed responses. An asterisk is used to distinguish the parameters which originate from $\mathbf{I}$. These include parameters of the tide-raising body, which may be different from the torquing body, and time-delayed quantities. Then (10) becomes

$$\frac{d(\mathbf{I}\boldsymbol{\omega})}{dt} + \boldsymbol{\omega}\times\mathbf{I}_{\text{rigid}}\,\boldsymbol{\omega} - \frac{3\,G\,M}{r^3}\,\mathbf{u}\times\mathbf{I}_{\text{rigid}}\,\mathbf{u} = k_2\,R^5\left[-\frac{3\,G\,M\,M^*}{r^3\,r^{*3}}\,\mathbf{u}\times\mathbf{u}^*\,\mathbf{u}\cdot\mathbf{u}^* + \frac{M}{r^3}\,\mathbf{u}\times\boldsymbol{\omega}^*\,\mathbf{u}\cdot\boldsymbol{\omega}^* + \frac{M^*}{r^{*3}}\,\boldsymbol{\omega}\times\mathbf{u}^*\,\boldsymbol{\omega}\cdot\mathbf{u}^* - \frac{1}{3\,G}\,\boldsymbol{\omega}\times\boldsymbol{\omega}^*\,\boldsymbol{\omega}\cdot\boldsymbol{\omega}^*\right]. \qquad (13)$$

When the tide-raising body and the torquing body are the same, the asterisk indicates the time-delayed parameters and $M^*=M$. When the tide-raising and torquing bodies are different, the asterisk indicates the time-delayed parameters of the tide-raising body and the right-hand side requires sums over the bodies (two sums for the first term and one sum for each of the second and third terms).

Note that if there is no dissipation ($r=r^*$, $\mathbf{u}=\mathbf{u}^*$, and $\boldsymbol{\omega}=\boldsymbol{\omega}^*$) and the tide-raising and torquing bodies are the same ($M=M^*$), then the first and fourth terms on the right-hand side of (13) are zero because of the cross products and the second and third terms cancel. Without dissipation, not only does a bulge directly under the attracting body exert no torque (first term on right-hand side), and not only is the apparent torque ($-\boldsymbol{\omega}\times\mathbf{I}\boldsymbol{\omega}$) from working in a rotating frame unable to interact with the spin-induced deformation (fourth term), but the torque from the spin deformation (second term) and the apparent torque from the tides (third term) cancel one another. In the rotating frame the same tide-plus-spin forces which elastically distort the Moon cannot also apply torque on that deformation since they are aligned. In an inertial frame the attracting body does apply torque on the rotation-caused bulge. The time variation of the angular momentum $\mathbf{I}\boldsymbol{\omega}$ in the rotating frame is not altered by the elastic deformations, but the rotation rates and Euler angles are still influenced because of the time variation of $\mathbf{I}$ in that product.

Another piece of information can be gleaned from (13). For multiple bodies raising tides and causing torques, there would be sums over the bodies (briefly use a subscript for the body): two sums in the first term on the right-hand side and one in each of the second and third terms. Without dissipation, for every term $M_n\,\mathbf{u}_n\times\boldsymbol{\omega}$ there is a term $M_n\,\boldsymbol{\omega}\times\mathbf{u}_n$ which cancels it, and for every $M_n M_m\,\mathbf{u}_n\times\mathbf{u}_m$ there is a $M_m M_n\,\mathbf{u}_m\times\mathbf{u}_n$. For a constant Love number, multiple attracting bodies cannot alter the angular momentum in the rotating frame through deformations without dissipation.

With dissipation the four deformation terms on the right-hand side of (13) are nonzero. The important torque terms arise from the Earth interacting with Earth-raised tides, while the Sun is only a minor influence. In component form the functions $U_{ij} = (a/r)^3\,u_i\,u_j$ and $\omega_i\,\omega_j/n^2$ are needed. The diagonals of the functions give $(a/r)^3$ and ω^2 which occur in $\mathbf{I}$ in the derivative on the left-hand side of (13). (The radius r is conveniently normalized by the semimajor axis a, and the spin is normalized by the mean motion n.) The series for these functions were developed using the lunar orbit theory of *Chapront-Touzé and Chapront* [1988, 1991] and the physical libration series by J. G. Williams et al. (manuscript in preparation, 2001) (hereinafter referred to as Williams et al., 2001). The functions with and without phase shifts/time lags are multiplied together to represent the four terms on the right-hand side of (13). When written out in component form, each of the three vector components of the differential equation has 24 terms on the right side, and each term has a series expansion. Economy of effort is achieved by combining the second-degree functions from Earth, Sun, and spin into one matrix. The coefficients are in proportion to the $-M/a^3$ and $n^2/3G$ that can be deduced from (7) and (9). Then the 24 terms for each component (54 if the Sun is included) can be replaced with six.

Since $u_1 \approx 1$ and $\omega_3/n \approx 1$, the larger deformation terms involve these components. As an example, the most important pair of terms on the right-hand side of the third component of the vector differential equation (13) is

$$-k_2\,R^5\,\frac{3\,G\,M^2}{a^6}\left[\,U_{11}\,U_{12}^* - U_{12}\,U_{11}^*\,\right]. \qquad (14)$$

Without dissipation this pair of terms will cancel, but with dissipation a component multiplying a phase shift is selected for each periodicity. The u_2 depends on orbit and physical libration variations, with the dominant periodic terms from the longitude variations of the lunar orbit. The largest of these is the monthly (27.555 days) eccentricity-caused term depending on mean anomaly ℓ, approximately $2e\sin\ell$. With this term as an example, the brackets in (14) plus a smaller contribution (indices 2212) yield

$$22{,}000''\,(\sin\ell^* - \sin\ell) \approx 22{,}000''\,(\ell^* - \ell)\,\cos\ell\,. \qquad (15)$$

For a positive frequency a positive time delay corresponds to a negative phase shift and a positive specific dissipation Q so $(\ell^* - \ell) \approx -1/Q_\ell$. Terms of the form of (15) arise from a constant torque coefficient multiplying a periodic deformation, minus a periodic torque times a constant deformation. Other terms result when a periodic torque multiplies a periodic deformation, and a constant results when the periods are equal. The phase for constant terms enters directly as a difference, e.g.,

$\sin(\ell^*-\ell)$, while mixes of different periods give arguments with angles mixed together, e.g., $\sin(2F^*-\ell^*-\ell) - \sin(2F-\ell-\ell^*)$.

The factor GM/a^3 is ubiquitous, and for analytical computation it is useful to relate it to sidereal mean motion n. Kepler's third law is modified for solar attraction [*Brouwer and Clemence*, 1961, chap. 12], and $1/a$ is set equal to the time-averaged $1/r$ for the perturbed orbit:

$$\frac{GM}{a^3} \approx n^2 \left(1 + \frac{n'^2}{2n^2} \right) \frac{M}{(M+m)}, \qquad (16a)$$

$$\frac{GM}{a^3} \approx 0.9906\, n^2 . \qquad (16b)$$

where n' is the mean motion of the Earth-Moon center of mass about the Sun. The Earth/Moon mass ratio is $M/m = 81.3006$, and for $R = 1738$ km the ratio $R/a = 1/221.17$.

The third component of the differential equation (13) describes the rotation about the polar axis. This rotation angle nearly follows the mean Earth as seen from the Moon, the Moon's orbital mean longitude L plus 180°. The small remaining part, the "longitude" angle of physical librations, is called τ. For the ecliptic definition of Euler angles in section 2, $\phi+\psi = L+\tau+180°$. The theory of the lunar rotation with torques on the lunar figure is a classic problem [*Eckhardt*, 1981; *Moons*, 1982a, 1982b; *Petrova*, 1996]. While the differential equations for rotation are nonlinear, a linearized form gives a good first approximation. For the present purpose, use $\omega_3 \approx n + \dot{\tau}$, ignore the small $\omega_1\omega_2$ term, extract a linear τ term from the rigid-body torque, and treat the remainder of that torque as a forcing function. Then the polar component of the differential equation becomes

$$C (\ddot{\tau} + 3\gamma n^2 \tau) + \dot{I}_{33}\, n = f_z . \qquad (17)$$

The forcing term f_z includes both the rigid-body forcing (without linear τ term) and the right-hand side of (13). The solution from the rigid-body forcing is not an objective here but is treated in the above three references (also see section 13). The resonant frequency $n\,(3\gamma)^{1/2}$ for the longitude variable has a period of 1056.1 days (including a correction factor $S_3 = 0.9759$ and adjustment for third-degree harmonics discussed by Williams et al. (2001)). As an example, the resulting solution with the forcing term proportional to (15) is $-1.3"\ (k_2/Q_\ell)\cos\ell$, but there is a small correction from the derivative of I_{33}, and the final contribution to τ is $-1.1"\ (k_2/Q_\ell)\cos\ell$. With the DE403 solution values the coefficient is $-0.0012"$ or ~1 cm at the lunar equator, which projects into a few millimeters in range.

The solution of the differential equation (17) for a periodic forcing term amplifies longer periodicities more than monthly terms. Libration amplitudes larger than the monthly example occur for annual, 206 day, and 1095 day periods. The latter requires the most care since it is near the resonance. Dissipation also induces a constant offset of τ which is larger than any of the periodic terms. Solar influences decrease the constant coefficient by 0.2%. The derivative of **I** plays only a minor role for longitude librations because it favors fast terms, while the solution of the differential equation favors slow terms.

The mean lunar orbit plane is inclined 5.145° to the ecliptic plane. The resulting ecliptic latitude motion of the Moon depends on the angle measured from the node, with period 27.212 days, and the polynomial representation of the angle is denoted F ($=L-\Omega$ or mean argument of latitude). The leading term for ecliptic latitude is $5.13° \sin F$, and this gives the strongest forcing term for the lunar pole. Additional forcing terms which depend on the mean anomaly result from the radial variation and the variation in orbit longitude. Consequently, forcing terms proportional to e sin i have arguments $F+\ell$ (1/2 month period) and $F-\ell$ (2190 days = 6.0 years). The strongest forcing functions for rigid or deformed motion of the lunar pole have arguments F, $F-\ell$, and $F+\ell$.

The influence of deformation on the pole direction, the latitude physical librations, is calculated using two orientation parameters. The p_1 and p_2 parameters are the x and y coordinates of the ecliptic pole, respectively, using the lunar principal axis frame:

$$p_1 = -\sin\theta\ \sin\varphi , \qquad (18a)$$

$$p_2 = -\sin\theta\ \cos\varphi . \qquad (18b)$$

The differential equations for p_1 and p_2 are coupled together [see *Eckhardt*, 1981]. The linear approximation to (13) comes from taking ω_3 constant, expressing the first two angular velocity components as functions of p_1 and p_2 and their derivatives, and extracting a linear term in p_1 from the rigid-body torque term (second component):

$$A (\ddot{p}_2 + n(1-\alpha)\dot{p}_1 + \alpha n^2 p_2) + \dot{I}_{13}\, n = f_x , \qquad (19a)$$

$$B (-\ddot{p}_1 + n(1-\beta)\dot{p}_2 - 4\beta n^2 p_1) + \dot{I}_{23}\, n = f_y . \qquad (19b)$$

The forcing functions about the x and y axes have been multiplied by the cosine of the equator's 1.54° tilt to the ecliptic plane to give f_x and f_y, respectively. Resonance frequencies are 27.29638 days and 74.63 years (Williams et al., 2001). The rigid or deformed forcing terms at 27.212 days (F) and 6 years ($F-\ell$) cause significant responses in the pole direction, but the 1/2 month response is weak. The first three terms on the right-hand side of (13) are important for the pole. The derivative of **I** plays a major role for the F term. The Sun increases the F term magnitude by 0.3%.

For the linear part of the rotational dissipation solution, six elements U_{ij} are considered for each of the constant plus 52 periodicities of the Earth-induced torque/tide functions. These include the largest functions plus smaller periodicities selected to give longer periods or near resonant terms. To these are added the Sun-induced functions for the constant and 13 periodicities plus the larger spin terms. The appropriate combination of elements for the right-hand side of (13) and the moment rate on the left-hand side are computed for 52 (constant times periodic) plus $2\text{x}52^2$ (periodic times periodic, giving sum and difference frequencies) combinations. Rotational coefficients are retained above a threshold size.

In addition to the first-order solution, selected nonlinear corrections from the rigid-body torques are added as second- and third-order corrections. This has the effect of increasing the τ constant by 3% and increasing the magnitude of the F coefficients for the pole by 2%. The pole response at 6 years is made larger.

5. Tidal and Rotational Dissipation: Series Solution

This section presents and discusses the lunar physical libration series solution for tidal and spin dissipation. Comparisons are made with the previous computations of *Yoder* [1979] and *Eckhardt* [1981].

Table 1. Longitude Libration Tidal and Spin Dissipation Terms are Given as a Function of Deformation Q Parameters[a]

Argument	Period,	Coefficients for Deformation Q Parameters																		
		$2D+\ell$	$2F$	$F+\ell$	2ℓ	$2D$	$\ell+\ell'$	$2F-\ell$	F	ℓ	$2\ell-F$	$3\ell-2F$	D	$\ell-\ell'$	$2D-\ell$	$2\ell-2D$	ℓ'	$\ell-D$	$2F-2\ell$	$F-\ell$
		9.6	13.6	13.7	13.8	14.8	25.6	26.9	27.2	27.6	27.9	28.3	29.5	29.8	31.8	206	365	412	1095	2190
	days	"	"	"	"	"	"	"	"	"	"	"	"	"	"	"	"	"	"	"
0	∞	0.5	−0.3	1.9	5.5	7.6			8.4	305.4					10.8					−0.2
ℓ	27.55									−1.1										
$2D-\ell$	31.81														−0.3					
$2\ell-2D$	205.89				−0.3	−0.3				−2.2					−2.3	0.9				
ℓ'	365.26						0.4							−0.4			8.5			
$\ell-D$	411.78									0.3			0.3					−0.3		
$2F-2\ell$	1095.18		−0.5		−0.5			−14.9	−5.9	−14.8	−5.3	−0.3							17.9	
$F-\ell-79°$	2190.35																			−0.8

[a]Each libration term is the product of a cosine of the argument at the left, with its period in days, times the sum of the coefficients (in arcseconds) to the right. Each coefficient is multiplied by the Love number k_2 and divided by the Q for the deformation period (days) and deformation argument at the top.

The arguments of the series solution depend on polynomial expressions for four angles. The polynomials are denoted ℓ for lunar mean anomaly (period 27.555 days), ℓ' for the mean anomaly of the Earth-Moon center of mass about the Sun (1 year), F for argument of latitude (27.212 days), and D for mean elongation of the Moon from the Sun (29.531 days). Also useful is the polynomial for the lunar orbit node Ω measured from the precessing equinox. It is also convenient to use L and L' for the polynomial expressions for the mean longitudes of the Moon and Sun, respectively, both measured from the precessing equinox, where $L = F + \Omega$ and $D = L - L'$.

By subtracting the uniform rotation and precession motion from the Euler angles, there results a set of small libration parameters τ, ρ, and σ. For the ecliptic definition of Euler angles (section 2) the conversions between Euler angles and the libration parameters are $\psi = \Omega + \sigma$, $\theta = I + \rho$, and $\varphi = F + 180° + \tau - \sigma$. Equations (18a) and (18b) provide the connection to p_1 and p_2. The angle I (not to be confused with the moment of inertia) is the 1.54° mean tilt of the precessing equator to the ecliptic plane. The product $I\sigma$ is convenient because it is comparable in size to ρ and τ.

The analytical dissipation series for the longitude libration (τ) is tabulated in Table 1, and the latitude librations (p_1 and p_2) are in Table 2. Coefficients down to 0.2 are presented (a borderline 188 day term was not included in Table 2). In Table 1 the 6 year term with phase is orthogonal to the rigid-body term owing to third-degree harmonics. The amplitude of each periodic term in the rotation depends on one or more of the Q parameters for the deformation frequencies. For example, in arcseconds the monthly p_1 term in Table 2 is

$$k_2 \left(\frac{217.4}{Q_F} + \frac{8.0}{Q_\ell} + \frac{4.7}{Q_{F+\ell}} + \frac{1.8}{Q_{2F}} + \frac{0.7}{Q_{F-\ell}} + \cdots \right) \cos F. \quad (20)$$

The coefficient is dominated by the Q for the 27.212 day month (north-south motion), but the Q for deformation at the 27.555 day anomalistic month and the Q at 1/2 month contribute a few percent. Most of the p_1 and p_2 coefficients for argument F are equivalent to a constant, negative shift of the equator's precessing node. The constant $I\sigma$ shift is given in arcseconds by

$$I\sigma_{\text{const}} = k_2 \left(-\frac{216.4}{Q_F} + \frac{0.2}{Q_\ell} - \frac{4.7}{Q_{F+\ell}} - \frac{1.8}{Q_{2F}} - \frac{0.7}{Q_{F-\ell}} + \cdots \right). \quad (21)$$

Compared to the monthly p_1 and p_2 coefficients, the Q_ℓ dependence has virtually disappeared, and the sensitivity to the three principal frequencies of latitude forcing remains. In

Table 2. Latitude Libration Tidal and Spin Dissipation Terms[a]

Argument	Period,	Libration	Function	Coefficient for Each Deformation Q						
				$2F$	$F+\ell$	$2D$	F	ℓ	$2D-\ell$	$F-\ell$
				13.6	13.7	14.8	27.2	27.6	31.8	2190
	days			"	"	"	"	"	"	"
F	27.212	p_1	cos	1.8	4.7	0.3	217.4	8.0	0.3	0.7
F	27.212	p_2	sin	−1.8	−4.7	−0.3	−216.0	−8.0	−0.3	−0.7
$F-\ell$	2190.350	p_1	cos		−0.2		−6.9	−5.8		−1.9
$F-\ell$	2190.350	p_2	sin		0.3		8.3	7.5		2.6
$2F$	13.606	$I\sigma$	cos				−1.1			
$2F$	13.606	ρ	sin				1.1			
$2F-\ell$	26.877	$I\sigma$	cos				0.3	−0.8		−0.3
$2F-\ell$	26.877	ρ	sin				−0.3	0.8		0.3
ℓ	27.555	$I\sigma$	cos				3.7	6.5		2.3
ℓ	27.555	ρ	sin				−3.6	−6.5		−2.3
0	∞	$I\sigma$	1	−1.8	−4.7		−216.4			−0.7

[a]Latitude libration parameters are p_1 and p_2 and, equivalently, ρ and $I\sigma$. Each libration term is the specified trigonometric function of the argument at the left (with its period) times the sum of the coefficients to the right. Each coefficient is multiplied by the Love number k_2 and divided by the Q for the deformation period (in days) and associated argument at the top.

addition to the p_1 and p_2 parameters in Table 2, an approximate conversion to ρ and $I\sigma$ is given. The latter pair is less complete since it omits some smaller combinations including differently phased mixes with F and Ω.

The physical libration p_1 is approximately the tilt of the lunar pole away from the Earth, and the monthly term is the largest observable dissipation periodicity. (The constant in longitude libration is not directly measurable since a change is compensated by a shift of reflector longitude coordinates during a solution.) The 27.212 day periodicity is the dissipation signature that has been seen by LLR for 2 decades. With Q proportional to 1/frequency and the DE403 value of $k_2/Q = 0.030/25.9 = 1.16\text{x}10^{-3}$, the coefficient of the p_1 term is 0.276". Since the coefficient in (20) is dominated by the monthly Q_F, the Q determined by the DE403 fit of LLR data to a time-delay tidal dissipation model effectively corresponds to a monthly period of 27.212 days. A different dependence of Q on frequency will change the Q inferred from observations by only a few percent. The $I\sigma$ shift is –0.265", and the node shift is –9.8".

For the DE403 value of k_2/Q a unit value in Tables 1 and 2 corresponds to a rotational displacement of 9.7 mm at the lunar radius. It is interesting to compare the tidal sensitivities for periodic rotation terms in the tables with tide heights. For the largest tides of ~0.1 m, with arguments ℓ and F, the Q_ℓ and Q_F are well represented among major rotation terms. Of the tides from 1 cm to several centimeters, namely, $2D-\ell$, $2D$, 2ℓ, $F+\ell$, the latter is most important in the rotation. Of the many tides from 1 mm to several millimeters, the rotation is sensitive to Q parameters for $F-\ell$, ℓ', $2\ell-2D$. The $2F-2\ell$ tide is only ~0.1 mm but is selected by the near resonant period. The phase-shifted part of the tide height is proportional to $1/Q$. So the larger sensitivities in Tables 1 and 2 correspond to phase-shifted tidal displacements of a few millimeters down to a few micrometers. For selected tidal frequencies the influence on the rotation exceeds the tide height in size.

The dissipation terms have been evaluated for two dependences of Q on frequency using the expressions in Tables 1 and 2 augmented with smaller coefficients. Table 3 evaluates the coefficients for Q independent of frequency, and Table 4 uses Q proportional to F/frequency. The latter corresponds to the time delay tidal model used for the numerical integration of the rotation. For the 6 year longitude term, only the cosine component is shown, but most of that term is in the sine component (see Table 1). Most noteworthy are the monthly and 6 year terms for (p_1 and p_2) latitude librations and the 3 year, 1 year, and 206 day terms for longitude libration. The most interesting terms for testing frequency dependence of Q are the 3 year and annual terms in longitude libration. Table 1 shows that the annual term is sensitive to the annual tidal Q, while the 3 year term is most sensitive to monthly Q and 3 year tidal Q. The series of Tables 1-4 scale inversely with C/mR^2, here taken as 0.3932 with an uncertainty of 0.0002 [*Konopliv et al.*, 1998].

Table 3 can be compared with *Eckhardt*'s [1981] computations, and Table 4 can be compared with *Yoder* [1979]. For the constant in longitude, Eckhardt (multiply his tabulated differences by –2000) gave 342, and Yoder gave 350.4. Eckhardt's values should be ~1/2% larger owing to his smaller value of C/mR^2, so the constant term here is slightly less than the two published calculations. For the 3 year longitude term, Eckhardt has –24, in good agreement with Table 3. Yoder's value for this near-resonant term is off by an order of magnitude. For the 206 day term, Yoder has the right magnitude (5.0), but the reversed sign, while for the difference between the annual terms of Tables 3 and 4 he gives 8.4. Eckhardt does not give terms smaller than 10. For the large term in latitude libration, Eckhardt gives 210 and –208 for the monthly p_1 and p_2 coefficients, respectively, and –208 for the Iσ constant. Compared with Table 3, his monthly magnitudes are 10% smaller and the $I\sigma$ magnitude is 7% smaller. The magnitude of the $I\sigma$ constant should be less (τ_{const} sin $I = 9$) than the average of the two monthly magnitudes, so there is a 4% internal inconsistency in Eckhardt. Yoder defines his latitude results as though a rotation of the ρ and $I\sigma$ variables, and the 229.6 value for the latter parameter (there is a sign ambiguity due to an apparently misplaced π in his definitions) is a good match with Table 4. The second term in latitude librations is elliptical in p_1 and p_2 and splits into ℓ and $2F-\ell$ terms in $I\sigma$ and ρ. Eckhardt gives –14 for p_1 and 20 for p_2, in reasonable agreement with Table 3, while

Table 3. Evaluation of the Coefficients of the Physical Libration Theory for Tidal Dissipation Using Q Independent of Frequency[a]

Argument	Period, days	τ cos, "	p_1 cos, "	p_2 sin, "	$I\sigma$ cos, "	ρ sin, "
0	∞	339.95			–223.88	
F	27.21		233.73	–232.41		
$F-\ell$	2190.35	–0.14	–15.02	18.96		
ℓ	27.56	–1.12			12.81	–12.75
$2\ell-2D$	205.89	–4.14			–0.11	
ℓ'	365.26	8.20			0.22	
$2\ell-F$	27.91		–0.01	0.03		
$2F-2\ell$	1095.18	–24.30			–0.61	–0.02
$\ell-D$	411.78	0.36			0.01	
$F+\ell-2D$	188.20		–0.34	0.46		
$2D-\ell$	31.81	–0.39			0.39	–0.40
$2D-F$	32.28		–0.16	0.22		
$2F-2D$	173.31	0.19			0.19	–0.19
$F+\Omega-81°$	27.32		–0.18	0.18		
81°–Ω	6798.38				0.18	–0.18
$2F-\ell$	26.88				–0.94	0.92
$2F$	13.61				–1.19	1.13
2ℓ	13.78	–0.03			0.30	–0.15

[a]Each coefficient (units arcseconds) should be multiplied by k_2/Q.

Table 4. Evaluation of the Coefficients of the Physical Libration Theory for Tidal Dissipation Using $Q = Q_F \dot{F}$ / Frequency[a]

Argument	Period, days	τ cos, "	p_1 cos, "	p_2 sin, "	$I\sigma$ cos, "	ρ sin, "
0	∞	349.30			−230.20	
F	27.21		240.30	−238.98		
$F-\ell$	2190.35		−13.39	16.86		
ℓ	27.56	−1.13			10.83	−10.76
$2\ell-2D$	205.89	−5.03			−0.14	
ℓ'	365.26	0.34			0.01	
$2\ell-F$	27.91		−0.21	0.23		
$2F-2\ell$	1095.18	−43.31			−0.93	−0.22
$\ell-D$	411.78	0.64			0.02	
$F+\ell-2D$	188.20		−0.31	0.44		
$2D-\ell$	31.81	−0.38			0.36	−0.37
$2D-F$	32.28		−0.18	0.26		
$2F-2D$	173.31	0.10			0.22	−0.22
$F+\Omega-81°$	27.32		−0.18	0.18		
$81°-\Omega$	6798.38				0.18	−0.18
$2F-\ell$	26.88				−0.68	0.66
$2F$	13.61				−1.19	1.14
2ℓ	13.78	−0.06			0.26	−0.12

[a]Each coefficient should be multiplied by k_2/Q_F. Units are arcseconds.

Yoder gives 12.5 by 15.2, which is similar to Table 4's entries. The numerical results of *Bois and Journet* [1993] are much smaller than the analytical results and are in error.

The most important dissipation terms are at monthly, 206 day, annual, 3 year, and 6 year periods. The series of this section will be used for interpretation of LLR data fits (section 18).

6. Average Values and Definitions

Section 3 pointed out that the tidal deformation of (7) and the spin deformation of (9) have constant parts. With deformations, the "rigid-body" moments of inertia of (5) are not the time-averaged moments. Since the second-degree harmonics J_2 and C_{22} depend on the moments, careful definitions must be given. The rigid-body moments A, B, and C are used to define $\alpha=(C-B)/A$, $\beta=(C-A)/B$, and $\gamma=(B-A)/C$. J_2 is taken as an independent parameter, while C_{22} and C/mR^2 are derived parameters:

$$C_{22\,\mathrm{rigid}} = \frac{J_{2\,\mathrm{rigid}}\ \gamma\ (1+\beta)}{2\,(2\beta-\gamma+\beta\gamma)}, \tag{22}$$

$$\frac{C}{mR^2} = \frac{4\,C_{22\,\mathrm{rigid}}}{\gamma}. \tag{23}$$

The constant part of the functions $(a/r)^3\, u_i\, u_j$ and $\omega_i\, \omega_j\, /\, n^2$ are used to compute the averages. For accurate time-averaged values of the moments normalized by mR^2 and the second-degree harmonics, add the corrections from the appropriate columns of Table 5 to the rigid-body values. There are very small tidal contributions to the off-diagonal moments, and two second-degree harmonics because two of the principal axes are not quite aligned with the mean Earth and mean spin directions. The principal axes of the rigid body and average deformed body do not quite match.

In the JPL LLR software, β, γ, k_2, and J_2 are the independent parameters, while C_{22} and C/mR^2 are derived. In the numerical integrator the mean spin values have been virtually nulled out of I_{spin}, which forces the mean spin effects into the "rigid-body" quantities. Only the average tidal contributions from the Earth (no Sun) should be added to rigid-body quantities to get averages. Thus the LLR-derived values of β and γ reported in this and past JPL papers depend on the rigid-body part without mean tides. *Ferrari et al.* [1980] gave expressions to link values of J_2 and C_{22} which include average Earth-raised tides with k_2 and rigid values of β, γ, and C/mR^2. Those expressions were used to report numerical values there and by *Dickey et al.* [1994]. The original rationale was that spacecraft-derived harmonics were generated without a tidal or spin deformation model, while LLR analyses did use a tidal model and a nulled average spin deformation. Tidal models are now used to analyze spacecraft data [*Lemoine et al.*, 1997; A. S. Konopliv, private communication, 1996] as well as LLR data. Table 5 can be used to recover average values for a variety of definitions.

A fluid or strengthless Moon would relax to the shape of the tidal plus synchronously rotating spin potential. To calculate the equilibrium moment differences or second-degree gravitational harmonics for the Moon, the fluid Love number $k_f = 1.44$ is appropriate rather than the smaller quantity from elastic theory. Such a calculation shows that J_2 is 22 times larger, β is 17 times larger, and γ and C_{22} are 8 times larger than the equilibrium figure for the present distance. The Moon is strong enough to support the stress elastically. It is appealing to conjecture that the tidal plus spin figure was frozen into an earlier Moon closer to the Earth [*Jeffreys*, 1915, 1937; *Kopal*, 1969; *Lambeck and Pullan*, 1980]. The spread of factors from 8 to 22, corresponding to distances of 0.50 to 0.36 times the present Moon, does not make it easy to embrace the hypothesis. Lambeck and Pullan invoke noise in the gravity field, the spectrum of power in the higher-degree field extrapolated to second degree, to explain the spread. Here the spectrum of *Konopliv et al.* [1998] is adopted for the extrapolation, and a linear combination, which would be zero for an equilibrium figure, is formed. The linear combination of harmonics is $J_2 - 10\,C_{22}/3 = (1.3\pm1.1)\times10^{-4}$, or the equivalent expression $\beta - 4\gamma/3 = (3.3\pm2.7)\times10^{-4}$, and the departure from

Table 5. Mean Values of Deformations for Moments and Harmonics[a]

Parameter	Rigid	Tide by Earth	Tide by Sun	Oblate Spin	Spherical Spin
I_{11}/mR^2	A/mR^2	-4.935×10^{-6}	-7×10^{-9}	-0.843×10^{-6}	2.529×10^{-6}
I_{22}/mR^2	B/mR^2	2.469×10^{-6}	-7×10^{-9}	-0.843×10^{-6}	2.529×10^{-6}
I_{33}/mR^2	C/mR^2	2.466×10^{-6}	1.4×10^{-8}	1.686×10^{-6}	2.529×10^{-6}
I_{12}/mR^2	0	2.3×10^{-9}	0	0	0
I_{13}/mR^2	0	-2.8×10^{-9}	0	0	0
I_{23}/mR^2	0	0	0	0	0
J_2	$J_{2\ \mathrm{rigid}}$	3.698×10^{-6}	2.1×10^{-8}	2.529×10^{-6}	0
C_{21}	0	2.8×10^{-9}	0	0	0
S_{21}	0	0	0	0	0
C_{22}	$C_{22\ \mathrm{rigid}}$	1.851×10^{-6}	0	0	0
S_{22}	0	-1.2×10^{-9}	0	0	0

[a]The tidal and spin deformations of the moments of inertia and the second-degree harmonics have mean values (columns 3–6). The symbol (or zero value) for the rigid-body quantity is given in the second column. The numerical values in columns 3–5 should be multiplied by the Love number k_2. The last column should be multiplied by s.

equilibrium is comparable to the extrapolated power. The frozen figure hypothesis is viable.

7. Frequency Shifts and Damping From Deformation

The forced lunar physical librations have three resonances: one in longitude libration and two for pole direction. The resonance periods are the same as the periods of the three free libration modes. The free librations are analogous to the solutions of the reduced equations for linear differential equations, and the unpredictable amplitude and phase must be established by observation. See Williams et al. (2001) for a study of free librations. Elastic deformation will shift the resonance periods from the rigid-body values, and dissipation will damp the free librations in addition to causing the forced terms of sections 4 and 5.

Elastic deformation without dissipation does not contribute forced terms from the right-hand side of (13). It does influence the rotation through the derivative of $\mathbf{I}$ in the $\mathbf{I\omega}$ term. The largest modification comes from the i=1, j=3 tidal term in (7). The u_3 component is a function of p_1, and its derivative is introduced into the differential equations. The square of the monthly resonance frequency for pole direction (precession/nutation mode) in the rotating frame is modified to

$$\nu_p^2 = n^2 [\, 1 - \frac{\dot{\Omega}}{n} \sin^2 I + 3 (S_1 \alpha + S_2 \beta') + k_2 \zeta \cos I \,], \quad (24)$$

where S_2=0.9778, S_1=0.0018, and $\beta'=629.978\times10^{-6}$ is a modification of β to include effects of third-degree harmonics (see Williams et al., 2001). The tidal part depends on the combination

$$\zeta = \frac{m R^2}{C} \frac{M}{m} \left(\frac{R}{a}\right)^3 = 1.91\times10^{-5}. \quad (25)$$

For the DE403 k_2 value, the tidal part shortens the monthly resonance period by 8×10^{-6} day. The equivalent 81 year period in the nonrotating frame is shortened by 9 days, and the 24 year period in the 18.6 year precessing frame is lengthened by 0.8 day. Other elastic effects on the three resonance frequencies multiply α, β, or γ and so are less important than the contribution in (24). While elasticity causes a dramatic increase in the wobble period for the Earth, this, as *Peale* [1973] realized, is not the case for the Moon.

The free libration in longitude has a 1056 day period (Williams et al., 2001). A variation of τ causes an east-west motion of the tidal bulge, and a delayed response in the bulge causes damping from the tidal torque term. A linear term for τ comes through u_2 in (14) and this is the source of most of the damping in (17). For damping like exp(–Dt) the damping time is 1/D. The damping for the longitude mode is

$$D_L = 0.497 \sqrt{\frac{3}{\gamma'}}\, n \zeta \frac{k_2}{Q_L}, \quad (26a)$$

$$D_L = 0.091 \frac{k_2}{Q_L} \ \mathrm{yr}^{-1}. \quad (26b)$$

The Q_L is at the 1056 day period, and γ', with value 228.6×10^{-6}, is a modification of γ for third-degree harmonics (Williams et al., 2001). The expression (26a) is similar to that given by *Eckhardt* [1993], and (26b) is 4% different from the numerical expression of *Peale* [1976].

The motion of the pole direction moves the tidal bulge in a north-south direction. The tidal torque term (first on right-hand side of (13)) is the main influence on damping the 27.296 day monthly mode. Terms from the derivative of the moment and the spin acting on the tidal bulge (third term) cancel. The spin on spin and torque on spin bulge terms are ineffective because the spin axis stays near the principal axis for the monthly mode. The damping is given by

$$D_p = 1.47 \zeta n \frac{k_2}{Q_p}, \quad (27a)$$

$$D_p = 2.35\times10^{-3} \frac{k_2}{Q_p} \ \mathrm{yr}^{-1}. \quad (27b)$$

The Q is at 1 month (27.296 days). The agreement with Peale's numerical value is excellent. For the DE403 value of k_2/Q the damping time is 3.67×10^5 years.

For the wobble mode the spin axis is displaced from the principal axis. The bulges from tides and spin are both effective

in damping the 74.6 year wobble. The expression for the damping of the elliptical wobble depends on the ratio E (=2.474) of the axis of the ellipse, where $E^2 = (\beta + 3S_2 \beta') / \alpha$.

$$D_w = \left(\frac{2.62}{E} + 0.168\, E \right) \zeta\, n\, \frac{k_2}{Q_w}. \qquad (28a)$$

$$D_w = 1.47\, \zeta\, n\, \frac{k_2}{Q_w}. \qquad (28b)$$

$$D_w = 2.36 \times 10^{-3}\, \frac{k_2}{Q_w} \quad \mathrm{yr}^{-1}. \qquad (28c)$$

The wobble Q is at 74.6 years. The numerical expression is 17% different from Peale's. The similarity of numerical coefficients for the damping of the two pole modes is coincidence.

Fits of the LLR data will be used to estimate Q as a function of frequency (section 18). Damping times will then be calculated (section 20).

8. Orbit Perturbations From Tidal Dissipation

The tidal and spin deformations not only affect the lunar rotation but also perturb the orbit. There are both elastic and dissipation effects, but only the latter are considered in this section. Dissipation causes the exchange of energy and angular momentum between the rotation and orbit. This section first presents the potentials for deformations and then gives numerical and analytical expressions for secular orbit changes.

An external body raises tides on the Moon, and those tides generate forces on the tide-raising and any other external bodies. The tidal distortion from a tide-raising body (denoted by *) has a potential energy at an external body of

$$V_{tide} = k_2\, G\, M\, M^*\, \frac{R^5}{r^3\, r^{*3}}\, P_2(\mathbf{u}\cdot\mathbf{u}^*). \qquad (29)$$

The potential energy at the external body from second-degree spin distortion is

$$V_{spin} = -k_2\, M\, \omega^{*2}\, \frac{R^5}{3\, r^3}\, P_2(\mathbf{u}\cdot\hat{\boldsymbol{\omega}}^*). \qquad (30)$$

P_2 is the second Legendre polynomial, and $\hat{\boldsymbol{\omega}}$ is the unit spin vector. The remaining notation is as before. For dissipation the phase-shifted or time-delayed variables (except M) indicated with an asterisk are displaced as seen from the frame of the rotating body. To calculate forces, the positive gradients of (29) and (30) are taken with respect to the position coordinates without an asterisk (sign convention for the point mass potential is plus). Along the Earth-Moon line the acceleration is inward toward the Moon.

A rotating frame is natural for computing time-delayed lunar deformation. Both the orbit motion and rotation are time delayed. For orbit computations it can be convenient to expand the vector and scalar radius through first order in the time delay Δt using a space-fixed frame

$$\mathbf{r}^* \approx \mathbf{r} - (\dot{\mathbf{r}} - \boldsymbol{\omega} \times \mathbf{r})\, \Delta t, \qquad (31a)$$

$$r^* \approx r - \dot{r}\, \Delta t. \qquad (31b)$$

The expression in parentheses is the conversion from space- to body-referenced velocity.

As seen from the rotating Moon, the Earth's angular and distance variations cause tides. Here secular orbit changes from energy and angular momentum exchange are considered. The orbit is perturbed in two ways by the deformations: directly from the forces calculated from the gradients of (29) and (30) and from forces due to the rigid figure of the Moon through the rotational displacements of its principal axes. To compute the power going into the orbit, calculate $\dot{\mathbf{r}}\cdot\nabla V$, where V is the sum of the rigid figure, tide, and spin potentials. With manipulation the equation for power is derived.

$$\dot{\mathbf{r}} \cdot \nabla V = \frac{dV}{dt} - \boldsymbol{\omega} \cdot \frac{d(\mathbf{I}\boldsymbol{\omega})}{dt}. \qquad (32)$$

Since the Euler equation (1) permits the derivative of the angular momentum to be replaced with the torque, this equation may seem self-evident, but the right-hand side is evaluated in the frame rotating with the Moon, which is computationally convenient, and the left-hand side is in the nonrotating frame, as needed for orbit perturbations. For the time derivative of V one differentiates the $\mathbf{u}$ and $\mathbf{r}$ variables but not the parameters with an asterisk. Simplifications can be made. Owing to the synchronous rotation, the power flowing into the rotation rate is only $C/ma^2 \approx 10^{-5}$ of the dissipated power, so the spin potential and the second term on the right-hand side can be ignored. The trigonometric series for $U_{ij} = u_i\, u_j\, (a/r)^3$ were developed for the computations of section 4, and these series appear in the rigid figure and tide potentials. The rigid figure potential is linear in the U_{ij}, and its time derivative gives periodic terms, but the tidal potential contains products $U_{ij}\, U^*_{ij}$, and its derivative contains periodic and secular terms. For Earth-raised tides acting back on the Earth the average power, P_{ave}, depends on the tidal potential through the constant part of

$$P_{ave} = \frac{k_2\, G\, M^2}{2\, a} \left(\frac{R}{a} \right)^5 \left(3 \sum_{ij} \dot{U}_{ij}\, U^*_{ij} - \sum_i \dot{U}_{ii} \sum_j U^*_{jj} \right). \qquad (33)$$

This power is drawn from the lunar orbit and dissipated in the Moon. The average power depends on squared tidal amplitudes times the frequency. Note that $\sum U_{ii} = (a/r)^3$. The average power from solar tides is three orders of magnitude smaller than the power from Earth-raised tides.

The power is related to the semimajor axis change through the derivative of the total energy $-GMm/2a$. The secular semimajor axis and mean motion changes ($3\Delta\dot{a}/a = -2\Delta\dot{n}/n$) are given in Table 6. The dependence on each tidal Q is explicit. In calculating the table, power is converted to semimajor axis change using a mean semimajor axis, rather than an osculating one. To convert $\Delta\dot{a}$ in mm yr^{-1} to average power in ergs yr^{-1}, multiply by 0.99×10^{24}.

For dissipative effects the torques on the lunar rotation and orbit, due to displaced second-degree figure and deformation, are equal in magnitude and opposite in sign (there are ignored figure-figure effects which are effectively fourth degree). About the polar axis the constant part of the torque due to tides is balanced against the constant part due to the rigid figure being displaced by tides. The average torque about the polar axis is zero. The tide-caused displacement of the pole direction is a dynamical rather than static response, and the sum of torques about the body y axis is not zero. This time-varying torque has a constant component projected along the line of the equator/ecliptic intersection. This component causes the Moon's equator to precess, but the dissipation-induced shift in the direction of the constant torque by σ from the orbit node on the ecliptic (section 5) causes secular orbit perturbations. Since the torque vector does not quite lie in the orbit plane, the orbital angular momentum is perturbed, and since it is not quite aligned with the

Table 6. Secular Orbit Changes From Periodic Tides[a]

Argument	Period, days	$\Delta\dot{n}$, " cent^{-2}	$\Delta\dot{a}$, mm yr^{-1}	$\Delta\dot{p}$, mm yr^{-1}	$\Delta\dot{e}$, 10^{-11} yr^{-1}	$\Delta\frac{di}{dt}$, μas yr^{-1}	$\Delta\ddot{\varpi}$, " cent^{-2}	$\Delta\ddot{\Omega}$, " cent^{-2}
ℓ	27.555	205	−302	−4	−705	15	−1.71	2.36
F	27.212	136	−201	−201	2	−601	−0.89	0.34
$2D-\ell$	31.812	6	−10	0	−22	0	−0.06	0.08
$2D$	14.765	10	−14	0	−33	0	−0.08	0.11
2ℓ	13.777	7	−10	0	−23	0	−0.05	0.08
$F+\ell$	13.691	6	−9	−4	−10	−13	−0.04	0.04
$2F$	13.606	1	−2	−2	0	−5	−0.01	0
$F-\ell$	2190.350	0	0	−1	2	−2	0	0
$2D+\ell$	9.614	1	−1	0	−3	0	−0.01	0.01
Sum for constant Q		373	−550	−212	−795	−606	−2.86	3.02
Sum for Q~1/frequency		394	−580	−218	−854	−623	−3.02	3.22

[a]Tidal argument and period are at left. The remaining columns are to be multiplied by k_2/Q, with Q appropriate to the tidal frequency. The last two lines give the sum of terms for Q constant and Q proportional to inverse frequency (multiply last line by k_2/Q_F).

node, the inclination is perturbed. The angular momentum component normal to the ecliptic plane is preserved.

For angular momentum exchange between rotation and orbit the torque $\mathbf{r}\times\nabla V$ is required. In section 4 the tidal torques were developed for physical libration calculations but must be rotated from body-referenced coordinates into the orbit frame. For the computations of Table 6 the total orbital angular momentum is proportional to the square root of the semilatus rectum $p=a(1-e^2)$, and the torque normal to the orbit plane gives the change in p. The eccentricity rate comes from the change in p and a. The torque component in the orbit plane directed 90° from the node gives the secular orbit inclination rate.

There are indirect effects of the above a, e, and i rates which cause the perigee and node precession rates to change. The solar-induced precession rates depend strongly on the mean motion and more weakly on eccentricity and inclination. Like the mean longitude, the node and perigee angles experience tidal accelerations. The partial derivatives of the longitude of perigee (ϖ) and node (Ω) precession rates [*Chapront-Touzé and Chapront,* 1988], with the tabulated tidal rates for a, e, and i, give the accelerations $\ddot{\varpi}$ and $\ddot{\Omega}$ in Table 6.

The model for the DE403 integration is based on tidal dissipation, but no core. The DE403 solution effectively sets a limit to the tidal contribution: $\Delta\dot{n}$ = 0.46 " cent^{-2} and $\Delta\dot{a}$ = −0.67 mm yr^{-1}. Additional rates are $\Delta\dot{p}$ = −0.25 mm yr^{-1}, $\Delta\dot{e}$ = −0.99x10^{-11} yr^{-1}, and $\Delta di/dt$ = −0.72 μas yr^{-1}. The accelerations are $\Delta\ddot{\varpi}$ = −0.0035 and $\Delta\ddot{\Omega}$ = 0.0037 " cent^{-2}. The inclination rate and the last two accelerations are too small to detect with the present data set. The secular acceleration $\Delta\dot{n}$ is positive. Tides on the Earth cause a negative secular acceleration of −26 " cent^{-2}. Tidal dissipation in the Moon contributes <2% of the total tidal secular acceleration. The above eccentricity rate is 70% of that from the Earth. The product $a\Delta\dot{e}$ = −3.8 mm yr^{-1}. With the above $\Delta\dot{a}$, lunar tides cause the perigee to increase 3.2 mm yr^{-1} and the apogee to decrease 4.5 mm yr^{-1}. These changes, along with the secular acceleration, are large enough to detect with the Lunar Laser data analysis, but other masking influences on these rates must be considered (see section 16).

Analytical approximations for the orbit changes are useful, e.g., for evolutionary calculations. For the effects due to the displaced figure axes the dissipation-induced constant τ and $I\sigma$ terms are needed. Analytical approximations are

$$\Delta\tau = \frac{k_2}{Q}\frac{M}{m}\frac{mR^2}{C}\left(\frac{R}{a}\right)^3\left[\frac{6e^2}{\gamma}+\frac{\sin(i+I)\,\sin I}{2\beta}\right], \quad (34a)$$

$$\Delta I\sigma = -\frac{k_2}{Q}\frac{M}{m}\frac{mR^2}{C}\left(\frac{R}{a}\right)^3\frac{\sin(i+I)\,\sin I}{\beta\sin i}. \quad (34b)$$

The Q is for a 1 month tidal period.

The analytical approximations correspond to the ℓ and F tides in Table 6. The leading terms in the U_{ij} series are $U_{11}\approx 1+3e\cos\ell$, $U_{12}\approx 2e\sin\ell$, and $U_{13}\approx\sin(i+I)\sin F$. These may be used with the power equation (33) and converted to the secular acceleration in orbital mean longitude $\Delta\dot{n}$:

$$\Delta\dot{n} = \frac{9}{2}\frac{k_2}{Q}\frac{M}{m}\left(\frac{R}{a}\right)^5 n^2\,[\,7e^2+\sin^2(i+I)\,]. \quad (35)$$

The orbit eccentricity is e (0.0549), the semimajor axis is a (384,399 km), and the mean motion is n (13.3685 rev yr^{-1}). The inclinations of the orbit and equator planes to the ecliptic plane are i = 5.145° and I = 1.543°, respectively. The numerical evaluation 348 k_2/Q " cent^{-2} may be compared with Table 6. The semimajor axis perturbation follows from $\Delta\dot{a} = -2a\,\Delta\dot{n}/3n$. The numerical evaluation is $\Delta\dot{a}$ = −515 k_2/Q mm yr^{-1}.

Analytical approximations for eccentricity and inclination rates follow from angular momentum transfer as before:

$$\Delta\dot{e} = -\frac{21}{2}\frac{k_2}{Q}\frac{M}{m}\left(\frac{R}{a}\right)^5 n\,e, \quad (36)$$

$$\frac{di}{dt} = -\frac{3}{2}\frac{k_2}{Q_F}\frac{M}{m}\left(\frac{R}{a}\right)^5 n\,\frac{\sin^2(i+I)}{\sin i}. \quad (37)$$

The Q is for a month. The numerical evaluations are $\Delta\dot{e}$ = −7.4x10^{-9} k_2/Q yr^{-1} and di/dt = −6.0x10^{-4} k_2/Q_F " yr^{-1}.

Lunar tidal dissipation extracts energy from the orbit and deposits it in the Moon. Angular momentum from the orbit keeps the lunar pole direction offset but does not change the spin rate (apart from the small secular acceleration $\Delta\dot{n}$). This is quite different from the Earth, where the spin energy and angular momentum power the orbit changes. (Zonal tides on the Earth do extract their energy from the orbit rather than the spin, but they affect tidal $\dot{n}$ by only ~1%.)

How does the Moon's spin rate follow the slowly increasing orbit period from dissipation on Earth and Moon? The rigid-body axis displaces slightly east of the mean Earth direction, so torques decrease the lunar spin. This is a rigid-body dynamical balance of deceleration against torque. The expression comes from solving the equivalent of (17) with a quadratic time term in the polynomial for mean longitude L:

$$\ddot{\tau} + \dot{n} + 3\,\gamma\, n^2\,\tau = 0\,. \tag{38}$$

Assuming fourth and higher derivatives of L are zero, the displacement in τ is

$$\Delta\tau = -\frac{\dot{n}}{3\,\gamma\, n^2}\,. \tag{39}$$

To follow the tidal deceleration of -26 " cent^{-2} requires a displacement of only 0.0006". The quadratic (t^2) term in L depends on the changing eccentricity of the Earth-Moon orbit around the Sun as well as the tidal acceleration. The total acceleration is -13 " cent^{-2} [*Simon et al.,* 1994], and it requires only 0.0003" shift of the axis for the lunar spin to follow the orbit change. The longitude libration follows slow orbital longitude accelerations as assumed in analytical theories and experienced in numerical integrations [*Bois et al.,* 1996].

The lunar tidal forces which give rise to the above secular orbit effects are part of the JPL numerical integration program for orbits and rotation. The numerical orbit integration does not use this section's approximations. The time-varying moments of inertia are converted to the five second-degree gravitational harmonics, and the orbit perturbations are computed from the harmonics. This is convenient because perturbations from the large rigid-body parts of the lunar J_2 and C_{22} must also be calculated. The detectability of these orbit effects will be considered further in section 16.

9. Computational Model for Core Dissipation

If a liquid lunar core exists, then dissipation at the core-mantle boundary is expected when the fluid moves at a different rate than the overlying mantle. This section presents the core model used in the numerical orbit and rotation integrations and theoretical computations.

Though motions in the fluid may be complex, we adopt a simplified model based on the average fluid rotation $\boldsymbol{\omega}'$. The differential angular velocity between the core and mantle is $\Delta\boldsymbol{\omega} = \boldsymbol{\omega}' - \boldsymbol{\omega}$. At a point on the surface of a spherical core-mantle boundary (radius R') the relative velocity of the fluid is $\Delta\boldsymbol{\omega}\mathrm{x}\mathbf{R}'$, and a viscous force proportional to the relative velocity gives a torque proportional to $\mathbf{R}'\mathrm{x}(\Delta\boldsymbol{\omega}\mathrm{x}\mathbf{R}') = R'^2\,\Delta\boldsymbol{\omega} - (\mathbf{R}'\cdot\Delta\boldsymbol{\omega})\,\mathbf{R}'$. When integrated over the spherical surface, the total torque is proportional to $\Delta\boldsymbol{\omega}$.

A core dissipation model is implemented in the LLR analysis software. The equations of sections 2 and 3 are now interpreted as applying to the mantle. To the large gravitational torques acting on the mantle in $\mathbf{T}$ on the right-hand side of (1) is added the small additional torque $\mathbf{T}_c$

$$\mathbf{T}_c = K\,(\,\boldsymbol{\omega}' - \boldsymbol{\omega}\,)\,, \tag{40}$$

where K is a dissipation parameter which couples mantle and core. The ratio of K to the mantle moment C is a parameter to be fit to data. The core-mantle boundary is taken as spherical, so the only torque on the core is $-\mathbf{T}_c$. The Euler equation governing the overall rotation of the core is then

$$\frac{d(\mathbf{I}'\boldsymbol{\omega}')}{dt} + \boldsymbol{\omega}'\mathrm{x}\mathbf{I}'\boldsymbol{\omega}' = -\mathbf{T}_c\,. \tag{41}$$

For a spherically symmetric core, the core moment matrix $\mathbf{I}'$ has equal diagonal elements C' (tidal distortions are ignored), and the above cross product is zero.

$$\frac{d\boldsymbol{\omega}'}{dt} = \frac{K}{C'}\,(\,\boldsymbol{\omega} - \boldsymbol{\omega}'\,)\,. \tag{42}$$

The moment ratio C'/C is an input parameter. For the Euler equations the torque on the core is in the core's rotating frame, while the opposite core torque on the mantle is expressed in the mantle's rotating frame.

If the (laminar) viscous force is replaced with a turbulent force proportional to the square of the relative velocity, then the total torque integrated over the sphere is proportional to $|\Delta\boldsymbol{\omega}|\,\Delta\boldsymbol{\omega}$ and the counterpart to (40) would require an additional factor of $|\Delta\boldsymbol{\omega}|$. *Yoder* [1981] concludes that a lunar core-mantle interaction would be turbulent. There is further discussion in section 11. The core-mantle coupling is weak, and $\boldsymbol{\omega}'$ shows less variation than $\boldsymbol{\omega}$. The magnitude of the difference $\boldsymbol{\omega}' - \boldsymbol{\omega}$ is nearly constant, and the direction is mostly uniform precession (the mantle rate varies $<10^{-4}\,n$, and the direction varies $<10^{-3}$ radians from uniform precession). The difference between turbulent and viscous interactions is subtle, and (40) is used in this paper for data analysis.

The equations of rotation for the mantle and core are numerically integrated along with the equations of motion for the orbits of the Moon and planets. The initial time is 1969. Partial derivatives of the lunar Euler angles and orbit with respect to K/C, the two initial angular velocity vectors, two sets of initial Euler angles, two mantle moment differences $(C-A)/B$ and $(B-A)/C$, gravitational harmonics, k_2, and lunar tidal dissipation are also integrated so that solutions can be made.

10. Precession of Core

The equator of the observed solid Moon is tilted 1.54° to the ecliptic plane, and its retrograde precession is locked to the 18.6 year precession of the orbit plane. It can be guessed that any core will exhibit some analogous precession. The core tilt angle is unknown. *Goldreich* [1967] considered viscous, turbulent, and shape effects and concluded that the coupling of the core to the mantle is too weak to align the rotation axes of solid and fluid parts. Thus the core's equator is likely to lie closer to the ecliptic plane than to the mantle's equator, but it should exhibit some precession-induced motion.

To compute the precession of core and mantle, a coordinate system rotating at the 18.6 year node rate is chosen. For the torques and angular velocities in the mantle system, the x axis points toward the intersection of the equator and ecliptic planes, and the z axis is normal to the equator plane; y completes the triad. There is an analogous set of axes for the core. The Euler angles are (1) the angle ψ from the equinox along the ecliptic plane to the descending equator plane, (2) the angle θ between the equator and ecliptic planes, and (3) the angle φ from the intersection to the lunar zero meridian. Primed quantities are for the core, and unprimed are for the mantle. For uniform precession of core and mantle plus uniform rotations of mantle about the z axis and core about the z' axis $\dot{\varphi} = \dot{F}$, $\dot{\psi} = \dot{\psi}' = \dot{\Omega}$, $\dot{\theta} = \dot{\theta}' = 0$, and $\theta = I$. Then the core/mantle angular velocity difference in the mantle xyz frame is

$$\boldsymbol{\omega}' - \boldsymbol{\omega} = \begin{pmatrix} -\dot{\varphi}' \sin\theta' \sin(\psi'-\psi) \\ \dot{\varphi}' [\cos\theta \sin\theta' \cos(\psi'-\psi) - \sin\theta \cos\theta'] \\ \dot{\varphi}' [\sin\theta \sin\theta' \cos(\psi'-\psi) + \cos\theta \cos\theta'] - \dot{\varphi} \end{pmatrix}. \quad (43)$$

To get the angular velocity difference in the core frame, interchange primed and unprimed quantities.

For steady state precession the differential equations for the mantle in the *xyz* frame are

$$-C\dot{\psi}\omega_z \sin\theta + \frac{(A+B)}{2}\dot{\psi}^2 \sin\theta\cos\theta = T_{gx} + K(\omega'-\omega)_x, \quad (44a)$$

$$0 = T_{gy} + K(\omega'-\omega)_y, \quad (44b)$$

$$0 = T_{gz} + K(\omega'-\omega)_z. \quad (44c)$$

A, B, and C are now the mantle moments, not the total lunar moments. The gravitational torque on the mantle is $\mathbf{T}_g$. The differential equations for the core in the primed frame are simpler:

$$-C'\dot{\varphi}'\dot{\psi}' \sin\theta' = K(\omega-\omega')_{x'}, \quad (45a)$$

$$0 = K(\omega-\omega')_{y'}, \quad (45b)$$

$$0 = K(\omega-\omega')_{z'}. \quad (45c)$$

There are no gravitational torques on a spherical core.

The core equations are solved first. The second and third components are combined to derive $\dot{\varphi}\cos\theta = \dot{\varphi}'\cos\theta'$. Since the precession rates of core and mantle are the same, their angular velocity components normal to the ecliptic plane, $\dot{\varphi}\cos\theta + \dot{\psi}$ and $\dot{\varphi}'\cos\theta' + \dot{\psi}'$, are equal. However, the angular velocity normal to the mantle's equator $\omega_z = \dot{\varphi} + \dot{\psi}\cos\theta$ is different from that normal to the core's equator $\omega_{z'} = \dot{\varphi}' + \dot{\psi}'\cos\theta'$. Define $\xi = -(K/C'\dot{\Omega})$, which is positive since the node rate is negative. Then the solution for the core is

$$\cot(\psi'-\psi) = \xi, \quad (46)$$

$$\tan\theta' = \frac{\xi\tan\theta}{\sqrt{1+\xi^2}}, \quad (47)$$

$$\dot{\varphi}' = \dot{\varphi}\cos\theta\sqrt{1+\tan^2\theta'}. \quad (48)$$

Since θ is expected to be bigger than θ', the core must spin at a rate of ~99.96% of the mantle rate.

To develope the gravitational torques $\mathbf{T}_g$ on the mantle in the *xyz* frame, analytical expressions for $U_{ij} = (a/r)^3 u_i u_j$ were first written in the body-fixed frame and then rotated by φ. Here the notation of libration theory is used for the mantle's uniform precession and rotation, so $\varphi = F+\tau-\sigma+180°$, $\psi = \Omega+\sigma$, and $\theta = I$. The largest terms are linear in $\sin i$ and $\sin I$, but third-degree terms which multiply $\sin i$ and $\sin I$ by $\sin^2 i$, $\sin i \sin I$, $\sin^2 I$, and e^2 were included. These small third-degree terms, plus periodic librations multiplying the torque functions, were evaluated and combined with the numerical factors of the linear terms. Solar torques make a small contribution. Only the constant part is retained below. The best accuracy is needed for the first of the three components.

$$T_{gx} = \frac{3}{2}n^2 \{ [0.9758(C-A) + 0.0048(C-B)] \sin I + [0.9872(C-A) + 0.0041(C-B)] \sin i \cos(\sigma-\tau) \}. \quad (49a)$$

$$T_{gy} = \frac{3}{2}n^2 \{ -[0.9833(C-A) + 0.0059(C-B)] \sin i \sin(\sigma-\tau) + \tau[(B-A)\sin I - (C-B)\sin i] \}. \quad (49b)$$

$$T_{gz} = -3S_3(B-A)n^2\left(\tau + \frac{I\sigma}{2}\sin i\right). \quad (49c)$$

Here τ and σ are constant, and $S_3 = 0.9759$.

For the mantle precession solution the notation of libration theory is used with $\dot{\varphi} = \dot{F}$, $\dot{\psi} = \dot{\Omega}$, and $\theta = I$. The three constant torques cause a tilt I, a shift in the equator's node σ, and a constant offset in longitude τ:

$$\tau = -\frac{K}{C(1+\xi^2)}\frac{\dot{F}\sin^2 I}{3S_3 n^2}\left(\frac{1}{\gamma} - \frac{1}{\beta}\right), \quad (50)$$

$$\sin(\sigma-\tau) = -\frac{K}{C(1+\xi^2)}\frac{2\dot{F}\sin I\cos I}{3n^2 \sin i\,(0.9840\beta + 0.0059\alpha)}. \quad (51)$$

An upper limit can be put on $K/C(1+\xi^2)$ by using the constant $I\sigma = -0.265"$ found from the DE403 pure tidal solution. The $K/C(1+\xi^2)$ limit is 3.4×10^{-8} d^{-1}, while the τ limit is $-0.021"$. Note that the τ offset has a sign opposite that for tidal dissipation.

The combination $\sin I \sin F$ enters the range observations in a direct manner (see section 17), and the tilt I may be considered a well-observed quantity. The following relation from the first component of (43), (44a), (49a), and the core solution links I to physical parameters:

$$G_t = -3n^2 \sin i \cos(\sigma-\tau)(0.9865\beta + 0.0041\alpha + E), \quad (52a)$$

$$G_b = 2.0002\dot{\Omega}\omega_z + 3n^2(0.9754\beta + 0.0048\alpha + E) - 1.9982\dot{\Omega}^2 - 2\dot{F}\frac{\xi K}{C(1+\xi^2)}. \quad (52b)$$

$$\sin I = \frac{G_t}{G_b}, \quad (52c)$$

The inclination $i = 5.145°$, and the elastic combination $E = k_2\zeta/3$, where ζ is defined by (25). The combination $\beta = (C-A)/B$ is the solution parameter which most strongly adjusts the mantle's tilt when analyzing data, but there are weaker dependences on Love number, third-degree harmonics, and $\xi K/C(1+\xi^2)$. To account for the influence of C_{31} and C_{33}, replace β and α with the primed quantities defined by Williams et al. (2001). Also, Williams et al. used a Fourier analysis to extract $I = 5553.63"$ from the DE403 numerical integration of physical librations. The physical parameters for the numerical integration were fit to the Lunar Laser data. The above expression is within 1" of the numerical result.

The magnitude of the spin rate difference between core and mantle is

$$|\boldsymbol{\omega}' - \boldsymbol{\omega}| = \frac{\dot{F}\sin I}{\sqrt{1+\xi^2}}. \quad (53)$$

If the core couples strongly to the mantle ($\xi >> 1$), then its spin pole nearly lines up with the mantle's pole. For weak coupling ($\xi << 1$), the core's spin pole is nearly normal to the ecliptic plane.

11. Core-Coupling Parameter *K*

The ratio K/C will be fit to data. The core-coupling constant K depends on fluid dynamics. In this section, interactions from two

possibilities, laminar and turbulent flow, are investigated. For these cases, K is a function of physical parameters, including core radius R', fluid density ρ', and kinematic viscosity ν.

At the core-mantle boundary a viscous interaction in a laminar boundary layer gives a stress proportional to $\nu\,\rho'\mathbf{v}$, where the core-mantle relative velocity $\mathbf{v} = \Delta\boldsymbol{\omega}\times\mathbf{R}'$. *Yoder* [1981, 1995] gives

$$\frac{K_\nu}{C'} = 2.6\,\frac{\sqrt{\nu\,\omega'}}{R'}\,. \tag{54}$$

By assuming a core of uniform density, K/C' can be converted to K/C. From the maximum value given in the preceding section, set the numerical value of $K/C = f_c\,(1+\xi^2)\,3.4\times10^{-8}\ \mathrm{d}^{-1}$, where f_c is the fraction of the observed $I\sigma$ offset which comes from the core. The core radius in kilometers is then $R' = 837\,[f_c\,(1+\xi^2)/\rho']^{1/4}\,/\,\nu^{1/8}$ with ρ' in gm cm^{-3} and ν in cm^2 s^{-1}. For the limiting case of f_c=1 a liquid iron core density of 7 gm cm^{-3} and a viscosity of 0.01 cm^2 s^{-1} give a 900 km core, which other lunar interior data indicate is unacceptably large (see discussion in section 19). As *Yoder* [1981] concluded, the viscous laminar interpretation fails for the Moon, and an alternative must be considered.

At a point on the core-mantle boundary the turbulent stress for relative velocity $\mathbf{v}=\Delta\boldsymbol{\omega}\times\mathbf{R}'$ is equal to $\kappa\rho'|\mathbf{v}|\mathbf{v}$, where ρ' is the fluid density and κ is a dimensionless parameter which depends on viscosity. (Topographic irregularities on the core-mantle boundary can give an additional stress.) Integrating the stress over the surface and computing the torque gives

$$K_t = \frac{3}{4}\,\pi^2\,\kappa\,\rho'\,R'^5\,\Delta\omega\,. \tag{55}$$

Concerned about the oscillating direction of the relative velocity, *Yoder* [1995] replaced the scalar speed $|\mathbf{v}|$ with its maximum value divided by $\sqrt{2}$, but that is not done here. With the mean density of the Moon ρ and $\Delta\omega$ from (53) one gets

$$\left(\frac{R'}{R}\right)^5 = \frac{16}{9\,\pi}\,\frac{C}{m\,R^2}\,\frac{K}{C\,\dot F}\,\frac{\rho\,\sqrt{1+\xi^2}}{\kappa\,\rho'\,\sin I}\,. \tag{56}$$

Using the limiting case for K/C scaled by f_c, the numerical expression for core size is then

$$R' = 145.2\ \mathrm{km}\,\left[\frac{f_c\,(1+\xi^2)^{3/2}}{\kappa\,\rho'}\right]^{1/5}\,. \tag{57}$$

Yoder [1981] used $\kappa = 0.002$. It is stated by *Dickey et al.* [1994] that κ is within a factor of 2 of 0.001. *Yoder* [1995] gives an approximate boundary layer theory. With some rearrangement (the κ symbol here and that used by Yoder are not the same parameter) and the addition of ξ, the functional and numerical (cgs units) forms for κ are

$$\sqrt{\kappa} = \frac{0.4}{\ln[\,0.4\,\sqrt{\kappa}\,R'^2\,\dot F\sin^2 I\,] - \ln[\,\nu\,(1+\xi^2)\,]}\,, \tag{58a}$$

$$\sqrt{\kappa} = \frac{0.4}{2\ln R' + \ln\sqrt{\kappa} - \ln[\,\nu\,(1+\xi^2)\,] - 21.0}\,. \tag{58b}$$

The Karman constant is set to 0.4. This equation is solved iteratively if the radius is known. The κ and R' equations are solved iteratively if f_c is known; κ depends logarithmically on the core size, kinematic viscosity, and ξ, so those uncertainties have modest effects. For a viscosity of 0.01 cm^2 s^{-1}, a 400 km core gives κ=0.00071, while a 300 km core gives κ=0.00076. For the limiting case (f_c=1) with the density of liquid iron (7 gm cm^{-3}), the core radius is 421 km. Topography on the boundary would decrease this core size. For reasonable core sizes the theoretical K from turbulent interactions exceeds that from laminar flow, so turbulence is expected as *Yoder* [1981] concluded. The limiting core size differs from Yoder's 330 km limit mainly owing to the smaller value of κ and slightly because of his 13% smaller pole offset.

For core radii between 300 and 400 km the peak monthly velocity difference between core and mantle is 2 to 3 cm s^{-1} ($R'\,n\sin I$). Since C' is proportional to mean core density times R'^5, the turbulent K/C' depends mainly on κ, which is weakly dependent on core radius and viscosity. The dynamics of the core depend on K/C'. For the above values of κ, the ξ is 0.02 and the core tilt to the ecliptic plane is 2', much smaller than the 93' mantle tilt. For dissipative effects, *Goldreich*'s [1967] assertion is upheld. The core's equator intersects the ecliptic plane 89° ahead of the mantle's equator intersection. The core changes the mantle tilt by –0.006", which will be compensated during LLR data fits by changing β and other parameters.

12. Core Differential Equations, Free Modes, and Damping

Torque on the Moon from the Earth's gravitational attraction drives the forced librations and causes the mantle's free librations to oscillate about the forced state. The dissipative core-mantle interaction causes slow damping of the three periodic free librations, just as damping is also caused by tidal dissipation (section 7). Moreover, the core is capable of its own rotational motion, so there are additional free modes. These are damping modes, not oscillatory motion. The development of the core and mantle differential equations for rotation, the free modes, and the damping are this section's subjects.

First, the coupled differential equations for the longitude librations are written for mantle and core. The uniform precession of mantle and core introduces functions of I, I' (mean θ'), and ξ. Small nonlinear terms are dropped. The mantle equation is

$$\ddot\tau + 3\,S_3\,\gamma\,n^2\,\tau + \frac{K}{C}\left(\dot\tau - \dot\tau'\,\frac{\cos I}{\cos I'} + \dot F\,\frac{\sin^2 I}{1+\xi^2}\right) = f_Z\,. \tag{59}$$

The core longitude libration τ' contains the periodic terms in $\psi' + \varphi'$. The mantle moment C is used for $\gamma = (B-A)/C$. C' is roughly three orders of magnitude smaller than C. The $\dot F\sin^2 I$ term gives rise to the linear contribution in the constant offset. This was previously computed (equation (50)) and will not be considered further here. Small nonlinear terms are also dropped in the core differential equation.

$$\ddot\tau' + \frac{K}{C'}\left(\dot\tau' - \dot\tau\,\frac{\cos I}{\cos I'}\right) = 0\,. \tag{60}$$

Since the core is assumed spherical without any gravitational torque, there are τ' derivatives but no τ' term. Mantle periodicities are driven by core periodicities through terms factored by K/C'. Since C'/C is small, the coupling terms will influence the core more than the mantle. The $\boldsymbol{\omega}' - \boldsymbol{\omega}$ component appears different in the two differential equations because two frames are used. The ratio $\cos I / \cos I'$ is computed from

$$\frac{\cos^2 I}{\cos^2 I'} = 1 - \frac{\sin^2 I}{1+\xi^2}. \qquad (61)$$

The $\xi = -(K/C'\dot{\Omega})$, defined in section 10, depends on the (negative) node rate.

The forcing term for the mantle comes from the $U_{12}=(a/r)^3 u_1 u_2$ function factored by $3\gamma n^2$ and the 0.9906 numerical factor of (16), but the forcing function on the right-hand side of (59) has the linear τ term removed to give the $3S_3\gamma n^2\tau$ on the left-hand side. The free librations are solutions of the mantle and core differential equations when the right-hand side of (59) is zero.

To investigate the free libration modes, substitute $\tau = a\exp(i\nu t)$ and $\tau' = a'\exp(i\nu t)$ into the linearized differential equations. Two linear equations for a and a' result. The complex determinant of the coefficients of a and a' is

$$\Delta_t = -\nu^2\left[(3S_3\gamma n^2 - \nu^2) + \frac{K}{C}\frac{K}{C'}\frac{\sin^2 I}{1+\xi^2}\right] + i\nu\left[(3S_3\gamma n^2 - \nu^2)\frac{K}{C'} - \nu^2\frac{K}{C}\right]. \qquad (62)$$

The inverse $1/\Delta_t$ is $\Delta_t^*/\Delta_t\Delta_t^*$, where the asterisk denotes the complex conjugate:

$$\Delta_t\Delta_t^* = \nu^4\left[(3S_3\gamma n^2 - \nu^2) + \frac{K}{C}\frac{K}{C'}\frac{\sin^2 I}{1+\xi^2}\right]^2 + \nu^2\left[(3S_3\gamma n^2 - \nu^2)\frac{K}{C'} - \nu^2\frac{K}{C}\right]^2. \qquad (63)$$

To find the free libration frequencies (real part of ν) and damping (imaginary part) for the longitude modes, find the roots with the determinant (62) set to zero. The zero root means that the spherical core can be rotated by an arbitrary angle. While an exact solution of the remaining cubic is possible, approximate solutions are presented here. To guide the approximations, the sizes of parameter combinations are needed. The combination $(3\gamma)^{1/2} = 0.026$ is well determined. For a small core, $K/C' > K/C$. For turbulent coupling $K/C'n \approx 10^{-4}$, which may be increased by boundary topography. From the limiting case, $K/Cn \le 1.5\times10^{-7}$. So for the lunar case the combinations $n(3\gamma)^{1/2} >> K/C' >> K/C$ are well separated.

One of the roots of the cubic is near iK/C'. If the core rotation rate is not at the steady state value of (48) plus forced librations, it will damp very nearly as $\exp(-Kt/C')$. This could have been guessed from the form of (42) and (60). For a homogeneous iron core, damping times of 140 years are expected for turbulent coupling. Topography would decrease the damping time.

The (mantle) free libration frequency for longitude, with period 1056 days, comes from the square root of $3S_3\gamma n^2$. For the Moon the free libration frequency is much larger than K/C', so the first bracket in (62) dominates the frequency. If the reverse were true, the free libration frequency would be determined most strongly by the second bracket and the $\gamma = (B-A)/C$ would be replaced by $(B-A)/(C+C')$. The core would rotate with the mantle. In general, there is a slight dependence of the free libration frequency on the strength of the core-mantle coupling.

The damping for the mantle free libration mode is

$$D_L \approx \frac{K}{2C(1+\xi_L^2)}, \qquad (64)$$

where $\xi_L = K/C'n\sqrt{3S_3\gamma}$ is the ratio of core damping constant to free libration frequency. For turbulent coupling, $\xi_L = 0.003$ (weak coupling). Then from the DE403 limiting case the core-induced damping time $(1/D_L)$ must be $\ge 1.6\times10^5$ years. The above damping expression agrees with *Peale* [1976].

The effect of the core on the latitude librations is more difficult. The Euler equations for the mantle (equations (1) and (40)) and core (equation (42)) are not in the same reference frame. The core differential equation can be expressed in the mantle body frame

$$\frac{d(\mathbf{I}'\boldsymbol{\omega}')}{dt} + \boldsymbol{\omega}\times\mathbf{I}'\boldsymbol{\omega}' = \frac{K}{C'}(\boldsymbol{\omega} - \boldsymbol{\omega}'), \qquad (65)$$

where $\mathbf{I}'\boldsymbol{\omega}'$ and the angular velocity difference are also in the mantle frame.

The differential equations for mantle and core rotation are nonlinear owing to the $\boldsymbol{\omega}\times$ operation as well as terms in the forcing torques. Except for the precession term of section 10, nonlinearities are small. A linear treatment suffices in most cases, but nonlinearities can be treated as additional forcing terms during an iteration. Analogous to the p_1 and p_2 which describe the motion of the mantle's pole, the core parameters p_1' and p_2' are defined as

$$p_1' = -\sin\theta'\sin(\varphi + \psi - \psi'), \qquad (66a)$$

$$p_2' = -\sin\theta'\cos(\varphi + \psi - \psi'). \qquad (66b)$$

This definition removes the rate difference between the core and mantle systems from the argument.

The difference in angular velocities is needed in the mantle coordinate frame. Some small nonlinear terms are discarded.

$$\boldsymbol{\omega}' - \boldsymbol{\omega} \approx \begin{pmatrix} -p_1\dot{F}\frac{\sin^2 I}{\cos I} - \frac{\dot{p}_2}{\cos I} + p_1'\dot{F}\frac{\sin^2 I}{2\cos I'} + \dot{p}_2'\frac{1+\cos I}{2\cos I'} \\ -p_2\dot{F}\frac{\sin^2 I}{\cos I} + \frac{\dot{p}_1}{\cos I} - p_2'\dot{F}\frac{\sin^2 I}{2\cos I'} - \dot{p}_1'\frac{1+\cos I}{2\cos I'} \\ -\dot{F}\frac{\sin^2 I}{1+\xi^2} + \dot{\tau}'\frac{\cos I}{\cos I'} - \dot{\tau} \end{pmatrix} \qquad (67)$$

The linearized differential equations for mantle and core rotation are

$$\ddot{p}_2 + \omega_3(1-\alpha)\dot{p}_1 + \alpha\omega_3^2 p_2 + \frac{K}{C}\cos I(\omega_1 - \omega_1') = f_x, \qquad (68a)$$

$$-\ddot{p}_1 + \omega_3(1-\beta)\dot{p}_2 - 4\beta\omega_3^2 p_1 + \frac{K}{C}\cos I(\omega_2 - \omega_2') = f_y, \qquad (68b)$$

$$\ddot{p}_2' + [\omega_3 + (1-\cos I)\dot{F}]\dot{p}_1' - p_2'(1-\cos I)\dot{F}\omega_3 + \frac{K}{C'}\frac{2\cos I'}{1+\cos I}(\omega_1' - \omega_1) = 0, \qquad (69a)$$

$$-\ddot{p}_1' + [\omega_3 + (1-\cos I)\dot{F}]\dot{p}_2' + p_1'(1-\cos I)\dot{F}\omega_3 + \frac{K}{C'}\frac{2\cos I'}{1+\cos I}(\omega_2' - \omega_2) = 0. \qquad (69b)$$

The mean spin rate component $\omega_3 = \dot{F} + \dot{\Omega}\cos I \approx n$. Terms of order $\sin^2 I$ have been retained in the core differential equations since the core rotation rate, $\omega'^2 = \omega^2 - \dot{F}^2\sin^2 I/(1+\xi^2)$ from section 10's steady state rotation, is slower by such an amount. There is some conflict between the objectives of linearity, retaining $\sin^2 I$ terms, and the wish to simplify the core

differential equations by removing small terms. In (69a) and (69b), terms of order $\xi^2 \sin^2 I$ have been eliminated, so terms of order $\sin^2 I'$ are not complete.

To get the free libration frequencies and damping, zero the forcing functions on the right-hand sides and substitute four unknowns multiplying $\exp(i\nu t)$ for the mantle and core p parameters. The matrix multiplying the four unknowns is 4x4, and setting its determinant equal to zero gives an eighth degree polynomial for the free frequencies and damping. So approximations are in order (free libration frequencies $>K/C'>>K/C$). A first approximation is to solve the core and mantle differential equations separately, eliminating core variables in the mantle equations and vice versa. In this approximation the motion of the mantle's pole causes interaction with the core, but the mantle does not sense any response of the core (in the longitude damping, the response of the core shows as the $1+\xi_L^2$ in the denominator). Similarly, the core does not sense the mantle's response.

The complex 2x2 core determinant may be written as

$$\Delta_c = [\, \nu^2 - \omega_3^2 - \left(\frac{K}{C'}\right)^2 - 2\, i\, \nu\, \frac{K}{C'} \,]\, [\, \nu^2 - (1-\cos I)^2 \dot{F}^2 \,] \,. \quad (70)$$

Setting it equal to zero gives four roots: $\pm\omega_3 + iK/C'$ and $\pm(1-\cos I)\,\dot{F}$. The first pair of roots means the core's pole of rotation could be tilted differently in space from that computed for core precession plus forced libration, but damping will move it toward the latter state. The K/C' damping parameter applies. The second pair of roots reflects the slower core rotation rate through the arguments in the definitions (66a) and (66b) based on the uniform solution of (48) and (61). A sphere does not have a unique principal axis, and there is no damping.

The 2x2 mantle determinant is approximately (smallest terms discarded)

$$\Delta_m \approx \nu^4 - \nu^2\, \omega_3^2\, (\, 1 + 3\,\beta + \alpha\,\beta \,) + 4\,\alpha\,\beta\,\omega_3^4 - i\,\nu\,\frac{K}{C}\,(\, 2\,\nu^2 - 2\,\dot{F}\omega_3 \sin^2 I - \alpha\,\omega_3^2 - 4\,\beta\,\omega_3^2 \,) \,. \quad (71)$$

The real part corresponds to the classical solid-body dynamics, and the imaginary part contains the dissipative terms. There are two free modes for the mantle pole. One is an 81 year free precession in space (frequency $\approx 3\beta n/2$), and the other is a 75 year wobble of the pole as seen in the rotating frame (frequency $\approx 2n(\alpha\beta)^{1/2}$). Dissipation affects these periods very little. A coupling-dependent shift of frequency analogous to the longitude mode is expected but does not come from the 2x2 approximation. The damping of the mantle's free precession is

$$D_p \approx \frac{K}{C\,(1+\xi_p^2)} \,. \quad (72)$$

The parameter $\xi_p = 2K/3\beta n C'$ is the ratio of the core damping to the free precession frequency. The dependence on ξ_p does not come out of the 2x2 treatment. It requires additional terms from the 4x4 matrix. For turbulent dissipation, $\xi_p \approx 0.1$ is the strongest coupling of the three mantle modes and the 18.6 year forced precession. Topography at the core-mantle boundary could strengthen the coupling. The core-caused damping time is $\geq 8.1\text{x}10^4$ years. *Peale*'s [1976] analytical expression is very complicated, and his numerical damping time is several times as large.

The damping parameter for the wobble is

$$D_w \approx \frac{K}{C}\left[\, 2\,\beta + \frac{\alpha}{2} + \frac{\sin^2 I}{1+\xi^2} \,\right], \quad (73a)$$

$$D_w \approx 2.19\text{x}10^{-3}\,\frac{K}{C} \,. \quad (73b)$$

From the limiting case the damping time is $\geq 3.7\text{x}10^7$ years. The above wobble damping does not agree with *Peale*'s [1976] stronger result. The difference appears to arise from the $\boldsymbol{\omega}\mathbf{x}\mathbf{I}'\boldsymbol{\omega}'$ term needed to express the core differential equation in the mantle frame. While there is a $\xi_w = K/C'n$, it is very small. *Yoder* [1981] gives numerical values for damping time but not analytical expressions. For all three free modes the values are four to five times larger than this paper's values.

To compare damping from turbulent core dissipation and tidal dissipation, consider cases with equal pole offsets. The core is more efficient than tides for damping the free precession. For the other two modes the core damping lies between the tidal cases for constant Q and Q~1/frequency.

While it is convenient to refer to core and mantle modes, there is a small influence of the classical free librations on the core, and there is a small reflection of the core damping modes in the mantle rotation. For the mantle modes the ξ parameters determine the core/mantle amplitude ratio. For the precession mode, with the largest coupling, that ratio is $(\, \xi_p^2 - i\,\xi_p \,)/(1+\xi_p^2)$. So the core response is nearly orthogonal in phase when ξ_p is small, but the core and mantle rotate together as ξ_p approaches infinity.

The core mode damping is very fast compared to the mantle damping. The damping of the three mantle free modes is too slow to allow K/C to be determined. In principle, the core-damping modes have a small influence on the mantle and if observed would be sensitive to K/C'. The expected mantle/core amplitude ratios are very small, and the short damping time (140 years for turbulent coupling) would make these effects more transient than the mantle modes. To be observable in the mantle rotation, the core modes would need strong stimulation in the recent past.

13. Core Forced Terms

Gravitational attraction acting on the mantle's figure ultimately drives all forced terms. The feeble interaction between the core and mantle induces weak mantle periodicities, orthogonal in phase to the main terms, and small core rotation terms. These small forced terms are computed in this section.

In differential equation (59) periodic orbit terms and nonlinear terms (orbit times libration and libration times libration) force the system. For the longitude librations the nonlinear effects are small except for the constant offset (β term in (50)). The forcing function depends on a sine series for the largest terms. Here a periodic forcing function with frequency ν is represented as $3\,\gamma\,n^2 H \exp[i(\nu t+\text{phase})]$. The solution for the libration amplitudes for mantle, $\tau = a\,\exp[i(\nu t+\text{phase})]$, and core, $\tau' = a'\exp[i(\nu t+\text{phase})]$, gives complex functions. For a sine forcing function, the real and imaginary parts of a and a' correspond to a sine and cosine, respectively.

Presented below are both the full solutions and the approximate solutions to (59) with the foregoing periodic form for the forcing function and solutions. As with the free libration calculations, the inequality $n\,(3\,\gamma)^{1/2} >> K/C' >> K/C$ guides the approximations. The solution for the sine (in-phase) mantle libration includes both the conventional solid-body response and the core effects (with K). It is very close to the solution without dissipation, and the coefficient of a periodic sine term is

$$a_s = \frac{3\gamma n^2 H \nu^2}{\Delta_t \Delta_t^*} \left\{ (3 S_3 \gamma n^2 - \nu^2) \left[\nu^2 + \left(\frac{K}{C'}\right)^2 \right] - \nu^2 \frac{K}{C} \frac{K}{C'} \frac{\cos^2 I}{\cos^2 I'} \right\}, \quad (74a)$$

$$a_s \approx \frac{3\gamma n^2 H}{(3 S_3 \gamma n^2 - \nu^2)}. \quad (74b)$$

The cosine mantle coefficient is

$$a_c = -\frac{K}{C} \frac{3\gamma n^2 H \nu^3}{\Delta_t \Delta_t^*} \left[\nu^2 + \left(\frac{K}{C'}\right)^2 \frac{\sin^2 I}{1+\xi^2} \right], \quad (75a)$$

$$a_c \approx -\frac{K}{C} \frac{a_s \nu}{(3 S_3 \gamma n^2 - \nu^2)(1+\xi_\nu^2)}. \quad (75b)$$

The ratio $\xi_\nu = K/C'\nu$ measures the strength of the coupling between core and mantle at the forcing frequency. Cosine terms which have frequencies either much lower or much higher than the resonance frequency are suppressed, but a response is favored near the resonance. The core-caused cosine terms, factored by the small quantity K/C, are very much smaller than the conventional solid-body sine terms (equation (74b)), but they are larger than the small change in the sine terms due to the core.

The mantle longitude series for the core effects is given in Table 7. The two largest planetary terms are too close to the resonance to separate from the free librations when fitting data. The remaining periodic terms are too small to detect. All of the periodic terms in Table 7 have weak coupling between core and mantle for the turbulent value of K/C'. For the annual term, the largest conventional longitude term, $\xi_\nu \approx 0.001$.

The core's sine and cosine forced longitude coefficients are

$$a_s' = \frac{K}{C'} \frac{3\gamma n^2 H \nu^2}{\Delta_t \Delta_t^*} \frac{\cos I}{\cos I'} \left[(3 S_3 \gamma n^2 - \nu^2) \frac{K}{C'} - \nu^2 \frac{K}{C} \right], \quad (76a)$$

$$a_s' \approx \frac{\xi_\nu^2 a_s}{1+\xi_\nu^2}, \quad (76b)$$

$$a_c' = -\frac{K}{C'} \frac{3\gamma n^2 \mathrm{H} \nu^3}{\Delta_t \Delta_t^*} \frac{\cos I}{\cos I'} \left[(3 S_3 \gamma n^2 - \nu^2) + \frac{K}{C} \frac{K}{C'} \frac{\sin^2 I}{1+\xi^2} \right], \quad (77a)$$

$$a_c' \approx -\frac{\xi_\nu a_s}{1+\xi_\nu^2}. \quad (77b)$$

For $|\xi_\nu| < 1$ the cosine term is larger than the sine term. For increasingly larger ξ_ν the amplitude grows and the phase rotates until, as $|\xi_\nu|$ approaches infinity, the core couples strongly to the mantle and they rotate together. Lower-frequency forced terms couple core and mantle more strongly than higher-frequency terms.

In the conventional longitude librations there is a 14" Venus-induced term with a 273 year period. The turbulent ξ_ν is estimated to be 0.3, so the core should have a long-period term of at least 4". Unfortunately, the influence of this term on the mantle librations is unobservable. For turbulent coupling the annual core term should be ~0.1", and an 18.6 year term is ~0.2".

Table 7. Maximum Terms in Longitude Libration Due to Dissipation From a Weakly Coupled Fluid Core[a]

Argument	Period, days	τ cos, mas
ℓ	365.260	0.2
$2F-2\ell$	1095.175	1.3
$3E-5M-59°$	1069.313	−0.2
$23E-21V+2D-\ell+15°$	1056.415	3.0
$V-2E-D+2\ell-F+257°$	1056.345	3.2
0	∞	−21.1

[a]All terms use cosines of arguments. Angular units are milliarcseconds (mas). Planetary mean longitudes for Venus, Earth, and Mars are denoted V, E, and M. Core parameters are $K/C(1+\xi^2) = 3.4\times10^{-8}$ rad d^{-1} and $C'/C = 1.7\times10^{-3}$, with $\xi = 0.022$.

Since the coupling is weak for all of the significant mantle longitude terms, and the LLR data analysis detects the resonant frequency through the coefficient a_s, the γ defined with the mantle moment C is much closer to the measurable quantity than if it had been defined with the total moment $C+C'$ (the difference in the numerator is the same with a spherical core). Holding the mantle C constant makes the differences of sine terms too small to list in Table 7. For the tidal acceleration, and the exceedingly long period (>10,000 years) "secular" terms in longitude, the core should couple strongly to the mantle. The γ in (39) should use the total moment, but the induced displacement of longitude libration is small and not directly observable. For secular terms in longitude, the core acceleration matches the mantle acceleration, but the core rate is different by $-\dot{n}C'/K$. There is no obvious way to use the secular terms to learn about the core.

The more complicated latitude terms are done as approximations. From the 2x2 mantle matrix (71) one gets forced terms for p_1 (complex coefficient a) and p_2 (complex b). The forcing functions on the right-hand sides of differential equations (68a) and (68b) have been set to $X \exp[i(\nu t+\text{phase})]$ and $-iY \exp[i(\nu t+\text{phase})]$. This choice makes X and Y real for the largest forcing terms (X with a cosine and Y with a sine), and it associates the real part of a and b with a cosine and the negative imaginary part with a sine. The X forcing function comes from $3\alpha n^2\, 0.9906\, U_{23} \cos I$, and the Y function comes from $-3\beta n^2\, 0.9906\, U_{13} \cos I$ with the linear $3\beta n^2 p_1$ moved to the left-hand side of (68b).

$$a \approx \frac{i[\nu \omega_3 (1-\beta) - i \frac{K}{C} \dot{F} \sin^2 I] X}{\Delta_m} - \frac{i[\nu^2 - \alpha \omega_3^2 - i \nu \frac{K}{C}] Y}{\Delta_m}, \quad (78a)$$

$$b \approx \frac{-[\nu^2 - 4\beta \omega_3^2 - i \nu \frac{K}{C}] X}{\Delta_m} + \frac{[\nu \omega_3 (1-\alpha) - i \frac{K}{C} \dot{F} \sin^2 I] Y}{\Delta_m}. \quad (78b)$$

Both numerator and denominator are complex. The main dissipation terms are factored by K/C, analogous to the longitude case. From the experiences with forced longitude librations, free

Table 8. Maximum Terms in Latitude Librations Due to Dissipation From a Weakly Coupled Fluid Core[a]

Argument	Period, days	p_1 cos, mas	p_2 sin, mas	$I\sigma$ cos, mas	ρ sin, mas
F	27.212	265.2	-265.0		
$F-\ell$	2190.350	-1.4	0.8		
0	∞			-265.6	-5.9
ℓ	27.555			-3.6	3.7
$2F-\ell$	26.877			1.5	-1.5
$2F$	13.606			-0.6	0.6

[a]The latitude physical libration parameters are p_1, p_2, ρ, and $I\sigma$. Angular units are milliarcseconds (mas). Core parameters are $K/C(1+\xi^2) = 3.4\text{x}10^{-8}$ rad d^{-1} and $C'/C = 1.7\text{x}10^{-3}$, with $\xi = 0.022$.

librations, and the solution in section 10 it can be guessed that core response would put $1 + \xi_\nu^2$ in the denominator, where $\xi_\nu = K/C'(|\nu|-n)$.

Table 8 gives the core-induced latitude series. It is dominated by the term for pole offset (the more elaborate solution of section 10 is used for this term). Most of the 2190 day term is from a nonlinear contribution. Table 8 also gives the approximate conversion to ρ and $I\sigma$ parameters.

Of the forced terms in Tables 7 and 8, only the large pole offset term is easily observable. The forced physical librations are mainly sensitive to K/C, and the sensitivity to K/C' (or ξ) is very small in the tables.

14. Sidereal Terms

The Moon's orbit precesses along a plane which nearly coincides with the ecliptic plane, but this mean plane of precession is tilted by two causes. The oblateness of the Earth induces an 8" tilt toward the equator, and the resulting plane is commonly referred to as the Laplacian plane. The second cause is the motion of the ecliptic plane. This induces a 1.5" tilt because the orbit does not quite follow the ecliptic motion. The two tilts are oriented differently. The ξ_ν in the latitude solution of the preceding section is infinite for a term at the sidereal period (27.322 days in the rotating frame or zero rate in the inertial frame), and the solution there should not be used for such calculations. Both tilt effects are very close to the sidereal rate; the first case differs by the 26,000 year precession of the Earth's equator.

The effect on librations of a fixed plane for orbital precession is intuitive. The rotating mantle and core precess along the same plane as the Moon's orbit whether that plane is the ecliptic plane or not. There are several reasons that this is not quite true for the Moon: the Sun is still in the ecliptic, there are figure-figure torques on the Moon from the Earth's oblateness, and the ecliptic plane is moving. The torques from the Sun will be ignored compared to the Earth's, and the figure-figure effect is 1% of the 8". As *Eckhardt* [1981] showed, the effect of the ecliptic motion is sizeable, 6" in addition to the 1.5", because the differential equations must be modified.

The differential equations for core and mantle can be written and solved in an inertial frame. The solution has a simple explanation. The pole of the ecliptic plane moves 0.470 " yr^{-1}, and the axis of that rotation is at ecliptic longitude $\Pi = 174.87°$ at J2000 and moves slowly (-8.7 " yr^{-1}). Both mantle and core precession nearly follow this motion. The solid-body rotation fails to follow by an angle given by the 0.470 " yr^{-1} rate divided by the free precession frequency (0.47 " yr^{-1} / 2π / 81 yr = 6.0"). For the steady state solution both spin axes move by the 0.47 " yr^{-1}, but there is a separation between the two axes such that the turbulent torque causes the core's axis to follow the motion. The core rotation axis is pulled along by the mantle owing to the core-mantle interaction. The core is fully coupled to the mantle, and the appropriate expression for the 6" term is $0.47\,(B+C')/1.5\,n\,(C-A)$. The phase is $L - \Pi + 90°$, where the orbital mean longitude is $L=F+\Omega$. The classical latitude libration terms have weak coupling between core and mantle and are very sensitive to $\beta = (C-A)/B$, so the sidereal term associated with ecliptic motion has independent information on the core moment C'. The core-sensitive terms are

$$\Delta p_1 = 6.0" \frac{C'}{C} \sin(L - 84.87°), \tag{79a}$$

$$\Delta p_2 = 6.0" \frac{C'}{C} \cos(L - 84.87°). \tag{79b}$$

The expression for the ecliptic-motion-induced separation between the core and mantle spin axes is 0.47 " yr^{-1} C'/K. For turbulent coupling the spin axis of the core lags the secular motion of ecliptic and mantle poles by ~1', while it also precesses with a 2' angle.

For turbulent coupling, section 11's limiting case of a 421 km iron core gives $C'/C = 1.7\text{x}10^{-3}$. This gives an upper limit of 0.010" for the sidereal core signature. The two closest terms (in frequency) are the forced precession, with an 18.6 year beat period, and the free precession, with an 81 year beat. There are solution parameters corresponding to all three frequencies, and the 81 year beat period will weaken the determination of C'. So the term is large enough to be useful, but the separation of parameters will be a challenge. Increasing data span will very much improve the direct determination of the core moment. All of the terms in Tables 7 and 8 are orthogonal to the major (solid-body) terms of the same period. This can be an advantage when solving for K/C. The core-induced sidereal term does not have this advantage.

The tidal dissipation Tables 3 and 4 have a sidereal term, but it was too small to include in Table 2. Split into the two phases and expressed in arc seconds, the two components are

$$\Delta p_1 = -\frac{k_2}{Q} [\, 0.01 \cos L + 0.18 \cos(L - 84.87°) \,], \tag{80a}$$

$$\Delta p_2 = \frac{k_2}{Q} [\, 0.01 \sin L + 0.18 \sin(L - 84.87°) \,]. \tag{80b}$$

The Q is monthly. The maximum for the tidal dissipation terms is 0.2 milliarcsecond (mas). This is much smaller than the maximum core effect, has different phase, and should be calculable from a monthly Q. The tidal elastic effect proportional to k_2 is orthogonal to the tidal dissipation, is several mas in size, and is more likely to correlate with C'.

An additional effect, core-mantle boundary oblateness, has not yet been investigated. Given this unknown, the two sources of sidereal terms with two phases, and the 81 year beat period, the sidereal terms are not pursued further in this paper. They offer a very interesting future opportunity for direct determination of core moment.

15. Orbit Perturbations From Core Dissipation

The gravitational attraction from a spherical core acts like a point mass and does not directly perturb the lunar orbit, but there is an indirect effect. The core-induced constant shifts in libration τ and σ (section 10) displace the mantle's principal axes from what would otherwise be their equilibrium orientations. The displaced figure of the Moon then perturbs the orbit. The effects are small, and leading-term approximations are used in this section. As is the case with tidal dissipation, the orbital perturbations are computed by the numerical integration programs from the accelerations. The approximations of this section do not enter those programs.

Orbit perturbations from a displaced figure were also considered for tidal perturbations (section 8). The important effects are in semimajor axis a, mean motion n, and inclination i. The computation can proceed in a manner similar to section 8 using the τ and σ offsets of section 10. Changes in a and n are also related to the power drawn from the orbit and deposited in the core:

$$P = -K(\boldsymbol{\omega}' - \boldsymbol{\omega})^2, \tag{81a}$$

$$P_{ave} = -\frac{K \dot{F}^2 \sin^2 I}{1+\xi^2}. \tag{81b}$$

The secular mean motion and semimajor axis changes are calculated (approximately) from the mean power. The mean motion change is

$$\Delta\dot{n} = \frac{K}{C(1+\xi^2)} \frac{C}{mR^2} \left(1+\frac{m}{M}\right) \left(\frac{R}{a}\right)^2 3\dot{F}\sin^2 I, \tag{82a}$$

$$\Delta\dot{n} = 1.11\text{x}10^6 \frac{K}{C(1+\xi^2)} \text{ " cent}^{-2}. \tag{82b}$$

The ξ is based on the node rate. The latter equation uses K/C in radians d^{-1} to give " cent^{-2}. The limiting case gives an upper limit of 0.038 " cent^{-2} from the fluid core. The influence on the semimajor axis comes from $\Delta\dot{a} = -2a\Delta\dot{n}/3n$, so the relation is

$$\Delta\dot{a} = -\frac{K}{C(1+\xi^2)} \frac{C}{mR^2} \left(1+\frac{m}{M}\right) \left(\frac{R}{a}\right)^2 2a\sin^2 I, \tag{83a}$$

$$\Delta\dot{a} = -1.64\text{x}10^3 \frac{K}{C(1+\xi^2)} \text{ m yr}^{-1}. \tag{83b}$$

Again, K/C is in radians d^{-1} to give m yr^{-1}. For the limiting case this is –0.056 mm yr^{-1}.

In the first approximation there are no torques perpendicular to the ecliptic plane, but there are torques normal to the orbit. The semimajor axis and semilatus rectum expand at the same rate so the eccentricity rate is zero. There is also a torque in the orbit plane 90° from the node which gives rise to an inclination rate

$$\frac{di}{dt} = -\frac{K}{C(1+\xi^2)} \frac{C}{mR^2} \left(1+\frac{m}{M}\right) \left(\frac{R}{a}\right)^2 \frac{\sin^2 I}{\sin i}, \tag{84a}$$

$$\frac{di}{dt} = -4.9 \frac{K}{C(1+\xi^2)} \text{ " yr}^{-1}. \tag{84b}$$

The last equation uses K/C in radians d^{-1} to give inclination rate in " yr^{-1}. The rate for the limiting case is $-1.7\text{x}10^{-7}$ " yr^{-1}. This is too small to detect. The core influence on node and longitude of perihelion acceleration is about an order of magnitude smaller than for tidal dissipation for the limiting cases.

For the same pole offset, tidal dissipation in the Moon provides an order-of-magnitude larger secular change of semimajor axis and mean motion than does core dissipation. Also, the tides change eccentricity, while the core does not. As with the lunar tides, the changes are opposite in sign to those from tidal dissipation on the Earth. The fluid-core-caused changes in a and n are three orders of magnitude smaller than rates caused by tides on the Earth. The differences in orbit perturbations from the three offer an opportunity to distinguish between them. This will be discussed further in the next section.

16. Separation of Orbit Perturbations

Can the secular rates of orbital semimajor axis, mean motion, and eccentricity be used to separate the contribution from lunar tidal and core dissipation? For semimajor axis and mean motion rates, tidal dissipation on the Earth is two orders of magnitude more important than lunar tides and three orders of magnitude more important than lunar core effects. In principle, one can subtract the Earth influence from the measured orbit changes to get the lunar effect. The measured pole offset gives a linear combination of the two lunar influences, and the total orbital effect depends on their proportion.

To the secular acceleration $\dot{n}$, the Moon contributes between 0.038 " cent^{-2} (all dissipation in core) and 0.46 " cent^{-2} (all dissipation tidal). Table 9 gives the secular acceleration and eccentricity rates computed from tides on Earth. Tidal components are deduced from artificial satellite and Lunar Laser Ranging. The LLR model has Love numbers and tidal time delays for three frequency bands: semidiurnal, diurnal, and long period. The semidiurnal and diurnal time delays are LLR fit parameters. The DE403 lunar ephemeris was generated in 1995, and its secular acceleration from Earth and Moon dissipation is –25.64±0.4 " cent^{-2}. The predictions of tidal acceleration from the artificial satellite laser ranging (SLR) deduced tides are systematically ~1 " cent^{-2} lower (in magnitude) than the LLR values. Half of this difference is understood. The SLR calculations of lunar acceleration do not correctly account for the finite mass of the Moon [*Williams et al.*, 1978], which requires a correction factor of $1+m/M = 1.0123$. A modified Kepler's third law (used in (16a)) contributes an additional factor of 1.0028 (using a=384,399 km from the average inverse distance). These two corrections increase the magnitude of the SLR values by 0.4 " cent^{-2}. A review of the conversion of the LLR Earth and Moon tidal time delays to $\dot{n}$ shows that the published (negative)

Table 9. Mean Motion and Eccentricity Rates Computed From Four Models of Earth Tides[a]

Tide Model	$\dot{n}$, " cent^{-2}	$\dot{e}$, 10^{-11} yr^{-1}	Reference
GEM-T1	–25.27	1.83	*Christodoulidis et al.* [1988]
GEM-T2	–24.94	1.68	*Marsh et al.* [1990]; *Dickman* [1994]
Cartwright-Ray	–24.88	1.59	*Ray* [1994]
LLR DE403	–26.10	1.35	this paper

[a]The first three models depend in whole or in part on multiple tidal components deduced from artificial satellite laser range data analysis. The last corresponds to the model used in the lunar and planetary integrator with two adjustable tidal parameters fit to LLR data.

values of $\dot{n}$ need to be corrected by +0.15 " cent^{-2}. Earth tides account for +0.10 " cent^{-2}, and lunar semimonthly tides in Table 6 add 0.05 " cent^{-2}. (The *Dickey et al.* [1994] value of $\dot{n}$ = –25.88±0.5 " cent^{-2} becomes –25.73±0.5 " cent^{-2}.) Adding dissipation in the Moon to Table 9 does not improve the SLR/LLR disparity. Because LLR is sensitive to the total secular acceleration while SLR senses only Earth tides, lunar tides increase the SLR/LLR spread more than core dissipation. At present, knowledge of tides on the Earth is not sufficiently accurate to extract the lunar contribution to the observed secular acceleration from the difference between SLR and LLR values.

The situation for eccentricity rate is more hopeful. The Moon contributes between -1.0×10^{-11} yr^{-1} (all dissipation from tides) and 0 (all dissipation in core). The contributions from Earth and Moon are close enough in size that eccentricity rate is useful for learning about the Moon's interior. An eccentricity rate of -1.0×10^{-11} yr^{-1} changes the perihelion distance by 3.2 mm yr^{-1}. The LLR determination of eccentricity rate should improve with increasing data span.

The internal accuracy of the determination of the dissipation-induced $\dot{n}$ is good. However, range perturbation exceeds 15 m during the data span! But the present uncertainty of tides on Earth does not permit this to be used for the lunar problem. Eccentricity rate is a much weaker signal, accumulating a few centimeters in range during the data span, but is easier to correct for tides on Earth. At present, the lunar rotation provides a direct test of lunar dissipation without corruption from external influences. Since the rotation effects are bounded while the orbit effects are secular, the orbit perturbations may assume greater importance in the future.

17. Determination and Separation of Lunar Variables

This section discusses how the lunar rotation terms affect the Lunar Laser ranges. It also discusses how the solution parameters separate from one another. The data analysis program uses rigorously derived partial derivatives of range with respect to the solution parameters, but for illustration, approximations are used.

The range vector $\mathbf{R}$ from an observatory on the Earth to a retroreflector on the Moon is

$$\mathbf{R} = \mathbf{r} - \mathbf{R}_s + \mathbf{R}_r . \tag{85}$$

The three position vectors are geocentric Moon $\mathbf{r}$, the geocentric ranging station $\mathbf{R}_s$, and the selenocentric retroreflector position $\mathbf{R}_r$. Orientation matrices for the Earth and Moon are used to transform between space-fixed coordinates and body-fixed coordinates. When accurately calculating the round-trip time delay, two $\mathbf{R}$ vectors are needed. One "leg" uses the transmit time and the lunar bounce time, while the other uses the bounce time and receive time. Since $R_s/r \approx 1/60$ and $R_r/r \approx 1/221$, a first approximation for the range projects the two smaller vectors along the Moon to Earth unit vector $\mathbf{u} = -\mathbf{r}/r$:

$$R \approx r + \mathbf{u}\cdot(\mathbf{R}_s - \mathbf{R}_r) . \tag{86}$$

At a given time, the difference in range to different retroreflectors depends on the reflector coordinates and the lunar orientation with respect to the Earth-Moon vector. In the lunar body-referenced frame, $\mathbf{u}$ is approximated by

$$u_1 \approx 1 - \frac{1}{2} u_2^2 - \frac{1}{2} u_3^2 , \tag{87a}$$

$$u_2 \approx \sin[\,(2e\sin\ell) - \tau\,] , \tag{87b}$$

$$u_3 \approx -\sin i \sin F - \sin(I+\rho)\sin(F-\sigma) . \tag{87c}$$

The direction of this vector is composed of the optical librations, due to the orbit (eccentricity e and inclination i terms), and the physical librations, due to rotation (I, τ, ρ, and σ). The e and i terms are leading terms of series for ecliptic longitude and sine latitude, respectively. See *Eckhardt* [1981] for the exact expressions. The selenocentric coordinates of a retroreflector project into the range direction as $-\mathbf{u}\cdot\mathbf{R}_r$, where $\mathbf{R}_r = (X, Y, Z)$ in the body frame. The main sensitivity of the range to the longitude libration comes from $Y u_2$, and the sensitivity to latitude librations comes from $Z u_3$. For the four retroreflectors, $1339<X<1653$ km, $-521<Y<803$ km, and $-111<Z<765$ km [*Williams et al.*, 1996]. Figure 1 shows the retroreflector locations. At the lunar surface a selenocentric angle of 1" is equivalent to 8.4 m, but the projection into the range direction is <4 m for the retroreflector positions. Thus a few centimeter range accuracy is sensitive to physical librations at the ≈0.005" level, and numerous observations will improve on this during a solution.

In the range data analysis program a partial derivative of the range (time delay) is required with respect to each solution parameter (P) for each leg of the round trip. For lunar parameters these partials are $\hat{\mathbf{R}}\cdot(\partial\mathbf{r}/\partial P + \partial\mathbf{R}_r/\partial P)$, in the space-fixed system. The orbit is separate from the orientation of and location on the Moon. For illustration, in lunar body-fixed coordinates the partial of the $-\mathbf{u}\cdot\mathbf{R}_r$ term is $-\mathbf{u}\cdot\partial\mathbf{R}_r/\partial P - \mathbf{R}_r\cdot\partial\mathbf{u}/\partial P$. The $\partial\mathbf{R}_r/\partial P$ includes partials with respect to the three selenocentric coordinates for each of the four retroreflectors plus partials for two Love numbers h_2 and l_2 for tidal displacements. The partials $\partial\mathbf{R}_r/\partial P$ come from the geometry and are not integrated. They are generated and projected into the range direction while processing data. The sensitivity to the reflector coordinates comes through the orientation of the Moon with respect to the Earth-Moon line. The tides vary with time, depend on location, and project according to variable orientation. A numerical integration program generates the partials of orientation $\partial\mathbf{u}/\partial P$ and orbit $\partial\mathbf{r}/\partial P$ with respect to dynamical parameters. These dynamical parameters include β, γ, seven third-degree gravitational harmonics, Love number k_2, tidal time delay Δt equivalent to a Q inversely proportional to frequency, K/C, rotation initial conditions for solid body and core, and lunar J_2. The projection into the range direction at the observation time is done when the range data is analyzed. Except for J_2, these dynamical parameters are most sensitive through the orientation. To distinguish Q values at different frequencies, analytical partials $\partial\mathbf{u}/\partial P$ are generated and projected at the time of data analysis. On the basis of the series solutions of section 5 and Tables 1 and 2, analytical partials are included for coefficients of five out-of-phase terms: 27.2 days and 2190 days for latitude librations, plus annual, 1095 days and 206 days for longitude librations. Since the p_1 and p_2 parameters are coordinates rather than angles, the analytical latitude partials are implemented using their equivalent terms for constant σ and 27.555 day variations in ρ and σ.

During solutions, how detectable and separable are the dissipation effects through lunar orientation? Except for the sidereal term, the dissipation terms are orthogonal in phase to the terms produced by the second-degree figure (triaxiality). There is little difficulty in separating orthogonal terms, even when they have identical periods, provided that the data span is long enough. Of the seven third-degree harmonics, three produce

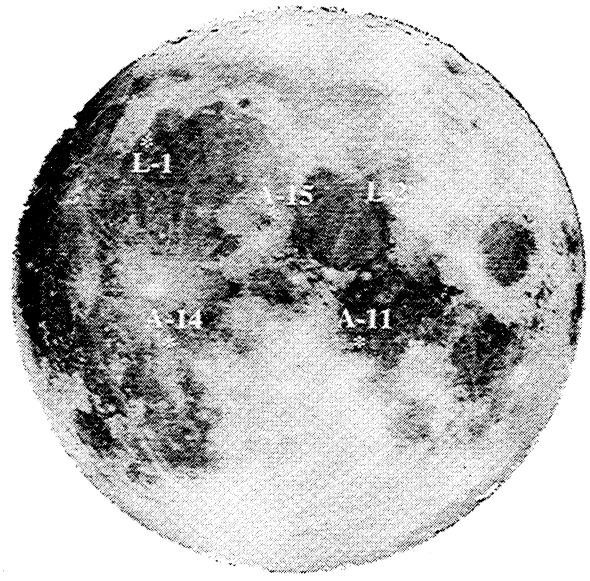

Figure 2. Location of the three Apollo retroreflectors and the two French reflectors on Soviet Lunakhods. The spread of locations aids separation of parameters during solutions.

terms orthogonal to the dissipation terms, and four (C_{30}, C_{32}, S_{31}, and S_{33}) produce terms that are phased like dissipation. The spherical harmonic functions for C_{30} and C_{32} are even in longitude and odd in latitude, while those for S_{31} and S_{33} are odd in longitude and even in latitude. The resulting libration series are dissimilar for the two pairs [*Eckhardt,* 1981; *Moons,* 1982b], but the paired members will correlate with each other. It is the separation of S_{31}, S_{33}, K/C, and Δt ($n k_2 \Delta t = k_2/Q$ for monthly Q) that needs further discussion.

Because of the good geometric spread of retroreflectors (Figure 2), the physical libration latitude and longitude components are distinguishable from each other and from the orbit. Table 10 displays the larger partial derivatives for S_{31}, S_{33}, K/C, and two tidal dissipation models (Q constant and Q~1/frequency). *Eckhardt* [1981] and *Moons* [1982b] are the sources for the two harmonic columns; this paper provides the dissipation columns. The constant in τ is not shown because it contributes nothing to the separation when reflector longitude (or X and Y) is adjusted during the solution. The τ partials are tabulated because they are the physical libration part of u_2 in (87b). Instead of u_3, the similar, but simpler, $p_1 - \tau \sin I \cos F$ is used (Moons tabulates p_1 and p_2 rather than ρ and $I\sigma$). The columns are normalized like unit vectors.

Table 10 may be used to understand what happens during the numerical solutions. Similarity down each column's series of arguments/frequencies causes correlation, while dissimilarity promotes separation. First, notice that the dissipation columns are dominated by the precession pole offset (cos F latitude term), but this offset is zero for the harmonics. Only dissipative effects contribute to the observed 0.26" pole offset. Separation during solutions depends on the largest dissimilar coefficients, provided the data span is comparable to or larger than their periods and beat periods with other major terms. The number of parameters in the fit must at least be matched by the number of detectable periodicities in the partials. In the simplest case the partials would be considered in decreasing order of size, but there are complications since of the three free libration modes one is near the 27.2 day F term (24 year beat period) and another is near the 1095 day term (81 year beat). Though the LLR data span exceeds 24 years, the earliest data is an order of magnitude less accurate than the recent data. While the determination of the F term is weakened somewhat, the 1095 day term is more strongly affected. With this reasoning the following statements are made. (1) For 2 decades the fits of ephemerides, including DE403, solved for harmonics plus the k_2 and Δt of the tidal model with Q~1/frequency (k_2 is phased orthogonal to the table's terms). Consequently, the 27.2 day, 3 year, and 6 year terms were of paramount importance aided by the 206 day term, which is next in size. (2) Adding K/C to the preceding solution parameters requires one or more additional distinct frequencies, e.g., the 27.6 day term. (3) The obvious way to distinguish a different tidal dissipation law such as constant Q is to use the annual term. There is very little interference from the core or harmonics terms. (4) To test Q values at other frequencies requires either detecting very small terms or using an independently derived gravity field of high accuracy. Adding more solution parameters forces the fits to rely on smaller periodic terms in the partials for separation.

Timescales from 1 month to 6 years are important for studying dissipation. Six years is a major periodicity in the rotation partials, and it is also a beat between the 27.2 and 27.6 day periodicities. For the broader goal of fitting lunar science parameters beyond those in Table 10, some rotation partials involve the same periodicities (but not the same coefficients), but

Table 10. Comparison of Larger Periodic Latitude and Longitude Out-Of-Phase Libration Terms for Two Gravitational Harmonics, Two Q Scalings, and Fluid Core Coupling[a]

Term	Libration	Period, days	S_{31}	S_{33}	Q~1/frequency	Q constant	K/C
cos F	Lat	27.212	0	0	0.982	0.992	1.000
cos(F–ℓ)	Lat	2190.350	–0.410	–0.178	–0.057	–0.066	–0.005
cos(2ℓ–F)	Lat	27.906	0.019	0.009	0.002	0.001	0
cos(2F–2ℓ)	τ	1095.175	–0.899	0.982	–0.181	–0.103	0.005
cos(2ℓ–2D)	τ	205.892	–0.142	0.060	–0.022	–0.018	0
cos ℓ'	τ	365.260	0	0.008	0.001	0.036	0.001
cos ℓ	τ	27.555	–0.037	–0.012	–0.005	–0.005	0
cos(2F–2D)	τ	173.310	0.023	0	0	0.001	0
cos(ℓ–D)	τ	411.784	0.021	–0.008	0.003	0.002	0

[a] The periodic latitude term is $p_1 - \tau \sin I \cos F$, the periodic longitude libration is τ, and fluid core coupling is proportional to K/C. The partial derivatives in each column are normalized to unit column length. Variety promotes separation during solutions. A periodic term is given if any coefficient in the row exceeds 0.020.

with sines rather than cosines. Other partials reverse the periodicities between longitude and latitude librations. Initial conditions of the rotation are equivalent to the three free libration modes at 27.3 days (with a 24 year beat with F), 1056 days (weakening the separation of the 1095 day terms), and 75 years. The reflector X partial starts with a constant and semimonthly terms. The leading terms for the Y and Z partials involve sines of ℓ and F, respectively. The tidal displacements project into range as a third-degree function of reflector coordinates. All this variety promotes separation during solutions. Important qualities for extracting lunar science information are accurate ranges, a long data span, and a broad spread of retroreflector locations.

18. Dissipation Solutions

The high accuracy of the Lunar Laser ranges (0.5×10^{-10} relative to the distance), the substantial data span, and the geometrical diversity of multiple ranging stations and multiple lunar retroreflectors permit solutions for a broad set of dynamical and geometrical parameters. Solutions for dissipation parameters, and the implied tidal Q values and core existence, are subjects of this section.

Lunar Laser ranges from March 1970 to July 1998 are the data set. Data from the earliest few years have uncertainties of 0.2–0.3 m. Ranges from the most recent years can be fit with a 2 cm root-mean-square (rms) residual. Ranges are from three sites on the Earth: McDonald Observatory, Texas, Observatoire de la Côte d'Azur (OCA), France, and Haleakala Observatory, Maui. The first two sites are currently operational. For further information on the ranging stations, consult *Dickey et al.* [1994] and *Samain et al.* [1998]. There are four actively used retroreflectors: Apollo 11, 14, and 15 and Lunakhod 2 (see Figure 2).

The set of lunar solution parameters includes β, γ, J_2, third-degree gravitational harmonics, Love numbers k_2, h_2, and l_2, tidal time delay associated with k_2, core-mantle coupling K/C, amplitudes for five dissipation-related analytical terms in rotation, and three-dimensional coordinates of the four retroreflectors. Also, integrator initial conditions for lunar orbit plus solid-body and core rotations comprise 18 parameters. The product of the gravitational constant and mass for the Earth and Moon ($G(M+m)$) and two (Earth) tidal dissipation parameters influence the orbit. Additional parameters include the Earth-Moon orbit about the Sun and, because the lunar and planetary data are fit jointly, planetary orbits. An analytical partial for an eccentricity rate is available. There are also geocentric coordinates for the terrestrial ranging sites, horizontal rates for plate motion, parameters for Earth orientation, precession and nutation, plus a stochastic procedure for Earth-rotation corrections which is important for the early observations. In addition to the choice of solving for a parameter or leaving it unchanged, parameters may be subject to linear constraints (e.g., one parameter may be forced to take a particular value, or two or three may be required to satisfy a linear relation).

As discussed in the previous section and demonstrated in Table 10, errors in the gravity harmonics S_{31} and S_{33} will corrupt dissipation solutions. Of the usable dissipation terms, the annual term and the large displacement of the pole direction are the least sensitive to the gravity field. The solutions in Table 11 vary both the treatment of the harmonics and the use of solution parameters based on numerically integrated and analytical partial derivatives. The tabulated parameters are extracted from the larger solution set. In Table 11 the Δ symbol indicates an increment using an analytical term. Total values are used for the remaining five parameters in the table which come from the numerically integrated tide, core, and gravity field models. To get a total value for an analytical dissipation term, it is necessary to add the model influences, computed from the tables of this paper, to an increment marked by Δ. The tabulated rms uncertainty is normalized to the observational uncertainties. The weightings of the LLR data and sets of planetary data are adjusted so that the normalized rms is near one. The 12,455 lunar ranges are 29% of the total number.

The first example in Table 11 (case A) uses numerically integrated partial derivatives to solve for the tide and core-mantle coupling parameters (k_2, tidal time delay, and K/C), the S_{31} and S_{33} harmonics, and the annual amplitude. Implicit in the numerical tide and core models is an additional 0.3 milliarcsecond (mas) for the annual term, giving a total dissipation effect of 3.7 mas. From the tidal and core parameters one computes the combined $I\sigma_{const} = -262.7 \pm 2.3$ mas (time delay and K/C are correlated –0.973, so the uncertainty in the combination is small). The core model causes 33% of that offset. This first case is limited to one analytical coefficient because the harmonics are included as solution parameters.

Luckily, the accuracy of the gravity field LP75G [*Konopliv et*

Table 11. Three Solutions for Dissipation and Related Parameters[a]

Parameter	Unit	Case A	Case B	Case C
Norm rms	1	0.8479	0.8490	0.8470
k_2	10^{-5}	2874±80	2867±80	2868±80
Time delay	day	0.1152±0.0140	0	0.1079
K/C	10^{-8} d^{-1}	1.122±0.257	0	1.317
$\Delta\tau_{206}$	mas	0	–1.0±1.6	2.7±1.6
$\Delta\tau_{365}$	mas	3.4±1.8	4.1±1.8	3.6±1.8
$\Delta\tau_{1095}$	mas	0	–26.7±5.9	3.0±5.9
$\Delta I\sigma_{27.6}$	mas	0	7.5±1.0	1.1±1.0
$\Delta I\sigma_{const}$	mas	0	–264.0±5.0	4.6±5.0
S_{31}	10^{-6}	5.64±0.64	5.869	5.869
S_{33}	10^{-7}	–2.58±0.11	–2.457	–2.457
$\Delta\dot{e}$	10^{-11} yr^{-1}	1.68±0.48	0.65±0.46	1.55±0.47
h_2	1	0.034±0.018	0.035±0.018	0.041±0.018

[a]Free solution parameters are displayed with uncertainties, while fixed parameters lack uncertainties. Angles are in milliarcseconds (mas). The first line is the normalized root-mean-square residual for all lunar and planetary observations.

al., 1998], based on Doppler tracking of Lunar Prospector (three months) plus earlier spacecraft, makes it practical to adopt one or both of the harmonics. With both tidal time delay and K/C forced to zero with constraints (the initial values for the numerical integration are not zero), which has the effect of canceling rotation and orbit effects from the numerical integration, and the LP75G values for S_{31} and S_{33}, the coefficients of five periodic dissipation terms are solved for. This solution is case B in Table 11. When noise from the gravity field is added to the uncertainties in the table, the uncertainty for the 3 year coefficient is 7.1 mas, and that for 27.6 days is 1.2 mas. The constant pole offset is correlated –0.93 with k_2 since the tidal contribution depends on the product of k_2 and time delay. The constraints on tidal time delay and K/C move the pole in one direction, while the analytical term moves it back the other way. This presumably explains the increased uncertainty from case A.

The case C solution fixes the tidal time delay and K/C to the numerical integration values used for data reduction (DE330 was generated using 2 years less data than the tabulated solutions) and fixes the S_{31} and S_{33} harmonics to the LP75G values. Analytical coefficients are solved for, but these are now corrections to the numerically integrated dissipation model. When those corrections are added to coefficients calculated from the model parameters, one gets –0.9, 4.0, –27.4, 7.4, and –262.6 mas, in the order of the table. The agreement between the second and third cases is quite good, which validates this paper's analytical theories for rotation.

The similarity of the total annual effect across the three solutions (3.7, 4.1, and 4.0 mas for cases A, B, and C, respectively) illustrates its insensitivity to the gravity field. The pole offset shows a range of 1.4 mas. To compute the pole offset better than 1 mas involves such complications as solar effects and nonlinearities in the solution from changes in moment and k_2. Of the three solutions the rms residual from case B is slightly larger than the other two, presumably because it lacks small dissipation terms, other than the five in the solution, which are implicit in the numerical integration.

Most of the annual term must be from tidal dissipation since the coefficient is insensitive to gravity field and core. The annual Q dominates the annual rotation term (Table 1). The annual tidal Q is ~60 (–19, +49, uncertainties are symmetrical for $1/Q$). The remaining terms require more interpretation.

Before attempting to interpret all five rotation terms, consider the influence of dissipation by both tides and core to give the observed (case B) –264±5.0 mas constant and 7.5±1.2 mas 27.6 day latitude corrections. For a –264 mas offset entirely due to tides, Table 3 (constant Q) would predict a 15.1 mas term at 27.6 days, while Table 4 (Q~1/frequency) predicts 12.4 mas. These predictions are larger than the observed correction by more than 6 and 4 times the uncertainty, respectively. Table 2 shows a dependence of the 27.6 day term on a 6 year Q as well as the monthly Q. Is it possible to adjust the monthly tidal Q and 6 year Q to match the two observed corrections? The mathematical solution gives a negative Q at 6 years. This is rejected as unphysical. To explain the two dissipation terms with core alone, Table 8 would predict –3.6 mas for the 27.6 day dissipation term. This prediction is too small by 9 times the uncertainty. The two observed latitude corrections of case B can be matched with a linear combination of tide and core dissipation. Define f_c as the fraction of the –264 mas offset due to core dissipation. Combinations based on a constant tidal Q yield $f_c = 0.41$, while those for tidal Q~1/frequency give $f_c = 0.31$. A combination of core and tidal dissipation matches the two latitude terms.

Tables 1 and 2 show that the five tidal dissipation terms of cases B and C depend on Q parameters at a variety of tidal periods. The number of independent Q parameters depends on the truncation level, and those parameters, if treated as unknown, can exceed the number of solution coefficients. A smooth function is needed for the Q dependence of tidal frequency. The Q is assumed to follow a power law $Q = Q_F$ (Frequency / $\dot{F}$)^w = Q_F (27.212 days / Period)^w. The two special cases previously considered are $w=0$ for Q independent of frequency and $w=-1$ for Q~1/frequency. A power law makes the tidally induced coefficients functions of two unknown parameters, the monthly Q_F and the exponent w. The strength of the core interaction provides a third unknown (f_c). So there are three adjustable parameters available to fit the four significant coefficients. The 206 day term does not have a significant detection and has a minor role in much of the following discussion. A power law has been used to model the frequency dependence of the solid Earth's Q (see section 20). In principle, expressions more complex than a power law are possible, and Tables 1 and 2 may allow more general forms to be tested in the future.

For the five coefficients of the case B and C solutions we return to the hypothesis that rotational dissipation can be explained by tidal dissipation acting alone. The tidal coefficients for the 27.6, 206, 365, and 1095 day terms are calculated for a sequence of w values using k_2/Q_F from the –264 mas pole offset ($24<Q_F\leq 25$ for $-1\leq w<0.6$). The small terms are scaled to the large term, which has the least relative uncertainty. Figure 3 shows the four curves for $-1\leq w\leq 1$ plus the solution coefficients from case B of Table 11. The time-delay model in the integrator matches $w = -1$, for which three solution magnitudes are smaller and one is larger than the tide-only prediction (they disagree by two to four times the uncertainties). Large positive values of w are incompatible with the sign of the 1095 day coefficient. The solution values for the annual and 1095 day coefficients cross their curves for small values of w, but the 27.6 day latitude term does not cross at all.

Instead of holding Q_F fixed to the large offset term, a Q_F curve for a sequence of w values can be derived for each case B solution coefficient. The resulting curves are shown in Plate 1. If the power law representation is valid, ideal curves (no noise) should intersect at a single point corresponding to the correct tidal w and Q_F, and curves generated from data should miss intersecting at that single point owing to noise. As can be seen, $w = -0.2$, $Q_F = 40$ is promising for three curves, but the pole offset gives $Q_F = 24.4$ for that w. A pure tidal solution is disappointing and does not reconcile these data within several times their uncertainties.

Tables 7 and 8 show that the pole offset provides most of the signature due to a core. If a core contributes a fraction f_c of the –264 mas offset term, then the (Plate 1a) tide-only Q_F for that term will be scaled upward by $1/(1-f_c)$, and the computed coefficient curves analogous to Figure 3 shrink to smaller magnitudes. The tidal and core tables (1, 2, 7, and 8) are used to compute the other four Q_F versus w curves. When a core is added to tides the 27.6 day term shifts to lower Q_F and the other three curves move slightly. Plate 1b shows the Q_F versus w curves for $f_c = 0.34$. Four curves pass near a single point. That point is $w = -0.19\pm0.13$, $Q_F = 36.8\pm5.0$ (correlation 0.25). The uncertainty for f_c is then 0.09. Either using $1/Q_F$ curves or including the 206 day Q_F curve changes the "intersection" very slightly. If $1/Q_F$ curves and the 206 day curve are used, then $w = -0.17\pm0.13$, $Q_F = 38.9\pm5.4$ (correlation 0.23), and $f_c = 0.37\pm0.09$. The use of $1/Q_F$ curves may be a more

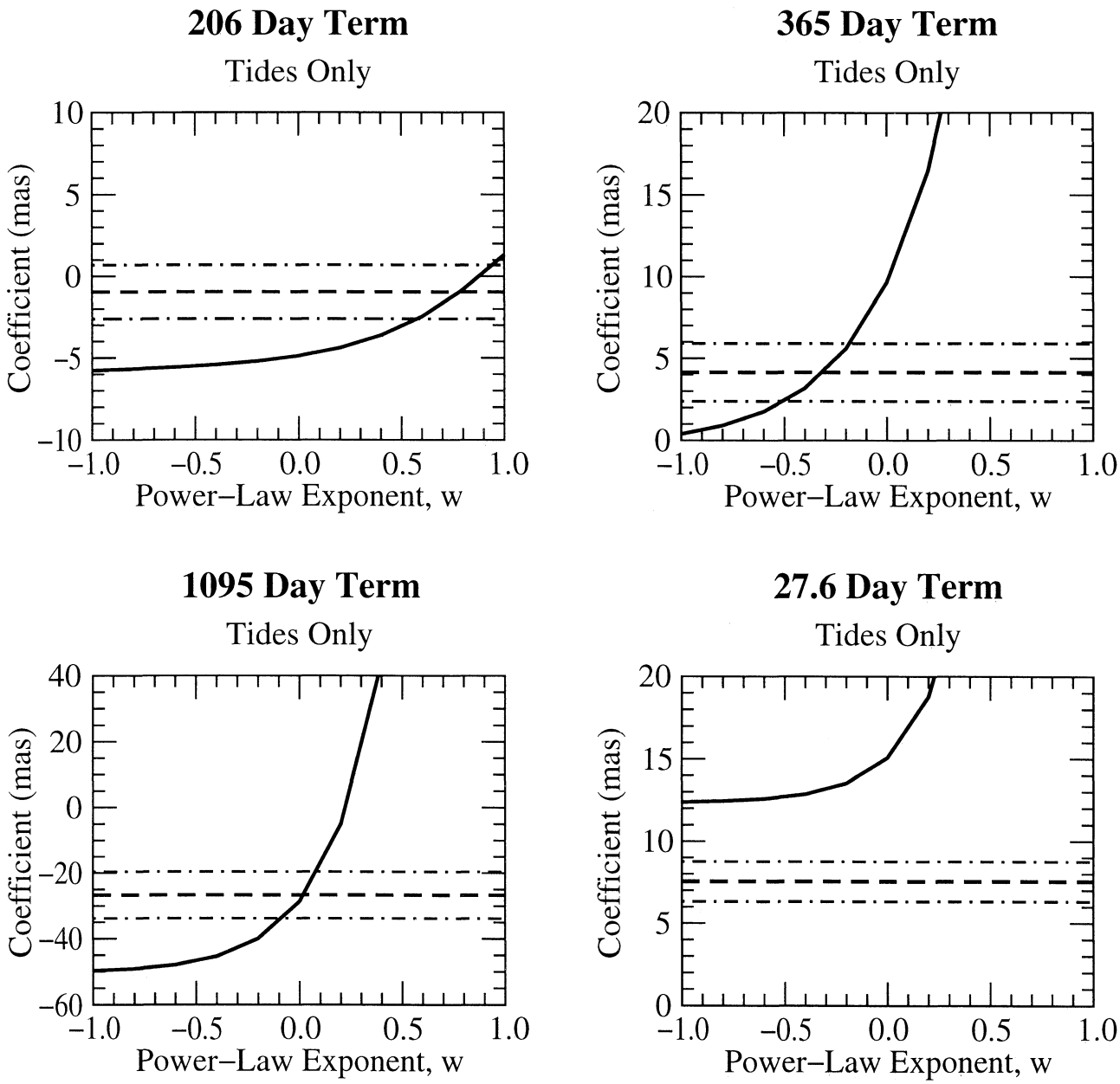

Figure 3. Dissipation signatures in rotation. The observed amplitudes (dashed lines), shown with uncertainties (dash-dot lines), are compared to theoretical amplitudes based on a power law dependence of tidal Q versus frequency (solid lines). The exponent of the power law is the abscissa. The measured amplitude of the largest term is used to scale the smaller terms. All of the dissipation is assumed to come from tides.

appropriate weighting since the rotation amplitudes are proportional to $1/Q$, but it only makes much difference if a curve is displaced from the intersection.

In Table 11 the case A solution corresponds to $f_c = 0.33 \pm 0.08$ and $Q_F = 37.6 \pm 4.6$, remarkably close to the above analysis despite the integrator's fixed value of $w = -1$. As seen in Plate 1, positive and negative curvatures help ameliorate systematic errors from the unadjusted w.

What are the model coefficients? The computed coefficients using the above $w = -0.19$, $Q_F = 36.8$, and $f_c = 0.34$ values are −3.4 mas for the 206 day coefficient, 3.9 mas for the annual, −25.7 mas for 1095 day, and 7.7 mas for 27.6 day. The 206 day term is discrepant at 1.5 times its uncertainty, and the other four are well within their uncertainties. The evaluation of the power law representation of Q as a function of tidal period gives the values in Table 12. The Q values for periods <1 month or >6 years are extrapolated outside of the most sensitive sampled band.

The anomaly of Table 11 is the eccentricity rate. In Table 9 the SLR-based terrestrial tidal models have more independently adjusted tidal components than the LLR model. An extra eccentricity rate of about $0.3 \times 10^{-11}\ \mathrm{yr}^{-1}$ would have been compatible with the SLR models. In the solutions with integrated core and tide effects, cases A and C, the anomalous eccentricity rate is >3 times its uncertainty and much larger than variations between terrestrial models can explain. An explanation for this anomalous perturbation is not evident. The case B solution zeros out the integrated orbit perturbations from lunar tides and core.

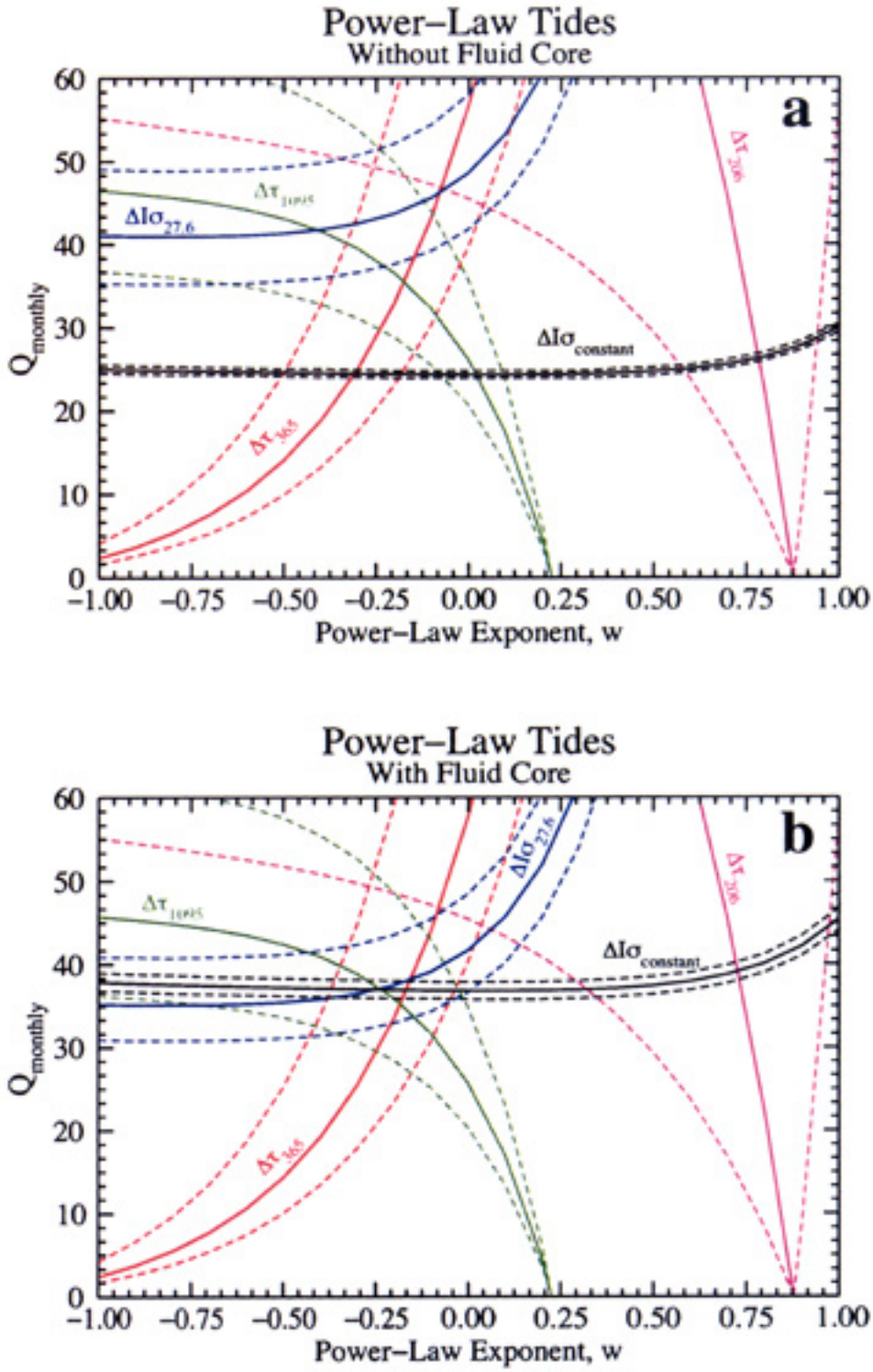

Plate 1. Observed dissipation amplitudes are used to calculate monthly Q for a power law dependence of tidal Q versus frequency. The curves (solid lines), shown with uncertainties (dotted lines), would intersect for an exact solution. (a) The tide-only case fails to represent the observed amplitudes within uncertainties. (b) Dissipation from tides plus core gives a consistent solution.

Table 12. Value of Q as a Function of Tidal Period Using the Power Law Representation $Q = 36.8\ (\ 27.212\ \text{days}\ /\ \text{Period}\ )^{-0.19}$

Tidal Period	Q	Uncertainties	
1/3 month	30	−5	+8
1/2 month	32	−5	+7
1 month	37	−4	+6
206 days	54	−11	+19
1 year	60	−15	+30
3 years	74	−24	+65
6 years	85	−30	+105
75 years	137	−64	+950

In section 15 no eccentricity rate was found from a core, so a core-only model (f_c=1) should give the rate correction of case B. That correction is 1.4 times its uncertainty, but eccentricity rate could be reconciled with its uncertainty if tides on the Earth give the higher rates of the SLR models. However, a core-only model (see Tables 7 and 8) is not compatible with three rotation terms of the case B solution. The 27.6 day coefficient is of opposite sign and the difference (solution minus Table 8) is 9 times its uncertainty, while the 1095 day and annual terms are 4 and 2 times their uncertainties, respectively. The solutions do detect tidal effects on the Moon. (Not solving for an anomalous eccentricity rate causes larger solution values for K/C.) There are several reasons that the rotation is preferred over the orbit for a core test. Four dissipation terms are detected for rotation, three of them exceeding 4 times their uncertainties, while the more weakly detected anomalous eccentricity rate is a single discrepancy. The rotation is influenced by lunar dissipation alone, while the orbit is influenced by dissipation in Earth as well as Moon. Still, the anomalous eccentricity rate serves notice that the dissipation is a complex problem and total understanding has not been achieved.

The differences between solutions can be used to check the secular orbit perturbations for n and e due to tides (Table 6) and core (section 15). When case B was subtracted from cases A and C, the change in the secular acceleration from dissipation in the Earth was the expected size but opposite in sign to that calculated from the Moon (the sum should nearly be invariant), confirming the theory for mean motion and semimajor axis change. For eccentricity rate the difference between solutions was 1.5 times that calculated, so the theory for eccentricity rate may be inadequate. Questions about the scale of the theory for eccentricity rate due to tides on the Moon are avoided by using case B, which gives a total rate of $2.0\text{x}10^{-11}\ \text{yr}^{-1}$. There is no comparable check on the theory of eccentricity rate for tides on the Earth, though other theoretical values are compatible [*Chapront-Touzé and Chapront,* 1988]. Thus not only does the orbital eccentricity rate appear to be higher than expected, but there is also an incompatibility between theory and numerical integration.

Tidal and core dissipation together match the LLR solutions (coefficients or integrated parameters) much better than tides acting alone. Notably, the failure of the 27.6 day coefficient to intersect the theoretical curve in Figure 3, or, equivalently, the wide discrepancy in Plate 1a between the Q_F derived from the 27.6 day and constant coefficients, is a major problem for a tide-only explanation of dissipation. Tides plus a fluid-core/solid-mantle interaction satisfactorily explain the lunar rotational dissipation data.

19. Molten Core: Implications and Comparisons

Detection of dissipation effects at four rotation frequencies supports both solid-body tidal dissipation and a molten core. What do these results indicate about the lunar interior, and how do they compare with other scientific information? This section discusses the core, and the next discusses the solid body.

The Lunar Laser data analysis indicates a liquid core and determines a coupling parameter. While the coupling constant depends on radius, and on the composition of the fluid core through density and viscosity, these are not separately measured. Much of the lunar core literature concerns a metallic core, usually iron and iron alloys, and that is reflected in the following discussion.

The core boundary pressure should be near 50 kbar. A fluid core is likely to include sulfur and nickel along with iron. Adding sulfur to iron reduces the density and markedly lowers the melting point. While pure Fe at 50 kbar melts at 1660°C, the Fe-FeS eutectic point is near 1000°C [*Brett,* 1973]. Adding nickel can further lower the eutectic temperature to ~940°C and can increase the density a few percent. The amount of sulfur in the core and the behavior of the Fe-FeS system are of considerable importance to the state of the liquid core; the effect of nickel is less dramatic.

Metallic iron is inferred in the mantle, and *Stevenson and Yoder* [1981] argue that a core would be on the iron-rich side of the Fe-FeS eutectic composition (25 wt % S). Cooling such an Fe-FeS melt in the liquid+solid part of the phase diagram would precipitate solid iron while concentrating the sulfur in the liquid phase. Freezing all of the liquid requires a temperature below the eutectic temperature. Liquid-outer/solid-inner core models are distinct possibilities. Completely fluid or solid cores are end-members. A completely solid core cannot have been reached since there must be at least a thin fluid shell to apply the torque that LLR analyses detect. Yoder's theory has a turbulent layer of thickness equal to the horizontal motion $R' \sin I \approx 10$ km, so this sets a minimum liquid shell thickness for the calculations to be meaningful. The relative sizes of the inner and outer cores would depend on the initial S/Fe proportion and the present core temperature. For a core of radius of 350 km with a present temperature of 1400°–1700°K, and evolutionary cooling of 50°–150°, Stevenson and Yoder calculate a sulfur mass fraction of 0.04–0.13 and a liquid shell thickness of 65–180 km.

The fluid-core/solid-mantle coupling constant is discussed in section 11. The solution parameter is K/C, but the moment C is known well enough to use K. Equation (57) relates core fraction f_c, fluid density, a theoretical parameter κ based on turbulent boundary layer theory, and core radius. The parameter κ is calculated for a thick turbulent layer adjacent to a thin laminar

Table 13. Limiting Cases, in Terms of 1 σ, for Four Core Configurations Composed of Iron and Sulfur[a]

Liquid Outer	Solid Inner	Max R', km	Max $\frac{m'}{m}$	Max $\frac{C'}{C}$ 10^{-4}	Min ξ	κ 10^{-4}
Fe	none	352	0.018	7.3	0.022	7.3
Fe	Fe	352	0.019	8.0	0.020	—
Eutectic	none	374	0.016	7.4	0.021	7.2
Eutectic	Fe	374	0.023	10.8	0.015	—

[a]Columns are given for radius, core/Moon mass ratio, core/Moon moment of inertia ratio, $\xi = -K/C'\dot{\Omega}$, and κ. The eutectic composition is 25 wt % S and 75 wt % Fe.

boundary layer using (58) based on Yoder's theory, but topography at the boundary has the effect of increasing κ. Consequently, the core sizes here are treated as upper limits.

The Lunar Laser Ranging determination gives $f_c = 0.34 \pm 0.09$. For a liquid iron core the corresponding radius is 335 (–21,+17) km. So the 1-σ upper limit of 352 km has the uncertainty added to the estimated value. Table 13 presents such upper limits for core radius and also core/Moon ratios for mass and moment of inertia. The two ratios assume a homogeneous core density. The four cases are (1) a liquid iron core, (2) a thin liquid iron shell over a solid iron inner core, (3) a liquid Fe-FeS core at the eutectic composition, and (4) a thin liquid Fe-FeS eutectic shell over a solid iron inner core. The adopted densities are liquid iron 7.0 gm cm^{-3}, solid iron 7.7 gm cm^{-3}, and the Fe-FeS eutectic 5.3 gm cm^{-3}.

The generation of Table 13 is subject to several caveats. An approximate turbulent boundary layer theory is used. A liquid shell thinner than 10 km would cause problems. Also, adding the uncertainty to the estimate gives a 1-σ limit, not a strict upper limit. Likely outweighing these concerns is the unknown size of core/mantle topography. Doubling κ reduces the size of the core by 13%, decreases the mass ratio by 44%, halves the moment ratio, and doubles the ξ. If there is a solid inner core, the liquid outer core has two surfaces for dissipation (and two values for κ), and like topography, this would cause the radius to be overestimated. An inner core could have its own rotation, increasing the complexity of the dynamics. It is assumed that the inner and outer cores rotate together to get those two limiting cases in Table 13.

The detection of the large pole offset term 2 decades ago did not allow separation of causes. *Yoder* [1981] argued that the tidal Q was not expected to be small enough to give the observed offset and therefore proposed a liquid core as the source. This paper finds both strong tidal dissipation and a substantial core. *Yoder's* [1995] boundary layer theory weakens the coupling constant by a factor of 3 over the 1981 skin friction value (κ=0.002), but since this paper finds that the core causes ~1/3 of the observed pole offset, the resulting core size is similar to that given in the 1981 paper.

How do the results of Table 13 compare with other information on a lunar core? Analyses of Apollo-era measurements on the magnetic induction of currents and of a magnetic dipole moment put an upper limit on core radius of 400–500 km [*Wiskerchen and Sonett,* 1978; *Goldstein,* 1979; *Russell et al.,* 1981; *Hood,* 1986]. Recent measurements of the induced dipole moment by the Lunar Prospector spacecraft give 340±90 km [*Hood et al.,* 1999].

Successful models of the lunar interior must be compatible with seismic results, plausible compositions, mean density, and moment of inertia. Such models favor a dense core. *Binder* [1980] finds the radius of an iron or iron-rich core to be between 200 and 400 km. Consideration of a variety of interior models by *Hood and Jones* [1987] led to metallic cores from 250 to 460 km (1–4% mass fraction). Their upper limit was set by the magnetic induction results. A study by *Mueller et al.* [1988] concluded that a metallic core of at least 150 km was necessary. A smaller core would require a crustal density below 2.9 gm cm^{-3}. *Kuskov and Kronrod* [1998a, 1998b] estimate a core of 320–390 km for iron and 490–600 km for FeS. The Apollo era provided most of the data for the models, but the recent improvement in the moment of inertia [*Konopliv et al.,* 1998] strengthened the model results. None of these conclusions conflicts with the limits of Table 13, though the tabulated limits are generally more restrictive on the upper limit. The LLR results require a liquid core or shell, while the model results can be solid or liquid.

Seismic waves have been successful at probing much of the Moon, but the deepest regions are more difficult. One ray traversing the core region was either very weakly detected and delayed [*Nakamura et al.,* 1974] or ambiguous [*Goins et al.,* 1981; *Sellers,* 1992]. If the late P wave arrival of Nakamura et al. is valid, then a molten core with radius 170–360 km is indicated. The inferred P wave speed through the core is lower than expected from pure iron, inspiring consideration of an FeS core. Sellers finds that a relocation of the impact would satisfy the data but suggests arrivals for two other events consistent with a low-velocity core about 400–450 km in radius. Free oscillations are sensitive to interior structure. *Khan and Mosegaard* [2001] have searched the seismic records for free oscillations following impacts. The spectra were stacked to give a signal-to-noise ratio of ~1.9. Their inversion does not show a liquid core, but a fluid shell could be unresolved by the 100 km granularity of their deep structure model.

Siderophile elements are expected to accompany iron into a core. Their abundances are depleted in lunar rock samples with respect to both primitive meteorites and the Earth's mantle. *Newsom* [1986] finds the depletion consistent with a metallic core of 5% mass fraction if the Moon formed from chondritic siderophile abundances. Starting with the Earth's mantle composition would generate a smaller core (mass fraction ≤1.2%). In a study of core formation, *Righter and Drake* [1996] get best agreement with siderophiles for a 5% core mass fraction but offer a 1% alternative. The sulfur mole fractions are 0.15 and 0.20, respectively. The larger core mass fractions are not compatible with the Lunar Laser results.

Thermal models exhibit variety. The example by *Toksöz et al.* [1978] has the center warming up with time, and it is stated that if a core is present, it is liquid. On the basis of several models, Toksöz states that the central temperature can be 1000°–1600°C. *Binder and Lange* [1980] present an initially molten Moon which mainly cools in the upper layers. *Schubert et al.* [1980] have most of the temperature gradient across a 290 km lithosphere, while a deeper convecting zone is isothermal. The central temperature has cooled up to 150°C. *Konrad and Spohn* [1997] and *Spohn et al.* [1999] start with a hot interior containing a liquid core. Cooling of the upper mantle forms a lithosphere, while the deepest zones cool only modestly. The former paper finds that the core remains molten to the present if its sulfur content is ~8% or more.

Many ancient lunar rocks with ages from 3.1 to 4.0 billion years show remanent magnetization. The strongest magnetization is from 3.6 to 3.9 billion years ago [*Cisowski et al.,* 1983; *Cisowski and Fuller,* 1986]. One interpretation is that the early Moon had a molten core with a dynamo which is no longer in evidence. There are several problems. Thermal evolution models which start with a cold interior do not heat the center fast enough (~1/2 billion years) to melt a core and provide an early dynamo. Sources of energy to power a dynamo have proved elusive [*Stevenson,* 1983]. A dynamo would turn off if the core solidified or if the vigor of fluid convection decreased below a threshold. *Stevenson* [1980] has proposed asymmetrical core formation with temporary dynamo action. The current absence of a global magnetic field does not preclude a partly or wholly molten core or a past field.

The power dissipated in the turbulent boundary layer is $(1.9 \pm 0.5) \times 10^{22}$ ergs yr^{-1}. This is a minor source of heating at present (see next section) but may have been important in the

past. This power scales in proportion to $\kappa n^3 \sin^3 I/(1+\xi^2)^{1.5}$. The dissipated power would have been strong when the Moon was near the Earth, but another maximum occurs near 200,000 km, just over half of the present distance. There the Moon passed through a change of spin state with the equatorial tilt I taking large values [*Ward,* 1975]. During this transition the core dissipation would have been ~10^{27} ergs yr^{-1}, provided that the core was liquid and of present size. *Stevenson* [1983] states that about 3×10^{24} ergs yr^{-1} is needed to drive a dynamo sufficiently powerful to explain the strongest remanent magnetization. The turbulent power per area is not spherically symmetrical; for power proportional to differential velocity cubed, the ecliptic poles receive $3\pi/4 = 2.36$ times the average along the equator. Even though it is deposited in the upper part of the liquid, such a nonuniform distribution of power can promote convection and, presumably, drive a dynamo. If there is an inner core, then some energy would be deposited at the lower boundary as well. If core dissipation was the source of energy for the generation of a paleofield, then the period of stronger magnetization could mark the time of high tilt near the change of spin state; the power would decrease sharply, and convection would stall as the Moon evolved outward.

Attributing part of the lunar rotational dissipation to a liquid-core/solid-mantle interaction is compatible with other lunar science data, though it is not compatible with large-core (>400 km) interpretations. Of the other lunar science information, only the uncertain seismic datum indicates a present molten core. Free oscillation data may favor a liquid shell over a fully molten core. The 1-σ limits of Table 13 indicate a small liquid lunar core with a mass fraction up to ~2%.

20. Solid Body: Implications and Comparisons

Solid-body tidal dissipation effects are detected at four rotation frequencies. This section discusses the implications for the lunar interior and the comparison with other science results.

An Earth analog would be useful for interpreting the tidal Q values for the Moon. The Earth's total response (solid body + oceans) can be measured at several periods: diurnal and semidiurnal through tidal effects, monthly and semimonthly through the response of the Earth's rotation to zonal tides, and 14 months through the Chandler wobble. Because of strong ocean responses, the solid-body tides are difficult to separate from the total measurements. At longer periods the oceans are expected to be closer to equilibrium. A determination of the solid-body semidiurnal Q of 370 (confidence interval 200–800) has been reported [*Ray et al.,* 1996]. Anelastic theory using a power law for Q favors a small positive value of w such as 0.09 [*Smith and Dahlen,* 1981]. In this paper (and in Ray et al.) the Q is defined from the phase shift of the k_2 tidal response which is the measurable quantity. Call this whole-body value the tidal Q. The properties of the Earth are not uniform, and the tidal Q is a function of the mantle Q, most strongly the lower mantle. If w=0.09 is used to extrapolate the Ray et al. value, then the tidal Q would be 260 at 1 month and 205 at 1 year. The corresponding lower mantle Q values are model dependent, but from tabulations of *Wahr and Bergen* [1986], $Q_{\text{mantle}} \approx 0.6\, Q_{\text{tidal}}$ for w=0.09. The monthly lunar tidal Q of 37 is surprisingly low by comparison with the Earth. There is less difference at the annual period, particularly if the uncertainties are considered. The lunar w=–0.19±0.13 from the power law fit indicates a slight dependence on frequency, but with a different sign than is used for Earth models.

Theories of viscoelastic rheology have the intent of connecting dissipation at a wide range of timescales [*Ross and Schubert,* 1986]. When $1/Q$ is small, then a Maxwell rheology gives Q nearly proportional to frequency (w≈1), while for a Kelvin-Voigt rheology, Q is nearly proportional to inverse frequency (w≈–1). The LLR result of w=–0.19±0.13 is in disagreement with both. The third model considered by Ross and Schubert has two adjustable parameters and can fit shallow frequency dependence over a restricted spread of frequencies.

There are lunar seismic determinations of local Q versus depth based on frequency bands near 1 and 8 Hz [*Nakamura,* 1983; *Goins et al.,* 1981]. The P and S wave seismic data show Q>1000 in the upper zones, much larger than for the Earth, perhaps owing to the anhydrous nature of lunar rocks, with Q decreasing with depth. *Nakamura and Koyama* [1982] find that the S wave Q increases with frequency above 5 Hz. Goins et al. call the region below 1100 km depth the attenuation zone. Both S and P waves are diminished, but the attenuation in this zone is stronger for S waves than for P waves. Goins et al. say Q<500 and *Nakamura et al.* [1982] say Q<100 for S waves. The Q values of both the LLR analysis and the S wave data correspond to dissipation associated with the rigidity or shear modulus. The anelastic theory for the Earth treats dissipation at seismic through Chandler wobble frequencies as arising from a common phenomenon. If the Moon can be treated similarly, then it suggests that the attenuation zone may be the cause of the low tidal Q. However, this would imply a very small local Q for the attenuation zone since it has only 4% of the lunar volume. If the bulk of the tidal dissipation is not in the attenuation zone, then the seismic and long-period tidal Q values are both larger than the monthly Q and a simple power law cannot connect them. It has been suggested that the seismic attenuation zone is due to a partial melt [*Nakamura et al.,* 1974; *Goins et al.,* 1981]. If the lunar tidal Q mainly arises from a partial melt, then it is unlike the Earth's solid-body tidal Q.

One of the consequences of anelastic theory is that it causes the Love numbers to be frequency dependent, violating one of the assumptions of this paper. There are pairs of terms which cancel because of this assumption. So there would be additional terms from the tidal torques, but orthogonal to this paper's dissipation terms.

Just above the attenuation zone lies a region (depth 700–1100 km) of deep-focus moonquakes. The juxtaposition of the two zones could indicate that an abrupt change in rheological properties is concentrating the strain [*Goins et al.,* 1981]. The deep moonquakes repeat monthly and appear to be triggered by tides.

For all of the solutions in Table 11, the secular acceleration $\Delta\dot{n}$ from tides on Earth and Moon plus core interaction is –25.9 " cent^{-2}, and the semimajor axis rate change is $\Delta\dot{a}$ = 38.2 mm yr^{-1}. For a lunar Q of 37±5 the tides cause changes of 0.29±0.04 " cent^{-2} and –0.43±0.06 mm yr^{-1}, respectively, while the core-mantle interaction gives only 0.013±0.003 " cent^{-2} and –0.019±0.005 mm yr^{-1}. The rate of energy deposited in the Moon is equal to the rate of energy drawn from the orbit: $(4.3\pm0.6)\times10^{23}$ ergs yr^{-1} for tides and $(1.9\pm0.5)\times10^{22}$ ergs yr^{-1} for the core-mantle interaction. The dissipation rate expressed as a steady state flow through the lunar surface is 3.8 nw cm^{-2}, much smaller than the (radiogenic+cooling) heat flow: 480 times smaller than the 1.8 μw cm^{-2} of *Langseth et al.* [1976] and 320 times smaller than the 1.2 μw cm^{-2} of *Warren and Rasmussen* [1987]. Though former assumptions about lunar Q are now removed, we concur

with earlier studies [*Kaula,* 1963, 1964; *Kaula and Yoder,* 1976; *Peale and Cassen,* 1978] that tidal heating for the present bulk Moon is not important compared to radiogenic heat sources.

How does the tidal power compare with the energy released by tidally triggered deep-focus moonquakes? *Goins et al.* [1981] give 8×10^{13} ergs yr^{-1} for the latter. It is plausible that tidal energy powers these moonquakes. The tidal power is ten orders of magnitude larger than the deep-focus energy release. On average the energy dissipation in a 2 km region is comparable to the total deep-focus seismic release. The A1 focus has a size of ~1 km [*Nakamura,* 1978]. The stress drop is compatible with tidal strains [*Toksöz et al.,* 1977; *Cheng and Toksöz,* 1978], and the moonquakes reverse direction during part of the tidal cycle. Whether tidal energy powers the moonquakes or not, it is clear that the energy dissipated in deep moonquakes does not contribute significantly to the tidal Q. For shallow-focus moonquakes, Goins et al. give an energy release of 2×10^{17} ergs yr^{-1}, but there is no evidence that these are tidally influenced.

The Lunar Laser analysis determines a bulk tidal Q, and it is unknown whether this low Q is a widespread property of lunar rock or whether there is a localized zone of high tidal dissipation. First consider the distributed case. For steady state thermal models with uniform conductivity (3.5 w m^{-1} $°C^{-1}$), uniform tidal energy deposition, and no convection, the mean temperature of the Moon would increase 3.5°C, and the center would rise 9°. This is minor compared to radiogenic heating. In addition to tidal dissipation, 4% of the total energy is being deposited in a thin boundary layer (roughly 10 km thick, according to Yoder's theory) at the core-mantle interface. This should raise the temperature at the core-mantle boundary ~4°. Uniform energy deposition is an idealization since even uniform elastic properties lead to strain and dissipation increasing with depth.

Consider a zone of high tidal dissipation. Since radioactive minerals tend to migrate upward, localized deposition at depth would increase the importance of tidal deposition with respect to radiogenic sources. An attenuation zone from 350 to 640 km radius has 4.2% of the lunar volume. This zone is known to be a sink for seismic energy, so it is possible that a substantial portion of the tidal energy is being deposited in a small volume just above the core. If most of the tidal energy is being deposited in the attenuation zone, then the (steady state) outward flow of tidal and turbulent power would raise the temperature ~32° at the top of the attenuation zone.

On evolutionary timescales, thermal effects from tides are more interesting. This question has been considered by *Peale and Cassen* [1978]. To scale their power calculations to the monthly k_2/Q of this paper, multiply by 3.45. The frequency dependence of this paper's Q would increase that further. Dividing the accumulated energy by the product of heat capacity (1.2×10^7 ergs gm^{-1} $°C^{-1}$) and mass (7.35×10^{25} gm) gives an upper limit for average temperature increase. Since the early tidal evolution is fast and deposits most of the energy early in the Moon's history, the limit may be close to the early temperature gain. Peale and Cassen estimated that tidal dissipation would increase the mean lunar temperature by 40°C, but the above factor raises it to 140°C. For a uniform Moon they also calculated the spatial distribution of power per volume, and the center receives about three times the average. Thus Peale and Cassen's scaled results indicate that even a uniform Moon could have tidally heated the center by ~400°C, and for a nonuniform Moon it could be higher.

Peale and Cassen stretched the timescale for tidal evolution to match the age of the two bodies, and their above total heating is proportional to the stretching. This was done because, extrapolated backward, the measured tidal acceleration brings the Moon close to the Earth in a time (1.6×10^9 years by our calculations) that is much less than the age of either. Even with a uniformly stretched timescale (a factor of ~2.7), the time to evolve outward to the distance (about half present) of *Ward*'s [1975] spin transition is fast, $<10^8$ years. The tilt of the lunar equator and, consequently, the tidal and (if the core is liquid) turbulent power are increased during and near the transition. In addition to the transition, high power occurs when the Moon is close to the Earth. However, computations based on the present measurements are not easily extrapolated to times before the figure froze or into the magma ocean era.

The Earth's tidal dissipation is mainly localized in the oceans. The extent, depth, and shape of the oceans depend on plate motion, so it is reasonable that the tidal Q varies, and it is plausible that the present tidal rate is higher than average. The tidal response of the oceans to the tidal forces at the tidal frequencies depends on the natural frequencies, strengths, and dissipation of oceanic normal modes. The normal modes depend on the changing configurations of the oceans and continents, and the tidal frequencies change owing to the evolution of the lunar orbit and Earth's spin. The timescale stretching is an important question, and one can look to the tidal paleorotation data for guidance. As reviewed by *Lambeck* [1980, 1988], paleorotation data are most dense for the past 4×10^8 years, but are noisy. The number of days per year seems to support an average rate of orbital evolution compatible with, or somewhat less than, the LLR-derived tidal recession. The number of days per month indicates either a lower rate, a nontidal acceleration of Earth rotation, or a systematic loss of tidal bands. Two older data may indicate a slightly stretched timescale for the past 9×10^8 years [*Sonett et al.,* 1996]. Any substantial stretching appears to be earlier. The timescale problem has been investigated using idealized ocean models. As summarized by *Bills and Ray* [1999], the most important influence is found to be the changing tidal frequency. The present semidiurnal tidal frequencies are higher than the most important normal mode frequencies, and the faster spin rate in the past would have decreased the tidal $1/Q$. Thus the timescale is stretched nonuniformly. The present tidal evolution is similar to measured values, and earlier rates are slower than those based on constant Q.

Peale and Cassen's [1978] tidal power computations kept the orbit eccentricity and inclination fixed while the distance changed. Preliminary calculations here indicate that an evolving orbit increases the power deposited in the Moon by both tides and core-mantle interaction. This occurs because, near the spin transition, both lunar tides and core dissipation cause a large negative orbital inclination rate, so a large inclination (>30°) is possible before the transition. A larger inclination causes increased tidal and turbulent dissipation. With evolution and this paper's k_2/Q the tidal power increase near the spin transition is an order of magnitude larger than that of Peale and Cassen. Without stretching the timescale it is possible to heat the center by ~200°C, provided a Q of 37 is appropriate; most (90%) of this heating occurs in the first 1.3×10^8 years ($<3 \times 10^7$ years to reach transition). Stretching the timescale increases the energy deposited in the Moon (a factor of 2.7 for a uniform stretch) and also increases the pretransitional orbital inclination. Stretching can also delay the evolution of semimajor axis through the transition distance if the Moon can extract as much power from

the orbit as the Earth deposits, but the decreasing inclination ends such a balance by reducing the power that the Moon extracts. Tides may be a significant source of heating for the early Moon, and much of that heating is deep.

During the spin transition a molten core comparable to that existing today would generate peak power (10^{27} ergs yr^{-1}) and accumulated energy similar to that from tides, but it would be deposited in <1% of the lunar volume. The liquid core formation history is not known. It may have originated during lunar formation. Another possibility is that a small core was present before transition, and the additional heating at the core-mantle boundary increased melting and core size. Yet another possibility is that the combination of heating by accretion, radioactive decay, and tides first generated a liquid core or layer before the Moon finished passing through the high-obliquity event. Once the turbulent dissipation starts with high equatorial tilt, that energy is deposited in a relatively small volume, and it can promote further melting, fluid convection, and a dynamo (see previous section). The unknown history makes the accumulated turbulent energy very uncertain. The possible upper range of energy densities would have caused a dramatic thermal event for the core and the adjacent mantle region.

If the strongest remanent magnetism in lunar rocks corresponds to the spin transition, then the timing is $5x10^8$ years late compared to a uniformly stretched tidal evolution timescale. Of the Earth's present tidal dissipation, 97% is in the oceans. On the earliest Earth the oceans were likely very different from now. The heavy bombardment would have supplied volatiles, but the largest impacts could remove atmosphere and ocean. For comparison, basin-forming events occurred on the Moon between 3.8 and 3.9 billion years ago; earlier basins either have been erased or were not sampled by missions. The early Earth was heated by both impacts and core formation. *Galer* [1991] considers that prior to about $3.8x10^9$ years ago, the warmer mantle would have prevented any continental masses from rising above the elevation of oceanic rock as they do today. It is plausible that intermittent oceans, less continental material, and reduced height difference would make the early Earth less effective at dissipating energy and evolving the lunar orbit outward. Even without oceans on Earth, the Moon would evolve outward owing to solid-body Q.

A qualification is in order. The preceding temperature increments are useful for relative comparisons of energy deposition, but strong heating of any part of the Moon can promote solid convection at the expense of temperature increase [*Schubert et al.,* 1980], and any melting would absorb heat. Starting a thermal model with a core 100°–200°C hotter than the mantle, *Konrad and Spohn* [1997] and *Spohn et al.* [1999] find that the early Moon had convection in the solid mantle. These computations generate mantle plumes which, for upwelling plumes, result in pressure release partial melting in the upper mantle. This melt is available for volcanism. The results of these two papers also seem appropriate if the initial excess core heat is replaced with turbulent heating at the core-mantle boundary, and *Petrova and Gusev* [1997] have suggested that a turbulent interaction could also cause plumes. Konrad and Spohn also find convection in the early lunar fluid core.

There are many uncertainties and concerns. It is not known when the core becomes molten. Near the spin transition both lunar tides and core dissipation cause large inclination changes, so a large orbital inclination is possible before the transition, and that increases both tidal and turbulent power deposited in the Moon. Any stretching of the timescale makes these even larger. If the present low tidal Q is due to a partial melt in the attenuation zone, the earlier Q could have been very different before heating or core formation.

The LLR fits of this paper indicate a present eccentricity rate of $2.0x10^{-11}$ yr^{-1}. The (Earth+Moon) theory predicts from $0.7x10^{-11}$ yr^{-1} to about $1.0x10^{-11}$ yr^{-1} with dissipation in the Moon canceling 40–50% of the effect from the Earth. This is a serious discrepancy. Stretching the timescale for tidal evolution of the orbit by reducing the dissipation in the Earth would make the average eccentricity rate negative for much of the time of evolution, on the basis of the theoretical calculations. However, the unexplained anomalies in the eccentricity rate and its computation make any extrapolation unclear. Higher eccentricity in the past would increase the dissipation in the Moon. *Goldreich* [1963] appreciated that dissipation in the Moon might reverse the sign of the eccentricity rate. Recent studies such as *Mignard* [1981] and *Touma and Wisdom* [1998] considered evolution for several values of lunar dissipation, but variable orientation with the spin transition was not modeled. The "problem" of a sizeable initial orbit inclination is increased when lunar orientation is included in calculations of dissipation and evolution. Tidal evolution is reviewed by *Peale* [1999].

At the lunar surface, tidal displacements from the largest monthly terms are ~0.1 m. Consequently, the Q of 37 corresponds to a few millimeters for the phase-shifted components. Tidal displacement is presently detected (h_2 in Table 11), but not with sufficient accuracy to see such effects. For the solutions of Table 11 the Love number l_2 is constrained to be 0.3 h_2, the relation expected for a homogeneous elastic solid.

The lunar science discussion of *Dickey et al.* [1994] points out that an oblate lunar core can bias the LLR solution values of k_2. Simple extrapolation of the seismic S wave mantle speeds through the attenuation zone predicts k_2 values lower than the LLR results by ~25% for the *Nakamura* [1983] S wave profile and 15% for the *Goins et al.* [1981] profile. Lowering the S wave velocities in the attenuation zone would increase the seismic predictions. Given this paper's evidence for a fluid core, the LLR values of k_2 may need to be reduced up to 25%. The solutions for tidal dissipation are sensitive to k_2/Q, so if the Love number is reduced, all of the Q values would scale in proportion, but the calculations of energy dissipation would be unchanged. Such a systematic scaling is not included in the random uncertainties in k_2 and tidal time delay in Table 11 and the Q values in the text or Table 12. In principle, the h_2 determination could detect such a scaling, but the present uncertainty is too large. Rotation signatures due to an oblate core should be orthogonal to the dissipation signatures and will be the subject of future study.

Damping of the free librations can be calculated from the equations of this paper (sections 7 and 12) or *Peale* [1976]. For the free libration in longitude the damping time is $2.7x10^4$ years. Most of the damping is from the tides, and the uncertainty in the inverse is 50% ($1/Q$ at 3 years in Table 12). The damping time for the wobble mode is about $2.0x10^6$ years and is dominated by tides. The uncertain extrapolation of the tidal Q to 75 years causes a 90% uncertainty for the inverse. The precession/nutation mode damping is $1.65x10^8$ years (15% uncertainty) with core damping 70% and tidal damping 30%. The energy in each free libration mode is proportional to the amplitude squared. Amplitudes are taken from *Newhall and Williams* [1997] and Williams et al. (2001). The free libration in longitude has an energy of $9.6x10^{16}$ ergs, and it is dissipating $7x10^{12}$ ergs yr^{-1}. For the two latitude modes the energy is not constant during one cycle, so an average energy is used here.

The average in the wobble mode is 2.9×10^{21} ergs, and the power loss is 3×10^{15} ergs yr^{-1}. The small precession/nutation mode has an average energy of 3×10^{13} ergs and a loss of only 2×10^{8} ergs yr^{-1}.

21. Summary

For 2 decades the analysis of Lunar Laser Ranging (LLR) data has detected a displacement in the Moon's precessing pole of rotation indicating energy dissipation. Two explanations have been offered: tidal losses in the Moon and interaction at the interface between a liquid core and solid mantle. The key to distinguishing the two causes is small additional influences on the rotation. Both numerical and analytical approaches are considered.

The orbit and lunar rotation are integrated numerically with a model for tides and fluid core. These numerical results are used to calculate the range during data fits. The differential equations for dissipation acting on rotation are set up (sections 2 and 3). Analytical series solutions are also developed for both interpretation and alternate fits. Section 4 continues the development for series solutions, and section 5 presents the series. Tables 1 and 2 give the dependence of each rotation term on each periodic tide's Q. Evaluations are given for two functions of tidal Q versus frequency: constant Q (Table 3) and Q proportional to inverse frequency (Table 4). The most useful terms influence the LLR data at periods of 1 month, 206 days, 1 year, 3 years, and 6 years. Tidal dissipation also damps free librations (section 7) and causes secular orbit perturbations (section 8, Table 6).

The mathematical model for a fluid-core/solid-mantle interaction (section 9) sets the torque proportional to the angular velocity difference between spinning core and mantle. This rule is used for numerical and analytical approaches. As the mantle orientation precesses in 18.6 years it induces a core precession, but with much smaller tilt and an offset node (section 10). The core orientation is closer to the ecliptic plane than to the mantle. The core does not rotate at the same rate as the mantle, and this causes a longitude offset for the direction of the principal axes. The core dissipation causes the node of the equator plane on the ecliptic and the pole direction to be shifted. The parameter K, which relates torque to angular velocity difference, is discussed in section 11. The K for turbulent coupling is a function of core radius, fluid density at the boundary, and several other parameters. Topography on the boundary may increase coupling.

For analytical investigation the coupled equations for core and mantle rotation are developed (section 12). The separate rotation of the core introduces core damping modes. The core modes damp rapidly; ~140 years is estimated. Expressions for slower damping of mantle free modes are also given. The forced terms are derived (section 13, Tables 7 and 8), but the precessing pole offset is by far the most observable core term. The forced terms, including the pole offset, are mainly sensitive to K. A special term, due to the secular motion of the ecliptic plane, is directly sensitive to core moment rather than K (section 14). It offers future possibilities to determine that moment.

Lunar core dissipation causes secular orbit perturbations (section 15). For a given pole offset, perturbations from a core are smaller than those caused by tides on the Moon. This difference permits an orbit test for separating core and tidal dissipation, with the eccentricity rate being the most useful of the perturbations (section 16). Tides on the Earth also cause secular orbit perturbations, so an orbit test is sensitive to more dissipation sources than a rotation test. At present, the lunar rotation is the preferred test to distinguish dissipation from core and tides (section 17).

Twenty-eight years of Lunar Laser Ranging data are used to make solutions for dissipation effects (section 18). Numerically generated partial derivatives and analytical coefficients are both used as fit parameters (Table 11). All solutions indicate substantial dissipation from both a molten core and tides. Four dissipation coefficients are detected, and Plate 1 compares them with calculations using tides alone and tides plus core. The core parameter exceeds three times its uncertainty. Core-only interpretations fare worse, failing by 9 σ. The tidal Q at 1 month is 37 (–4,+6), and at 1 year Q is 60 (–15,+30). If a power law is used for Q versus frequency, the exponent is -0.19 ± 0.13, so Q increases slowly with period. The orbit eccentricity rate from fits is 2×10^{-11} yr^{-1}. This is two to three times the expected rate and is not understood.

With turbulent core-mantle coupling the inferred core radius is 335 (–21,+17) km if it is assumed to be iron (section 19). Because topography at the core-mantle boundary would increase the coupling, the core radius is presented as a 1-σ upper limit: 352 km for iron and 374 km for an Fe/Fe-S eutectic. Table 13 gives core parameters for a spread of possibilities: the two extreme compositions and liquid cores with and without solid inner cores. Other lunar science information is compatible with or supports a presently solid or molten core.

The power drawn from the orbit and dissipated in the Moon is $(4.3 \pm 0.6) \times 10^{23}$ ergs yr^{-1} for tides and $(1.9 \pm 0.5) \times 10^{22}$ ergs yr^{-1} for the core-mantle interaction (section 20). These are minor compared to radiogenic heating. Deep-focus moonquakes are thought to be triggered by tides and a small fraction of the tidal energy is sufficient to power them. The low tidal Q is surprising. The highest seismic damping is just above the core, and it has been suggested that this is a zone of partial melt. It is plausible that this zone dominates the tidal damping. Damping times for the free librations are calculated from the core and tide dissipation.

Both tide and core dissipation may have been significant heat sources in the early Moon. The dissipated power would have been high when the Moon was near the Earth and decreased as the Moon evolved outward owing to tidal dissipation in the Earth, but an additional peak would occur at about half the present distance. A transition between two spin states would have caused temporary high lunar obliquity and an increase in the energy dissipation from lunar tides and core. Tidal dissipation could have heated the central region by several hundred degrees. If the tidal dissipation is localized in the attenuation zone adjacent to the core, this region could have been heated even more. If the lunar core was its current size, a similar amount of energy would have been deposited in the smaller volume of the core-mantle boundary. This early energy could have caused major thermal activity in core and lower mantle, temporarily driving convection in the fluid core and solid convection in the lower mantle and powering a magnetic field. Thus the remanent magnetization in lunar rocks, peaking circa 3.8×10^{9} years ago during the time of mare volcanism, may record the passage of the Moon through the spin transition as the Moon evolved outward under the action of the Earth.

Detection of an independently rotating molten core through its drag on the mantle exceeds three times its uncertainty. The association of high core dissipation during a change of spin state with peak remanent magnetization is plausible but unproved. There are ample opportunities for future investigation.

Appendix A: Spherically Symmetrical Distortion

In (8) the rotational potential was separated into degree two and spherically symmetrical parts. To describe a body's elastic response, the second-degree Love number k_2 is more familiar than the spherically symmetrical parameter designated s in sections 3 and 4. *Love* [1944] presented the displacement due to the rotational potential $r^2\omega^2/3$ for the incompressible homogeneous sphere. *Dahlen* [1976] considered a more general body. He gave differential equations for displacement, and he also addressed the moment of inertia change. Working with perturbed rotation ($\Delta\omega^2 = 2\,\omega\Delta\omega$), Dahlen introduced a factor of 2 in his definition of displacement that is not used by Love. *Yoder et al.* [1981] followed Dahlen, while *Yoder* [1982] used the unperturbed potential with Love's solution. This appendix uses Love's potential, considers the moment change, and presents Love's displacement and the resulting moment change for the homogeneous case.

For an incompressible homogeneous sphere with density ρ, radius R, bulk modulus K, and shear modulus or rigidity μ, Love's solution (his article 175) for the radial displacement $U(r)$ using the spherically symmetrical rotational potential is

$$U(r) = \frac{\rho\,\omega^2 R^2 r}{15\left(K + \frac{4}{3}\mu\right)}\left(\frac{5K + \frac{8}{3}\mu}{3K} - \frac{r^2}{R^2}\right). \quad \text{(A1)}$$

This problem is analogous to the self-gravitating sphere (Love's article 98). The strain dU/dr reverses sign in the interior. The displacement at the surface depends on K, but not μ.

$$U(R) = \frac{2\,\rho\,\omega^2 R^3}{45\,K}. \quad \text{(A2)}$$

Dahlen [1976] defined a parameter d_0 that with the U here would be $3g(R)U(R)/\omega^2R^2$, where $g(R)$ is the surface gravitational acceleration (1.623 m s^{-2} for the Moon).

A solid's mass element $dm = 4\pi r^2 \rho\, dr$ is invariant to spherical distortion. Evaluate the moment of inertia from the integral

$$\frac{2}{3}\int_0^R (r + U(r))^2\, dm. \quad \text{(A3)}$$

For small distortions the change in the moment is

$$\Delta I = \frac{16\pi}{3}\int_0^R \rho(r)\, U(r)\, r^3\, dr. \quad \text{(A4)}$$

The moment matrix change is ΔI times the identity matrix. To put ΔI into the form of (9) and (12), define

$$s = \frac{16\pi G}{\omega^2 R^5}\int_0^R \rho(r)\, U(r)\, r^3\, dr. \quad \text{(A5)}$$

This looks like *Dahlen*'s [*1976*] expression for n_0, but his $U(r)$ has an additional factor of 2, so $s = n_0/2$.

For a homogeneous sphere, use a constant density and the displacement (A1) in the integral of (A5).

$$s = \frac{16\,G\,M\rho}{525\,R\,K}\,\frac{\left(5K + \frac{14}{3}\mu\right)}{\left(K + \frac{4}{3}\mu\right)}. \quad \text{(A6)}$$

Note that $GM/R = g(R)R = v_c^2$, where v_c is the surface circular orbital speed (1.680 km s^{-1} for the Moon). When the above result for s is doubled, it agrees with *Yoder*'s [1982] value for n_0. The elastic parameters are related to the P and S wave speeds:

$$V_P^2 = \frac{\left(K + \frac{4}{3}\mu\right)}{\rho}, \quad \text{(A7)}$$

$$V_S^2 = \frac{\mu}{\rho}. \quad \text{(A8)}$$

While k_2 is sensitive to V_S and the shear modulus μ, both speeds and both elastic parameters influence s. The phase shifts and specific dissipation Q parameters associated with s are not expected to be the same as those for k_2.

The seismic speeds are well determined in the upper zones of the Moon but uncertain for the deepest regions [*Goins et al.*, 1981; *Nakamura*, 1983; *Khan et al.*, 2000]. For computation, V_S = 4.4 km s^{-1} and V_P = 7.8 km s^{-1} are used here. The Love number k_2 should be between 0.02 and 0.03, and both s and d_0 should be about 0.010–0.012. The spherical radial displacement of the lunar surface is ~5 cm owing to the rotation. For comparison, a Love number h_2 = 0.04 causes the surface at the pole to decrease 18 cm and the equator to increase 9 cm (ignoring the question of whether this Love number is appropriate for the static part of the distortion). The net surface change is 13 cm downward at the pole and 14 cm outward at the equator. The relative change of rotation rate $\Delta\omega/\omega$ is ~10^{-4}, so the spin-induced surface variations are ~0.03 mm. By contrast, tides raised by the Earth are ~0.1 m, while those raised by the Sun are 2 mm.

The time variation of tidal distortion greatly exceeds the variation of spin distortion, and the effects on rotation are similarly stark. The largest rotation effect due to s displaces the pole by $(\Delta p_1, \Delta p_2) = -0.05''\ s\ (\sin F, \cos F)$. The largest tidal k_2 effect is $(\Delta p_1, \Delta p_2) = 74''\ k_2\ (\sin F, \cos F)$. The s pair of terms comes from the constant part of ΔI and would disappear if the mean moments were put in the "rigid" moments A, B, and C. The k_2 pair is dominated by variable moment effects. The largest dissipation term in longitude from s is $0.003''\ (s/Q)\cos 2(F-\ell)$, very small compared to Tables 1–4 for k_2/Q. Consequently, the Love number k_2 and associated Q values can be determined from analyses of Lunar Laser data while the effects of s and s/Q are too small to fit those parameters.

Appendix B: Toroidal Distortion

Acceleration of the rotation will cause forces on a body. In the rotating coordinate system the acceleration is $\mathbf{r}\times\dot{\boldsymbol{\omega}}$. The resulting distortion is toroidal about the axis of spin acceleration. *Bills* [1995] suggested that the toroidal distortion could be mimicking rotation and corrupting fits of the Lunar Laser ranges, but he did not compute its size. *Yoder* [1982] computed the form of the distortion solution for the homogeneous case. Below, Yoder's solution is modified to give distortion without a change in rotation.

Yoder [1982] gives the solution for the incompressible homogeneous sphere. The acceleration $\dot{\boldsymbol{\omega}}$ causes a twisting distortion about the axis of angular acceleration. Here the particular solution is chosen so that the acceleration-induced distortion does not modify the angular momentum. For a distortion vector $\mathbf{U}$ and mass element dm, set $\int \mathbf{r}\times\dot{\mathbf{U}}\, dm = 0$. Restricting our interest to periodic variations of the magnitude of $\dot{\boldsymbol{\omega}}$, there results

$$\mathbf{U}(\mathbf{r}) = \frac{\rho}{10\,\mu}\left(r^2 - \frac{5}{7}R^2\right)\mathbf{r}\times\dot{\boldsymbol{\omega}}. \quad \text{(B1)}$$

The notation for density, shear modulus, and radius are the same as used for the spherical distortion. The reversal of sign in the interior keeps the angular momentum from changing. The distortion at the surface is

$$\mathbf{U}(\mathbf{R}) = \frac{\rho R^2}{35\,\mu}\,\mathbf{R}\times\dot{\boldsymbol{\omega}}. \quad \text{(B2)}$$

The surface distortion does look like a rotation about the angular acceleration axis and it can mimic a rotation, but the distortion with depth only resembles solid rotation for the particular solution.

The two largest accelerations of the body-referenced spin axis are from the monthly variation of physical libration in longitude and a periodic variation of the precessing spin pole direction with respect to the body z axis. The resulting distortion at the surface expressed in micrometers is

$$\mathbf{U}(\mathbf{R}) = -4\,\hat{\mathbf{R}}\mathbf{x}\mathbf{k}\,\sin\ell + 12\,\hat{\mathbf{R}}\mathbf{x}\mathbf{j}\,\sin F. \quad \text{(B3)}$$

The unit vectors $\mathbf{j}$ and $\mathbf{k}$ are in the direction of the y and z body axes, while the unit $\hat{\mathbf{R}}$ vector is toward a surface point such as a lunar retroreflector. The toroidal distortion is not a significant influence on the LLR fits and is not large enough to warrant modeling.

Notation

a	orbital semimajor axis of Moon.
a, b	amplitudes in section 13; subscripts s, c mean sine and cosine components.
a', b'	core amplitudes in section 13; subscripts s, c mean sine and cosine components.
A, B, C	constant lunar moments of inertia.
C'	core moment.
C_{21}, C_{22}	second-degree gravity harmonics of Moon.
D	mean elongation of Moon from Sun.
D	with subscripts L, w, p, a damping coefficient.
e	orbital eccentricity for Moon.
E	combination of parameters used in (28) and separately in (52); Earth mean longitude in Table 7.
F	mean argument of latitude of Moon.
f_c	core fraction for precession offset.
f_x, f_y, f_z	forcing terms in differential equations.
G	gravitational constant.
g	gravitational acceleration.
H	forcing amplitude for longitude libration.
h_2	vertical displacement Love number.
i, j	subscripts are indices running 1–3.
i	orbital inclination of Moon to ecliptic, 5.145°; imaginary in section 13.
I	mean tilt of lunar equator to ecliptic, 1.543°.
I'	mean tilt of core equator to ecliptic plane.
$\mathbf{I}$	moment of inertia matrix.
$\mathbf{I}'$	core moment of inertia matrix.
$\mathbf{I}_{\text{rigid}}$	moment of inertia matrix, rigid body part.
$\mathbf{I}_{\text{tide}}$	moment of inertia matrix, tidal deformation.
$\mathbf{I}_{\text{spin}}$	moment of inertia matrix, spin deformation.
J_2	second-degree gravity harmonic of Moon.
k_2	potential Love number.
k_f	fluid Love number.
K	core-mantle coupling parameter; sometimes used with subscripts t and v.
l_2	horizontal displacement Love number.
ℓ	mean anomaly of Moon.
ℓ'	mean anomaly of Earth-Moon orbit about Sun.
L	mean longitude of Moon.
L'	mean longitude of Sun with respect to Earth-Moon center of mass.
M	mass of Earth; Mars mean longitude in Table 7.
m	mass of Moon.
n	mean motion of Moon.
n'	mean motion of Earth-Moon orbit about Sun.
p	orbital semilatus rectum for lunar orbit.
p_1, p_2	physical libration in latitude; overdots are time derivatives.
p_1', p_2'	core physical libration in latitude; overdots are time derivatives.
P	power; fit parameter in section 17.
P_{ave}	average power.
P_2	second Legendre function.
Q	specific dissipation for tides; various subscripts indicate frequency.
r	distance from Moon.
$\mathbf{r}$	position vector from Moon to Earth or Sun.
rms	abbreviation for root-mean-square.
R	radius of Moon, 1738 km; range in section 17.
R'	radius of lunar core.
$\mathbf{R}$	range vector from an observatory on the Earth to a retroreflector on Moon.
$\mathbf{R}_s$	vector for geocentric ranging station.
$\mathbf{R}_r$	vector for selenocentric retroreflector position.
s	spherical spin parameter.
S_1, S_2, S_3	numerical factors.
S_{21}, S_{22}	second-degree gravity harmonics of Moon.
S_{31}, S_{33}	third-degree gravity harmonics of Moon.
t	time.
$\mathbf{T}$	torque vector.
$\mathbf{T}_2$	torque vector, second-degree contribution.
$\mathbf{T}_c$	torque vector, core contribution
$\mathbf{u}$	unit vector from Moon to Earth or Sun.
u_1, u_2, u_3	components of unit vector from Moon to Earth or Sun in lunar body-fixed coordinates.
u'	unit vector to point on lunar surface.
U_{ij}	matrix components, $(a/r)^3\,u_i\,u_j$.
$\mathbf{v}$	core-mantle relative velocity vector at boundary.
V	Venus mean longitude in Table 7.
V_{tide}	tidal potential.
V_{spin}	spin potential.
w	exponent in Q versus frequency power law.
x, y, z	coordinates.
X, Y	forcing amplitudes in section 13.
X, Y, Z	Moon centered reflector coordinates in section 17.
α	$(C–B)/A$.
β	$(C–A)/B$.
γ	$(B–A)/C$.
δ_{ij}	delta function.
Δ	used to indicate a change, e.g., Δa, Δe, and Δn.
Δt	time delay.
Δ_c, Δ_m, Δ_t	determinants.
κ	fluid core parameter, equation (58).
ν	frequency; kinematic viscosity of core in section 11.
ν_p	frequency of free precession, a resonance frequency.
π	mathematical symbol for pi.

Π	ecliptic longitude of axis of ecliptic plane rotation, 174.87° at J2000.
ρ'	fluid core density.
ρ	physical libration angle.
σ	physical libration angle.
τ	physical libration in longitude.
τ'	core physical libration in longitude.
ω	angular velocity.
$\boldsymbol{\omega}$	angular velocity vector.
$\omega_1, \omega_2, \omega_3$	angular velocity components.
$\boldsymbol{\omega}'$	core angular velocity vector.
$\hat{\boldsymbol{\omega}}$	unit angular velocity.
ϖ	mean longitude of perigee of lunar orbit.
Ω	mean orbital node of Moon; overdots are time derivatives.
ξ	combination of parameters for core computations, dimensionless, section 10; in section 13 it is used with subscripts L and ν.
ζ	combination used with tides; see equation (25).
φ, θ, ψ	Euler angles for lunar orientation; overdots are time derivatives.
φ', θ', ψ'	Euler angles for core orientation; overdots are time derivatives.

Mathematical Operations

d	derivative.
∂	partial derivative.
$\boldsymbol{\nabla}$	mathematical symbol for gradient.
x	mathematical symbol for cross product.
·	mathematical symbol for dot product; overdots are time derivatives.
*	indicates time delayed, e.g., $fn^* = fn(t-\Delta t)$; used for complex conjugate in section 12.
Σ	summation.
$\int$	integral.

Units

"	seconds of arc
'	minutes of arc

Appendices

d_0	Dahlen's spherical displacement parameter.
$\mathbf{j}, \mathbf{k}$	unit vectors.
K	bulk modulus.
n_0	Dahlen's spherical spin parameter.
r	radius to point in Moon.
$\mathbf{R}$	vector to point on surface.
$\hat{\mathbf{R}}$	unit vector to point on surface.
$U(r)$	elastic displacement.
V_P, V_S	P and S wave speeds.
v_c	circular orbit speed.
ΔI	change in moment of inertia.
μ	shear modulus or rigidity.
ρ	density.

Acknowledgments. We acknowledge and thank the staffs of the Observatoire de la Côte d'Azur, University of Texas McDonald Observatory, and the Haleakala Observatory, and the LLR associates. X X Newhall contributed to the early numerical work. DE403 was a cooperative effort with E. M. Standish. Bruce Bills provided helpful comments on the manuscript. The research described in this paper was carried out at the Jet Propulsion Laboratory of the California Institute of Technology, under a contract with the National Aeronautics and Space Administration.

References

Bills, B. G., Discrepant estimates of moments of inertia of the Moon, *J. Geophys. Res., 100*, 26,297-26,303, 1995.

Bills, B. G., and R. D. Ray, Lunar orbital evolution: A synthesis of recent results, *Geophys. Res. Lett., 26*, 3045-3048, 1999.

Binder, A. B., On the internal structure of a Moon of fission origin, *J. Geophys. Res., 85*, 4872-4880, 1980.

Binder, A. B., and M. A. Lange, On the thermal history, thermal state, and related tectonism of a Moon of fission origin, *J. Geophys. Res., 85*, 3194-3208, 1980.

Bois, E., and A. Journet, Lunar and terrestrial tidal effects on the Moon's rotational motion, *Celestial Mech. Dyn. Astron., 57*, 295-305, 1993.

Bois, E., F. Boudin, and A. Journet, Secular variation of the Moon's rotation rate, *Astron. Astrophys., 314*, 989-994, 1996.

Brett, R., A lunar core of Fe-Ni-S, *Geochim. Cosmochim. Acta, 37*, 165-170, 1973.

Brouwer, D., and G. M. Clemence, *Methods of Celestial Mechanics*, Academic, San Diego, Calif., 1961.

Cappallo, R. J., C. C. Counselman III, R. W. King, and I. I. Shapiro, Tidal dissipation in the Moon, *J. Geophys. Res., 86*, 7180-7184, 1981.

Chapront-Touzé, M., and J. Chapront, ELP 2000-85: A semi-analytical lunar ephemeris adequate for historical times, *Astron. Astrophys., 190*, 342-352, 1988.

Chapront-Touzé, M., and J. Chapront, *Lunar Tables and Programs from 4000 B. C. to A. D. 8000*, Willmann-Bell, Richmond, Va., 1991.

Cheng, C. H., and M. N. Toksöz, Tidal stresses in the Moon, *J. Geophys. Res., 83*, 845-853, 1978.

Christodoulidis, D. C., D. E. Smith, R. G. Williamson, and S. M. Klosko, Observed tidal braking in the Earth/Moon/Sun system, *J. Geophys. Res., 93*, 6216-6236, 1988.

Cisowski, S. M., and M. Fuller, Lunar paleointensities via the IRMs normalization method and the early magnetic history of the Moon, in *Origin of the Moon*, edited by W. K. Hartmann, R. J. Phyllips, and G. J. Taylor, pp. 411-424, Lunar and Planet. Inst., Houston, Tex., 1986.

Cisowski, S. M., D. W. Collinson, S. K. Runcorn, A. Stephenson, and M. Fuller, A review of lunar paleointensity data and implications for the origin of lunar magnetism, *Proc. Lunar Planet. Sci. Conf. 13th* , Part 2, *J. Geophys. Res., 88*, Suppl., A691-A704, 1983.

Dahlen, F. A., The passive influence of the oceans upon the rotation of the Earth, *Geophys. J. R. Astron. Soc., 46*, 363-406, 1976.

Dickey, J. O., J. G. Williams, and C. F. Yoder, Results from lunar laser ranging data analysis, in *High-Precision Earth Rotation and Earth-Moon Dynamics*, edited by O. Calame, pp. 209-216, D. Reidel, Norwell, Mass., 1982.

Dickey, J. O., et al., Lunar laser ranging: A continuing legacy of the Apollo program, *Science, 265*, 482-490, 1994.

Dickman, S. R., Ocean tide effects on Earth's rotation and on the lunar orbit, in *Gravimetry and Space Techniques Applied to Geodynamics and Ocean Dynamics*, *Geophys. Monogr. Ser.*, vol. 82, edited by B. E. Schutz et al., pp. 87-94, AGU, Washington, D. C., 1994.

Eckhardt, D. H., Theory of the libration of the Moon, *Moon Planets, 25*, 3-49, 1981.

Eckhardt, D. H., Passing through resonance: The excitation and dissipation of the lunar free libration in longitude, *Celestial Mech. Dyn. Astron., 57*, 307-324, 1993.

Ferrari, A. J., W. S. Sinclair, W. L. Sjogren, J. G. Williams, and C. F. Yoder, Geophysical parameters of the Earth-Moon system, *J. Geophys. Res., 85*, 3939-3951, 1980.

Galer, S. J. G., Interrelationships between continental freeboard, tectonics and mantle temperature, *Earth Planet. Sci. Lett., 105*, 214-228, 1991.

Goins, N. R., A. M. Dainty, and M. N. Toksoz, Lunar seismology: The internal structure of the Moon, *J. Geophys. Res., 86*, 5061-5074, 1981.

Goldreich, P., On the eccentricity of satellite orbits in the solar system, *Mon. Not. R. Astron. Soc., 126*, 256-268, 1963.

Goldreich, P., Precession of the Moon's core, *J. Geophys. Res., 72*, 3135-3137, 1967.

Goldstein, B. E., Electrical conductivity of the lunar interior: Theory, error sources, and estimates, *Proc. Lunar Planet. Sci. Conf. 10th*, 2357-2373, 1979.

Hood, L. L., Geophysical constraints on the lunar interior, in *Origin of the Moon*, edited by W. K. Hartmann, R. J. Phillips, and G. J. Taylor, pp. 361-410, Lunar and Planet. Inst., Houston, Tex., 1986.

Hood, L. L., and J. H. Jones, Geophysical constraints on lunar bulk composition and structure: A reassessment, *J. Geophys. Res., 92*, E396-E410, 1987.

Hood, L. L., D. L. Mitchell, R. P. Lin, M. H. Acuna, and A. B. Binder,

Initial measurements of the lunar induced magnetic dipole moment using Lunar Prospector magnetometer data, *Geophys. Res. Lett.*, *26*, 2327-2330, 1999.

Jeffreys, H., Certain hypotheses as to the internal structure of the Earth and Moon, *Mon. Not. R. Astron. Soc.*, *60*, 187-217, 1915.

Jeffreys, H., On the figures of the Earth and Moon, *Mon. Not. R. Astron. Soc.*, *Geophys. Suppl.*, *4*, 1-13, 1937.

Kaula, W. M., Tidal dissipation in the Moon, *J. Geophys. Res.*, *68*, 4959-4965, 1963.

Kaula, W. M., Tidal dissipation by solid friction and the resulting orbital evolution, *Rev. Geophys.*, *2*, 661-685, 1964.

Kaula, W. M., and C. F. Yoder, Lunar orbit evolution and tidal heating of the Moon (abstract), *Lunar Sci. VII*, 440-442, 1976.

Khan, A., and K. Mosegaard, New information on the deep lunar interior from an inversion of lunar free oscillation periods, *Geophys. Res. Lett.*, *28*, 1791-1794, 2001.

Khan, A., K. Mosegaard, and K. L. Rasmussen, A new seismic velocity model for the Moon from a Monte Carlo inversion of the Apollo lunar seismic data, *Geophys. Res. Lett.*, *27*, 1591-1594, 2000.

Konopliv, A. S., A. B. Binder, L. L. Hood, A. B. Kucinskas, W. L. Sjogren, and J. G. Williams, Improved gravity field of the Moon from Lunar Prospector, *Science*, *281*, 1476-1480, 1998.

Konrad, W., and T. Spohn, Thermal history of the Moon: implications for an early core dynamo and post-accretional magmatism, *Adv. Space Res.*, *19*(10), 1511-1521, 1997.

Kopal, Z., *The Moon*, D. Reidel, Norwell, Mass., 1969.

Kuskov, O. L., and V. A. Kronrod, A model of the chemical differentiation of the Moon, *Petrology*, *6*, 564-582, 1998a.

Kuskov, O. L., and V. A. Kronrod, Constitution of the Moon, 5, Constraints on composition, density, temperature, and radius of a core, *Phys. Earth Planet. Inter.*, *107*, 285-306, 1998b.

Lambeck, K., *The Earth's Variable Rotation: Geophysical Causes and Consequences*, Cambridge Univ. Press, New York, 1980.

Lambeck, K., *Geophysical Geodesy: The Slow Deformations of the Earth*, Clarendon, Oxford, England, 1988.

Lambeck, K., and S. Pullan, The lunar fossil bulge hypothesis revisited, *Phys. Earth Planet. Inter.*, *22*, 29-35, 1980.

Langseth, M. G., S. J. Keihm, and K. Peters, Revised lunar heat-flow values, in *Proc. Lunar Sci. Conf. 7th*, 3143-3171, 1976.

Lemoine, F. G. R., D. E. Smith, M. T. Zuber, G. A. Neumann, and D. D. Rowlands, A 70th degree lunar gravity model (GLGM-2) from Clementine and other tracking data, *J. Geophys. Res.*, *102*, 16,339-16,359, 1997.

Love, A. E. H., *A Treatise on the Mathematical Theory of Elasticity*, Dover, Mineola, N. Y., 1944.

Marsh, J. G., et al., The GEM-T2 gravitational model, *J. Geophys. Res.*, *95*, 22,043-22,071, 1990.

Mignard, F., The lunar orbit revisited, III, *Moon Planets*, *24*, 189-207, 1981.

Moons, M., Physical libration of the Moon, *Celestial Mech.*, *26*, 131-142, 1982a.

Moons, M., Analytical theory of the libration of the Moon, *Moon Planets*, *27*, 257-284, 1982b.

Mueller, S., G. J. Taylor, and R. J. Phillips, *J. Geophys. Res.*, *93*, 6338-6352, 1988.

Nakamura, Y., A1 moonquakes: Source distribution and mechanism, *Proc. Lunar Planet. Sci. Conf. 9th*, 3589-3607, 1978.

Nakamura, Y., Seismic velocity structure of the lunar mantle, *J. Geophys. Res.*, *88*, 677-686, 1983.

Nakamura, Y. and J. Koyama, Seismic Q of the lunar upper mantle, *J. Geophys. Res.*, *87*, 4855-4861, 1982.

Nakamura, Y., G. Latham, D. Lammlein, M. Ewing, F. Duennebier, and J. Dorman, Deep lunar interior inferred from recent seismic data, *Geophys. Res. Lett.*, *1*, 137-140, 1974.

Nakamura, Y., G. V. Latham, and H. J. Dorman, Apollo lunar science experiment - final summary, *Proc. Lunar Planet. Sci. Conf. 13th*, Part 1, *J. Geophys. Res.*, *87*, *Suppl.*, A117-A123, 1982.

Newhall, X X, and J. G. Williams, Estimation of the lunar physical librations, *Celestial Mech. Dyn. Astron.*, *66*, 21-30, 1997.

Newsom, H. E., Constraints on the origin of the Moon from the abundance of molybdenum and other siderophile elements, in *Origin of the Moon*, edited by W. K. Hartmann, R. J. Phillips, and G. J. Taylor, pp. 203-230, Lunar Planet. Inst., Houston, Tex., 1986.

Peale, S. J., Some effects of elasticity on lunar rotation, *Moon*, *8*, 515-531, 1973.

Peale, S. J., Excitation and relaxation of the wobble, precession, and libration of the Moon, *J. Geophys. Res.*, *81*, 1813-1827, 1976.

Peale, S. J., Origin and evolution of the natural satellites, *Annu. Rev. Astron. Astrophys.*, *37*, 533-602, 1999.

Peale, S. J., and P. Cassen, Contribution of tidal dissipation to lunar thermal history, *Icarus*, *36*, 245-269, 1978.

Petrova, N., Analytical extension of lunar libration tables, *Earth Moon Planets*, *73*, 71-99, 1996.

Petrova, N., and A. Gusev, Clue about the planet interior: Convective motion and core-mantle rotation in the Earth and the Moon, paper presented at International Conference "Geometrization of Physics III", Kazan State Univ., Russia, 1997.

Ray, R. D., Tidal energy dissipation: Observations from astronomy, geodesy, and oceanography, in *The Oceans: Physical-Chemical Dynamics and Human Impact*, edited by S. K. Majumdar et al., pp. 171-185, Pa. Acad. of Sci., Pittsburgh, 1994.

Ray, R. D., R. J. Eanes, and B. F. Chao, Detection of tidal dissipation in the solid Earth by satellite tracking and altimetry, *Nature*, *381*, 595-597, 1996.

Righter, K., and M. J. Drake, Core formation in Earth's Moon, Mars, and Vesta, *Icarus*, *124*, 513-529, 1996.

Ross, M. and G. Schubert, Tidal dissipation in a viscoelastic planet, *Proc. Lunar and Planet. Sci. Conf. 16th* , Part 2, *J. Geophys. Res.*, *91*, Suppl., D447-D452, 1986.

Russell, C. T., P. J. Coleman Jr., and B. E. Goldstein, Measurements of the lunar induced magnetic moment in the geomagnetic tail: Evidence for a lunar core?, *Proc. Lunar Planet. Sci. Conf. 12th*, 831-836, 1981.

Samain, E., et al., Millimetric lunar laser ranging at OCA (Observatoire de la Côte d'Azur), *Astron. Astrophys. Suppl. Ser.*, *130*, 235-244, 1998.

Schubert, G., D. Stevenson, and P. Cassen, Whole planet cooling and the radiogenic heat source contents of the Earth and Moon, *J. Geophys. Res.*, *85*, 2531-2538, 1980.

Sellers, P. C., Seismic evidence for a low-velocity lunar core, *J. Geophys. Res.*, *97*, 11,663-11,672, 1992.

Simon, J. L., P. Bretagnon, J. Chapront, M. Chapront-Touzé, G. Francou, and J. Laskar, Numerical expressions for precession formulae and mean elements for the Moon and planets, *Astron. Astrophys.*, *282*, 663-683, 1994.

Smith, M. L., and F. A. Dahlen, The period and Q of the Chandler wobble, *Geophys. J. R. Astron. Soc.*, *64*, 223-282, 1981.

Sonett, C. P., E. P. Kvale, A. Zakharian, Marjorie A. Chan, and T. M. Demko, Late Proterozoic and Paleozoic tides, retreat of the Moon, and rotation of the Earth, *Science*, *273*, 100-104, 1996.

Spohn, T., W. Konrad, D. Breuer, and R. Ziethe, The longevity of lunar volcanism: Implications of thermal evolution calculations with 2D and 3D mantle convection models, submitted to Icarus, 1999.

Stevenson, D. J., Lunar asymmetry and paleomagnetism, *Nature*, *287*, 520-521, 1980.

Stevenson, D. J., Planetary magnetic fields, *Rep. Prog. Phys.*, *46*, 555-620, 1983.

Stevenson, D. J., and C. F. Yoder, A fluid outer core for the Moon and its implications for lunar dissipation, free librations, and magnetism (abstract), *Lunar Planet. Sci. XII*, 1043-1044, 1981.

Toksöz, M. N., N. R. Goins, and C. H. Cheng, Moonquakes: Mechanisms and relation to tidal stresses, *Science*, *196*, 979-981, 1977.

Toksöz, M. N., A. T. Hsui, and D. H. Johnston, Thermal evolutions of the terrestrial planets, *Moon Planets*, *18*, 281-320, 1978.

Touma, J., and J. Wisdom, Resonances in the early evolution of the Earth-Moon system, *Astron. J.*, *115*, 1653-1663, 1998.

Wahr, J., and Z. Bergen, The effects of mantle anelasticity on nutations, Earth tides, and tidal variations in rotation rate, *Geophys. J. R. Astron. Soc.*, *87*, 633-668, 1986.

Ward, W. R., Past orientation of the lunar spin axis, *Science*, *189*, 377-379, 1975.

Warren, P. H., and K. L. Rasmussen, Megaregolith insulation, internal temperatures, and bulk Uranium content of the Moon, *J. Geophys. Res.*, *92*, 3453-3465, 1987.

Williams, J. G., W. S. Sinclair, and C. F. Yoder, Tidal acceleration of the Moon, *Geophys. Res. Lett.*, *5*, 943-946, 1978.

Williams, J. G., X X Newhall, and J. O. Dickey, Lunar gravitational harmonics and reflector coordinates, in *Figure and Dynamics of the Earth, Moon, and Planets*, edited by P. Holota, pp. 643-648, Astron. Inst., Czech. Acad. of Sci., Prague, 1987.

Williams, J. G., X X Newhall, and J. O. Dickey, Lunar moments, tides, orientation, and coordinate frames, *Planet. Space Sci.*, *44*, 1077-1080, 1996.

Wiskerchen, M. J., and C. P. Sonett, On the detectability of a metallized lunar core, *Proc. Lunar Planet. Sci. Conf. 9th*, 3113-3124, 1978.

Yoder, C. F., Effects of the spin-spin interaction and the inelastic tidal

deformation on the lunar physical librations, in *Natural and Artificial Satellite Motion*, edited by P. E. Nacozy and S. Ferraz-Mello, pp. 211-221, Univ. of Texas Press, Austin, 1979.

Yoder, C. F., The free librations of a dissipative Moon, *Philos. Trans. R. Soc. London, Ser. A*, *303*, 327-338, 1981.

Yoder, C. F., Tidal rigidity of Phobos, *Icarus*, *49*, 327-346, 1982.

Yoder, C. F., Venus' free obliquity, *Icarus*, *117*, 250-286, 1995.

Yoder, C. F., W. S. Sinclair, and J. G. Williams, The effects of dissipation in the Moon on the lunar physical librations (abstract), *Lunar Planet. Sci., IX*, 1292-1293, 1978.

Yoder, C. F., J. G. Williams, and M. E. Parke, Tidal variations of Earth rotation, *J. Geophys. Res.*, *86*, 881-891, 1981.

D. H. Boggs, J. O. Dickey, J. T. Ratcliff, J. G. Williams, and C. F. Yoder, Jet Propulsion Laboratory, MS 238-332, 4800 Oak Grove Drive, Pasadena, CA 91109, USA. (james.g.williams@jpl.nasa.gov)

(Received September 19, 2000; revised August 15, 2001; accepted August 23, 2001.)